Chapter 10 The rock coast of South and Central America

Article *in* Geological Society London Memoirs · July 2014

DOI: 10.1144/M40.10

Ramon Blanco-Chao
University of Santiago de Compostela

Kevin Pedoja
Université de Caen Normandie

Cesar Witt
Université de Lille

J. Martinod
Université Savoie Mont Blanc

Geological Society, London, Memoirs

Chapter 10 The rock coast of South and Central America

R. Blanco-Chao, K. Pedoja, C. Witt, J. Martinod, L. Husson, V. Regard, L. Audin, M. Nexer, B. Delcaillau, M. Saillard, D. Melnick, J. F. Dumont, E. Santana, E. Navarrete, C. Martillo, M. Pappalardo, L. Ayala, J. F. Araya, A. Feal-Pérez, D. Correa and I. Arozarena-Llopis

Geological Society, London, Memoirs 2014, v.40; p155-191.
doi: 10.1144/M40.10

Notes

Chapter 10

The rock coast of South and Central America

R. BLANCO-CHAO*, K. PEDOJA[1], C. WITT[2], J. MARTINOD[3], L. HUSSON[4], V. REGARD[3], L. AUDIN[5], M. NEXER[1], B. DELCAILLAU[1], M. SAILLARD[3], D. MELNICK[6], J. F. DUMONT[7], E. SANTANA[7], E. NAVARRETE[7], C. MARTILLO[7], M. PAPPALARDO[8], L. AYALA[9], J. F. ARAYA[10], A. FEAL-PÉREZ[11], D. CORREA[12] & I. AROZARENA-LLOPIS[13]

[1]*Laboratoire de Morphodynamique Continentale et Côtière, CNRS, Université de Caen, 14000 Caen, France*

[2]*CNRS UMR 8217 Géosystèmes UFR des Sciences de la Terre Bâtiment SN5, Avenue Paul Langevin 59655 Villeneuve D'Ascq cedex France*

[3]*Université de Toulouse; UPS (OMP); GET; 14 Av Edouard Belin, F-31400 Toulouse, France*

[4]*Géosciences-Rennes (UMR6118 du CNRS, Université de Rennes 1, 35042 Rennes, France*

[5]*Institut des Sciences de la Terre (ISTerre) CNRS: UMR5275 – IRD: UR – IFSTTAR – U. de Savoie – U. J. Fourier - Grenoble I – INSU – OSUG, 38000 Grenoble, France*

[6]*University of Potsdam, Institute of Earth and Environmental Science Building Am Mühlenberg 3, Room 17 Karl-Liebknecht-Str. 24-25 14476 Potsdam-Golm, Germany*

[7]*ESPOL, Facultad de Ingeneria en Ciencia de la Tierra, La Prosperina, Guayaquil, Ecuador*

[8]*Dipartimento di Scienze della Terra, University of Pisa, Via S. Maria 53, 56126 Pisa, Italy*

[9]*Universidad Nacional Mayor de San Marcos, Facultad de Ingeniería Geológica, Peru*

[10]*Department of Geography, University of Chile, Santiago, Chile*

[11]*Department of Geography. Universidad de Santiago de Compostela. Praza da Universidade, 1. 15782, Santiago, Spain*

[12]*Departamento de Geología, Universidad EAFIT, Medellín, Colombia*

[13]*Universidad Nacional-Costa Rica, Costa Rica*

**Corresponding author (e-mail: ramon.blanco@usc.es)*

Abstract: The great variety of climatic conditions, tidal ranges and wave regimes of South and Central America act on a complex geology and tectonic framework. Many of the rock and cliffed coasts of South America are strongly controlled by the occurrence of extensive Cenozoic and Pleistocene sediments that crop out at the coast. Geology and the different uplift rates are a major factor in the whole coastal geomorphology of South and Central America, and consequently are a very important control of the processes and landforms of rock coasts. This chapter covers several aspects of the rock coast of South and Central America, with special attention to the combination of tectonic movements and Quaternary Pleistocene–Holocene sea-level changes.

South and Central America is a vast geographical area extending from the tropics to subpolar zones encompassing a great diversity of coastal environments (Fig. 10.1). From the Caribbean to Cape Hornos South America is a huge continent with a great diversity of geological and tectonic contexts and a wide variety of climatic conditions because of the latitudinal extent, and the role of the Andian Mountains in the west. Long rivers such as the Amazon, the Orinoco and the Paraná have their mouths on the Caribbean and Atlantic coasts, a very large source of sediments that have developed extended low-lying coastal areas. On the contrary, on the Pacific Andean coast the high reliefs and small fluvial basins, together with the southward-increasing aridity, reduce the sedimentary supply. This dissymmetry in the magnitude of the river catchments was in part responsible for the differences in the development of the coastal sedimentary complexes of the Atlantic and Pacific coasts of South America. There is a great diversity in wave energy environments with long swell waves in the exposed mid latitude Atlantic and Pacific coasts, frequent storms at the south end of the continent and hurricanes affecting the Caribbean coasts. Tides on the Pacific coast decrease from a near macro-tidal range in Central America and in the north of Colombia to meso-tidal in the most of the Andean coast, although in the deep fiords of the south coast of Chile the tidal amplification can reach 5.8 m. The southernmost coast of America is meso-tidal, but the Patagonian coast is macro-tidal, with spring tidal ranges of 10 m. The tidal range decreases to the north, being micro-tidal in Uruguay, increasing again on the Brazilian coast (2.2 m in Belén). The Caribbean coasts are micro-tidal, with less than 1 m of spring tidal range.

The variety of climatic conditions, tidal ranges and wave regimes act on a complex geology and tectonic framework. Many of the rock and cliffed coasts of South America are strongly controlled by the occurrence of extensive Cenozoic and Pleistocene sediments that crop out at the coast. Geology and the different uplift rates are a major factor in the whole coastal geomorphology of South and Central America, and consequently are a very

From: KENNEDY, D. M., STEPHENSON, W. J. & NAYLOR, L. A. (eds) 2014. *Rock Coast Geomorphology: A Global Synthesis*. Geological Society, London, Memoirs, **40**, 155–191. http://dx.doi.org/10.1144/M40.10

Fig. 10.1. General map with locations cited in the text.

important control of the processes and landforms of rock coasts. This chapter covers several aspects of the rock coast of South and Central America, with special attention to the geological and tectonic framework. The chapter is organized by countries with some more extended sections reviewing research in progress.

A geodynamic and geological introduction to the coasts of South America through the perspective of Quaternary stair-case coastal landscapes

Staircase coastal landscapes (e.g. sequence or flight of marine terraces) are extremely frequent because emerged Plio-Quaternary sequences of palaeocoasts are widely spread on the world coastlines. Along the coasts of South America, coastal sequences are present in 10 countries: Ecuador, Peru, Chile, Argentina, Uruguay, Brazil, French Guiana, Suriname, Venezuela and Colombia (Figs 10.2 & 10.3). These emerged coastal sequences are a long-standing geological curiosity (e.g. Darwin 1846; d'Orbigny, 1834–1847; Sheppard 1927; Feruglio 1933, 1950; Hoffstetter 1948; Paskoff 1970), which has been attributed to the results of various processes. Some uplifted coasts, Holocene in age, are due to the postglacial rebound and the related Global Isostatic Adjustment (Rostami *et al.* 2000), and are mainly present in the south of South America. Nevertheless, Holocene coastal barriers are also frequently described in Brazil (Martin *et al.* 1988, 1996). The majority of the coastal sequences found on South American shores is the geomorphic expression of late Pliocene and Quaternary highstands superimposed on tectonically uplifting coastlines. Some of these sequences have been studied from both local tectonic and geodynamic perspectives (Paskoff 1980; Hsu 1992; Leonard & Wehmiller 1991, 1992; Ota *et al.*, 1995; Ortlieb *et al.* 1996; Marquardt *et al.* 2004; Cantalamessa & Di Celma 2004; Pedoja *et al.* 2006*a*, *b*, 2008, 2009, 2011*a*, *b*; Melnick *et al.* 2009; Regard *et al.* 2010; Saillard *et al.* 2009, 2011, 2012), but many regions of these thousands of kilometres of coastlines remain poorly documented.

Since the pioneering descriptive works of Darwin (1846), it is evident that the coastal sequences of South America reflect a

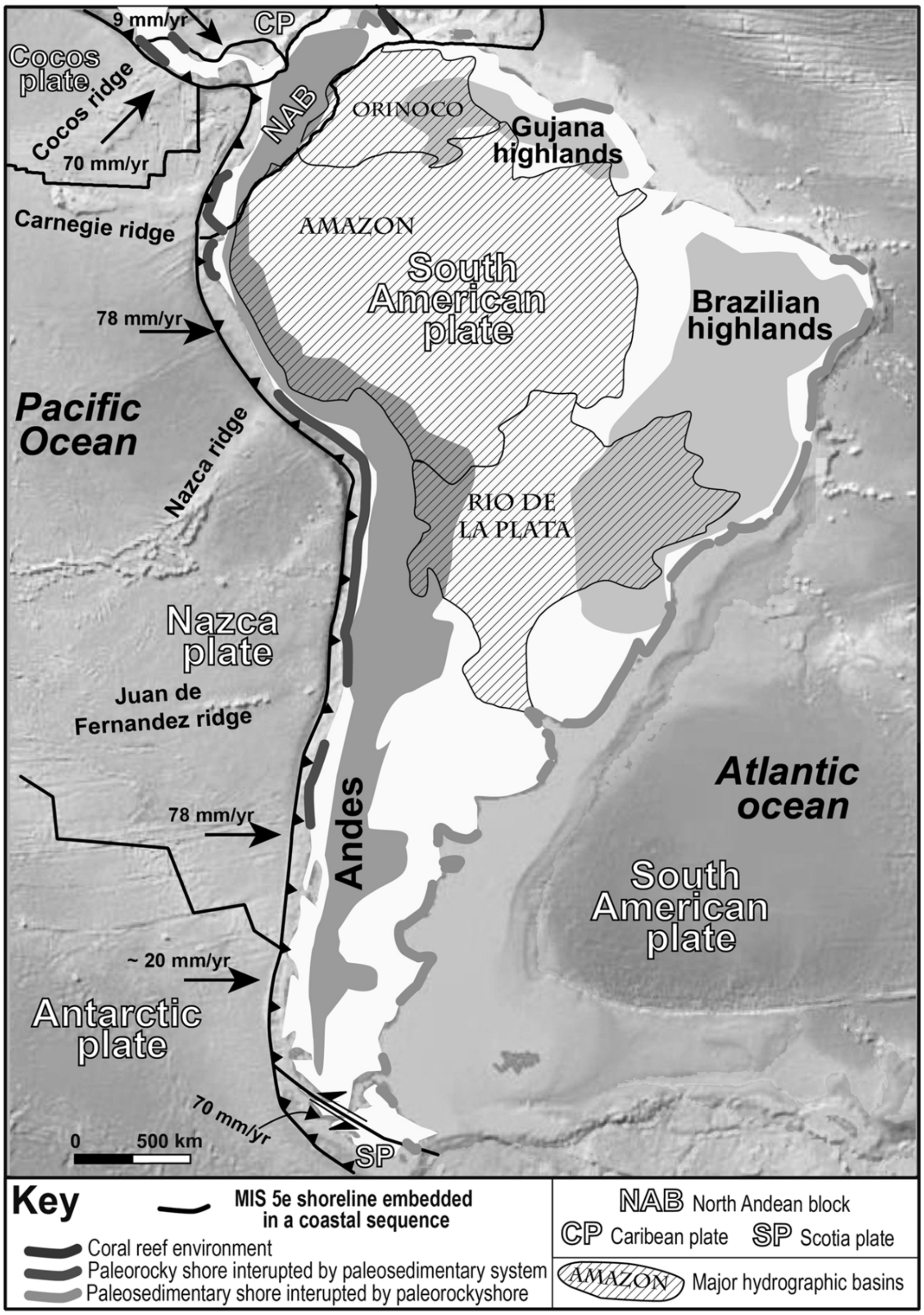

Fig. 10.2. South and Central American coastal sequences.

dissymmetry in their nature and distribution between the east (mainly Brazil and Argentina) and the west (Ecuador, Peru, Chile). Intuitively, one can accept that this dissymmetry is a consequence of the geodynamic setting. Consequently, in order to briefly describe the coastal geology of South America, we first present the nature and distribution of Quaternary coastal sequences, which we then tentatively interpret in the frame of their geodynamical and geological context.

South and Central American plio-Quaternary coastal sequences

In South America, out of 119 references we identified 79 sites where palaeoshorelines were created during the last interglacial maximum (MIS 5e, 122 ka). At all sites, this particular palaeoshoreline (referred herein as MIS 5e palaeoshoreline) is embedded in a coastal sequence whose formation may have started as early as the Pliocene (DeVries 1988). However, there are also sites where Holocene and/or Pleistocene shorelines are described, but the precise age or altitude of MIS 5e palaeoshorelines is not available in the literature. This is the case in Colombia and Suriname (Wong 1992).

At one site, different interpretations of the same coastal sequence have led to the establishment of two distinct morpho-stratigraphies (and consequently different uplift rates) being developed by different authors. At Valdivia (Chile), MIS 5e is identified either at 12.5 ± 3 m by Paskoff (1977) or at 69 ± 1 m by Pino *et al.* (2002).

Looking at the distribution of coastal sequences along the South American shores, one first striking observation is the east–west

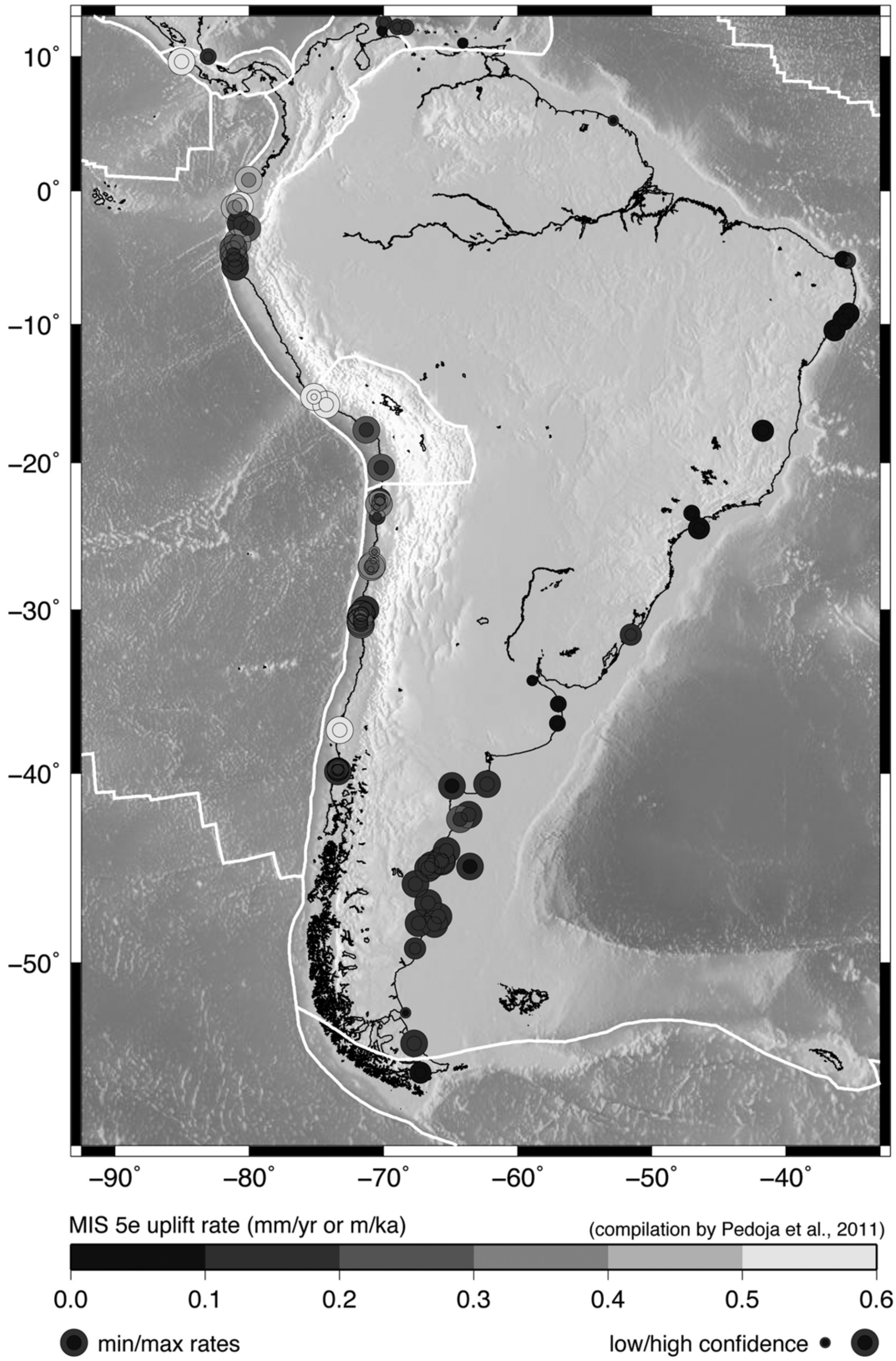

Fig. 10.3. South and Central American coastal uplift based on MIS 5e palaeoshoreline.

dissymmetry, which is marked by: (a) the nature of the indicators; (b) the length of the coastal tract covered by coastal sequences; and (c) the elevation of the MIS 5e indicators and corresponding uplift rates (Figs 10.2 & 10.3).

Nature of indicators. Quaternary palaeoshorelines of South America either correspond to (a) palaeorockyshores interrupted by palaeosedimentary systems to the west (Pacific side); and (b) palaeosedimentary shores interrupted by palaeorockyshores to the east (Atlantic side; Fig. 10.2). Such dissymmetry is also marked in the modern shoreline (e.g. Inman & Nordstrom 1971): the west coast of South America is rock-dominated whereas the east coast is predominantly sedimentary. As a counterpart to this observation, we need to re-iterate the observation made previously (Pedoja *et al.* 2011*a*) that the type of coast and palaeocoast (erosional, depositional and constructional) can change so rapidly that it is often difficult to fit a single site within this classification scheme.

Coastal tracts. On the eastern coast of South America, coastal sequences are extensively well developed and are present along very long continuous coastal tracts with very few interruptions.

For example, in Brazil, sequences are described over more than 3000 km and the coastal stretch covered by coastal sequences in eastern Patagonia (Argentina) reaches 2000 km. To the west, coastal sequences are more discontinuous. Long stretches without any described coastal sequence are present in Central Peru (between *c.* 7 and 15°S).

Deformation. Palaeocoasts from the last interglacial maximum (MIS 5e) range in altitude from -7 ± 2 to 235 ± 5 m. Corresponding uplift rates (corrected from eustasy), range from -0.08 ± 0.02 to 1.88 ± 0.1 mm a^{-1} (or m ka^{-1}). The highest uplift rates (>0.15 mm a^{-1}) are all located on the western side of the continent (Costa Rica, Ecuador, Peru, Chile) whereas to the East (Brazil, Argentina, Uruguay, French Guyana) the uplift is slower and more homogeneous.

Relation with geology and geodynamics

Plates kinematics and associated mantle flow. The South American continent is bounded by the passive Atlantic margin on its eastern side and by active subduction margins with the Nazca and Antarctic oceanic plates on its western boundary. Strike-slip faults separate South America from the Scotia plate at the southernmost boundary of the continent, and from the Caribbean plate, to the north.

The convergence velocity between the South America and Nazca plates is *c.* 78 mm a^{-1}, *c.* 75°N (Nuvel-1A model; DeMets *et al.* 1994), or 66 mm a^{-1} according to geodetic measurements (GPS, VLBI and SLR data; e.g. Argus *et al.* 2010; Prawirodirdjo & Bock 2004), which may reflect a decrease in the subduction velocity of the Nazca oceanic plate beneath South America. Plate reconstructions confirm that the convergence velocity between the two tectonic plates has been decreasing since the Early Miocene (Pardo-Casas & Molnar 1987; Somoza 1998; Somoza & Ghidella 2012). This decreasing velocity has been attributed to the growth of the Andean relief that increases the interplate contact (Iaffaldano *et al.* 2006), to the appearance of horizontal slab segments beneath northern Peru and north-central Chile (Martinod *et al.* 2010), or to slab interaction with the lower mantle (Husson *et al.* 2008; Quinteros & Sobolev 2013).

The absolute motion of South America with respect to hot spots (i.e. the lower mantle reference frame) is oriented towards the west since the separation of this continent from Africa in the Cretaceous (Silver *et al.* 1998; Sdrolias & Muller 2006). The westward drift of South America is probably one of the major parameters responsible for the compressive stress regime in western South America that explains continental shortening and the growth of the Andes (Russo & Silver 1996). This motion implies that the oceanic slab beneath South America retreats westward. This slab retreat, in turn, requires upper mantle flow to the west beneath the Pacific ocean, and toroidal mantle flow on both sides of the slab (i.e. eastward-oriented flow beneath Patagonia and the Caribbean plate, south and north of the Nazca slab, respectively, see below; e.g. Russo & Silver 1996; Husson *et al.* 2008; Guillaume *et al.* 2010).

At *c.* 46°S, the Chile Spreading Ridge that separates the Nazca plate from Antarctica collides against the western margin of South America. The associated triple junction was located close to the Strait of Magellan 14 Ma ago (Cande & Leslie 1986), and migrated northward to its present-day location offshore the Taitao Peninsula. Because the Nazca plate subducts approximately 50 mm a^{-1} faster than the Antarctica plate, a slab window has opened underneath Patagonia. The mantle flows eastward through this window and helps the westward retreat of the Nazca slab (Russo *et al.* 2010; Guillaume *et al.* 2010). This flow is responsible for the post-Middle Miocene back-arc basaltic magmatism in southern Patagonia (e.g. Gorring *et al.* 1997), the long-wavelength uplift of southern Patagonia (Guillaume *et al.* 2009), the cessation of active thrusting in the eastern foreland (e.g. Lagabrielle *et al.* 2004; Blisniuk *et al.* 2005) and possibly the onset of incipient extensional collapse (Scalabrino *et al.* 2010). Further to the SE of Tierra del Fuego, the Scotia plate moves eastward at a rate of *c.* 7 mm a^{-1} with respect to South America (Thomas *et al.* 2003).

From Ecuador to Colombia the current convergent margin occurs on previously accreted oceanic fragments originated at the Galapagos hot spot and most likely related to the Caribbean plate (e.g. Jaillard *et al.* 2009). On the northern boundary of South America, the contact with the Caribbean Plate is transpressive. The Caribbean plate moves *c.* 20 mm a^{-1} to the east with respect to South America (e.g. De Mets *et al.* 2010), but the amount of convergence that occurred between these two plates and the length of a possible Caribbean slab segment beneath northern Colombia and Venezuela remains controversial (Taboada *et al.* 2000; Duerto *et al.* 2006).

Possible causes of coastal uplift in South America

Vertical displacements of shorelines may reflect the interplay of the overriding plate with the subducting plate. The active continental margin of South America is one of the most segmented active margins in the world. The first-order segmentation is related to the presence of regions domminated by flat v. normal subduction. However, significant segmentation also results from ridge and oceanic asperities subduction as well as triple point collision and subduction, among others. It is commonly accepted that forearc basins may have recorded the evolution of the subduction regime because of their position above the plate interface. However, forearc basin structure as a function of the dynamics of subduction is an aspect that is poorly known.

The tectonic regime of subduction (accretion v. erosion) may play an important role in vertical movements at forearc basins and along the coastline. Most of the active Nazca–South American subduction zone has been considered as a typical example of a tectonically erosive margin (e.g. von Huene and Lallemand; von Huene & Ranero 2003), mainly defined by: (a) the absence of an accretionary prism; (b) extensional rather than contractional strain regime at the continental slope; and (c) landward migration of the volcanic arc. The deformational wake of an erosive margin may be linked to the sense of its vertical motion (subsidence or uplift), as proposed by Armijo & Thiele (1990). Complex retroactions occur, linked to changes in plate interface coupling, rate of sediment input to the trench, sediment underthrusting and underplatting or thrust generation at the plate interface (e.g. Hartley *et al.* 2000; Clift & Hartley 2007).

At the forearc scale, vertical displacements may result as well from mantle dynamics: mantle flow around the subducting slabs can exert a vertical traction underneath the overriding plate, and may influence coastal uplift. Because the subduction underneath South America is not steady, the magnitude of these tractions changes through time and causes vertical movements: the Amazon basin may be tilting to the east (Shephard *et al.* 2010), the Sierras Pampeanas subsided in response to the subduction of a flat slab (Davila *et al.* 2010), and an uplifting wave crosses Patagonia towards the north, accompanying the migration of the Chile triple junction (Guillaume *et al.* 2009). If dynamic topography can reasonably be invoked to explain the coastal uplift of Patagonia, it is clear that coastal vertical displacements resulting from dynamic topography may also occur in other segments of South American coasts.

The subduction of the Nazca plate beneath South America is segmented. Two major horizontal slab segments appeared in the late Miocene beneath both northern Peru and north-central Chile (e.g. Espurt *et al.* 2008 and references therein). These flat-slab segments correspond to major changes in the offshore morphology of the fore-arc area (e.g. absence of any longitudinal valley separating the Coastal Cordillera from the Andean

Piedmont). However, their effect on coastal dynamics is not clear. It has been proposed that the appearance of these horizontal slab segments marks the subduction of buoyant oceanic plateaus or aseismic ridges (e.g. Espurt *et al.* 2008). The subduction of major oceanic ridges (Carnegie ridge beneath Ecuador, Nazca Ridge beneath Peru) clearly triggers local coastal uplift at high rates (Macharé & Ortlieb 1992; Pedoja *et al.* 2006*a*; Saillard *et al.* 2011). In Ecuador, 2–3 million years of orthogonal subsidence of the Carnegie ridge (Witt *et al.* 2006; Michaud *et al.* 2009) produced coastal uplift that is twice more significant at the ridge axis than at both flanks (Pedoja *et al.* 2006*a*). In Peru, the subducting Nazca Ridge being oblique with respect to the convergence vector, the locus of ridge subduction progressively migrates southward (von Huene & Lallemand 1990; Hampel 2002) and the vertical motions resulting from the subduction are more ephemeral (Macharé & Ortlieb 1992; Saillard *et al.* 2011). The coastal area is uplifting to the south of the ridge, whereas the northern part in central part of Peru, where no uplift is reported, is probably subsiding after ridge subduction and migration (Le Roux *et al.* 2000; Hampel 2002).

Climate on the Pacific side of the Andes is equally segmented. Along-strike climatic variations are believed to be responsible for a high v. low frictional interface and have been related to major or minor topographic growth at the scale of the chain (e.g. Lamb & Davis 2003). The Central Andes are bounded by the driest desert worldwide. Hence, the oceanic trench adjacent to the Central Andes is mostly starved of sediments. The southern Andes, in contrast, are affected by southern westerlies, resulting in a humid climate on the Pacific side of the Cordillera and consequently in a filled trench with >2 km of sediments and an accretionary tectonic regime. The increase in exhumation rates in the southern Andes after the onset of Patagonian glaciations at *c.* 7–5 Ma (Mercer 1983) resulted in a shifting of the margin from erosive to accretionary (Melnick & Echtler 2006). Forearc basins between 33 and 46°S were uplifted *c.* 1.5 km associated with this shift. Based on the observation that the highest topography in the Andes occurrs in areas where trench sediment fill is below 0.5 km (between 10° and 33°S), Lamb & Davis (2003) propose that the absence of subducted trench sediments in the plate interface may increase friction, allowing for stresses to be transmitted from the lower to the upper plate, resulting in more intense shortening. This parameter does not appear to exert a major influence on coastal uplift, since emerged palaeo-shorelines are preserved both in the Atacama Desert (e.g. Regard *et al.* 2010 and references therein) and in very humid zones of southern Chile (e.g. Melnick *et al.* 2009). However, coastal uplift in the erosive part of the margin occurs at rates of *c.* 0.1–0.3 mm a^{-1}, whereas in the southern part it may exceed *c.* 1 mm a^{-1}. As suggested before temporal and spatial changes (across and along-strike) of the subduction-regime may be considered as a mechanism to explain forearc uplift.

Finally, the Pacific coasts of South America also present a seismic segmentation. It has been noted that the propagation of seismic ruptures during large (M > 8) plate-boundary earthquakes usually tends to stop in regions that often correspond to a morphological anomaly of the coastal area. For instance, the Mejillones Peninsula is considered to be a major seismic barrier since all the historical megathrust earthquakes that occurred in the region stopped beneath it (e.g. Delouis *et al.* 1998; Lomnitz 2004; Victor *et al.* 2011). In southern Chile, both the 1960 M = 9.5 and the 2010 M = 8.8 earthquakes terminated beneath the Arauco Peninsula (Plafker & Savage 1970; Moreno *et al.* 2012), and based on similarities of deformation patterns at 10^2–10^5 years across the peninsula, Melnick *et al.* (2009) proposed that this seismotectonic boundary has been stable over millions of years. Along these lines, Audin *et al.* (2008) noted that the southern limit of the 2001 M = 8.4 Arequipa earthquake is coincident with a major fault system in the upper plate striking oblique to the coastline. These examples suggest that long-term coastal uplift and deformation at geological timescales is linked to mechanical properties of the interplate contact and upper plate that in turn have an effect on the dynamics of seismic ruptures (Audin *et al.* 2008). However, some earthquake rupture ends are definitely not related to any particular morphological feature of the coastline, such as for example the northern limit of the 2010 Maule earthquake. This boundary was crossed by M ≥ 8 historical earthquakes in 1730, 1751 and 1906 (Lomnitz 2004; Okal 2005). Thus, it seems that only major anomalies of the coastline, or oblique fault systems in the upper plate, may control the rupture ends of great subduction earthquakes.

Although tectonic and geodynamic processes associated with plates kinematics may explain part of the observed uplift and subsidence around the South American continent, more local phenomena resulting in an increase or decrease of the load applied on the lithospheric plate may also result in vertical displacements of the coastal areas.

In the southern part of the continent, the load exerted by the Patagonian ice-fields deflects coastal areas, on both the Pacific and Atlantic side of South America, despite glaciers only reaching the Atlantic coast close to the Straits of Magellan and in Tierra del Fuego. The maximum ice volume during the last glacial period may have reached *c.* 3.5×10^5 km^3 (Hulton *et al.* 2002). Glacio-isostatic rebound models, however, suggest small present-day vertical motions on the Atlantic coast of Patagonia north of 50°S (Ivins & James 2004; Klemann *et al.* 2007). In fact, Rostami *et al.* (2000) note that glacial isostatic models do not explain the large amount of Holocene uplift found in Patagonia over the last 7000 years, and that other geodynamic processes may be responsible for part of this uplift. The glacial isostatic signal is minor when considering Pleistocene markers of coastal uplift. Preserved sequences of palaeoshorelines formed during Pleistocene interglacial periods also indicate that Patagonian coasts are not undergoing a discrete episode of uplift but rather are continuously rising, which confirms that the observed uplift does not result from glacial isostasy.

Surface load transfer may also influence coastal uplift by modifying accommodation space or by controlling the subduction regime (see below). This first aspect is well illustrated by the observed subsidence of the Rio de la Plata region, and possibly the Amazon Basin, and is at odds with the overall generalized uplift of the Atlantic coastline (Pedoja *et al.* 2011*c*).

The South American continent is separated from the Atlantic Ocean by a passive margin from the Mesozoic. Pedoja *et al.* (2011*c*) propose that uplift may occur close to a passive margin as a result of increasing horizontal margin-perpendicular compression of the lithospheric plate. In the Atlantic passive margins of South America, increasing compression may result either from a global Cenozoic increase of compressive stresses reflecting the accretion of India, Africa and Australia to the Eurasian continent (Pedoja *et al.* 2011*c*), and/or from the increasing coupling between the Nazca and South America plates, evidenced by the decreasing trenchward velocity of the Nazca plate since the Early Miocene (see references above). Leroy *et al.* (2004), indeed, show that higher magnitudes of compressive stresses at passive margins favour crustal uplift and tectonic inversion (e.g. Cogné *et al.* 2011). Of course, the above-mentioned mechanism may explain the uplift of Brazilian coasts that are very close from the shelf break, but not that of Patagonian coasts that are situated more than 500 km from the continental slope.

Holocene sea-level

The postglacial marine transgression in South America had a very different influence on recent coastal evolution and present dynamics. The complex tectonic framework together with other factors such as seismic activity and the glacial- and hydro-isostatic affects makes it difficult to draw a generalized sea-level curve of the Holocene for South America. The postglacial marine transgression in South America followed the general trend of the Holocene global curve, with a rapid sea-level rise prior to 6000–5000 BP caused by the glacial eustatic component and a second period dominated by the redistribution of water masses (Pirazzoli 1991; Mörner 2005), with local to regional differences owing to tectonics and isostasy. The general trend shows a southward increasing elevation for the Holocene marine terraces, in part predicted by the geoidal models (Rostami *et al.* 2000). In the far-field areas of low latitudes a relative sea-level higher than the present has been observed around mid-Holocene that was probably related to the hydroisostatic processes triggered by the collapsing forebulges or by the continental levering described by the eustatic models (Mitrovica & Milne 2002; Milne *et al.* 2005; Milne & Shennan 2007; Fig. 10.4). On the Atlantic coast data suggest that sea level over the last 5000 a was characterized by a progressive fall modulated by several oscillations, but the timing and amplitude of these osillations show great variability.

On the coast of Brazil a maximum relative sea-level of 2–4 m above present occurred between 5100 BP and 5700 cal. years BP (Bezerra *et al.* 2003; Angulo *et al.* 2006), followed by a sea-level fall and a second sea-level rise about 2100–1100 cal. years BP (Bezerra *et al.* 2003). In Uruguay the sea level reached +5 m round 6000 years BP, with a major regressive events at 3800–3600 BP and 2800–2500 BP (Bracco *et al.* 2005). In Argentina the maximum sea-level was dated around 6000 years BP in the Rio de la Plata (Cavallotto *et al.* 2004). In Patagonia maximum sea-level was dated around 7000 BP (Rostami *et al.* 2000; Zanchetta *et al.* 2012) and around 7000–8000 in Tierra de Fuego. The increasing higher elevation from north to south of the Holocene terraces in Patagonia can be related to the hydro-isostasy behaviour of the broad continental shelf but probably also to the occurrence of a tectonic uplift associated with the subduction-related tectonic deformation close to the Chilean trench (Rostami *et al.* 2000).

The physical models of geoidal deformation do not predict the occurrence of the sea level oscillations in the last 5000 years that were identified in several areas of South American coasts (Bezerra *et al.* 2003; Angulo *et al.* 2006; Schellmann & Radtke 2010). There is still no agreement on the causes of this sea-level variation, and it could be the result of glacio-isostasy (Schellmann & Radtke 2010) or local tectonics (Barreto *et al.* 2002; Zong 2007). The discrepancies in the maximum elevation of the mid-Holocene sea-level and amplitude may be due to lack of data or inaccuracy in the radiocarbon dating caused by regional variations in the ^{14}C reservoir effect (Schellmann & Radtke 2010). It is very important to reconsider the interpretation of the sea-level markers used to reconstruct past sea-levels (Zanchetta *et al.* 2012), and the energetic environment that can introduce important differences in elevation (Schellmann & Radtke 2010).

The available data for Holocene sea-level changes in the tectonically active Pacific coastlines are scarce. The Pacific coast seems to have been uplifted relatively continuously during the late Quaternary, at least since MIS 11, but with regional and local differences in the rates of uplift related to the dynamics of plate tectonics (Pedoja *et al.* 2006*b*; Regard *et al.* 2010; Saillard *et al.* 2011). It seems there is a trend of a decrease in the uplift rate through the Pleistocene to the Holocene (Pedoja *et al.* 2006*a*).

Rocky coasts in Central America

Pacific coasts of Central America

The Pacific coast of Central America extends along six countries (Guatemala, El Salvador, Honduras, Nicaragua, Costa Rica and Panamá) for about 2200 km (Fig. 10.5). There is considerable geological and geomorphological diversity (Yanez-Arancibia 2005), reflected by the variety of different coastal configurations. Tidal ranges vary from 1.5–2 m in Guatemala and 2–3 m in El Salvador and Nicaragua, to 4 m in the Gulf of Fonseca and 4.5–6 m in the Gulf of Panama (Gierloff- Emden 1982). Pacific Ocean swell generates average waves at the coast of up to 2 m high (Gierloff- Emden 1982) and longshore currents run predominantly southeastward, (Scheffers & Browne 2010). Climate varies from semi-arid in northern Guatemala to humid tropical conditions in Costa Rica and Panama (Scheffers & Browne 2010). Following the description of Marshall (2007), 15 physiographic provinces can be recognized in Central America (Fig. 10.5), but rock coasts only appear on the SE coast of Belize in the Maya block, Chortis and Chorotega fore arc (the main ones), Chocó fore and back arc areas and some parts of the Chorotega back arc (Figs 10.5 & 10.6).

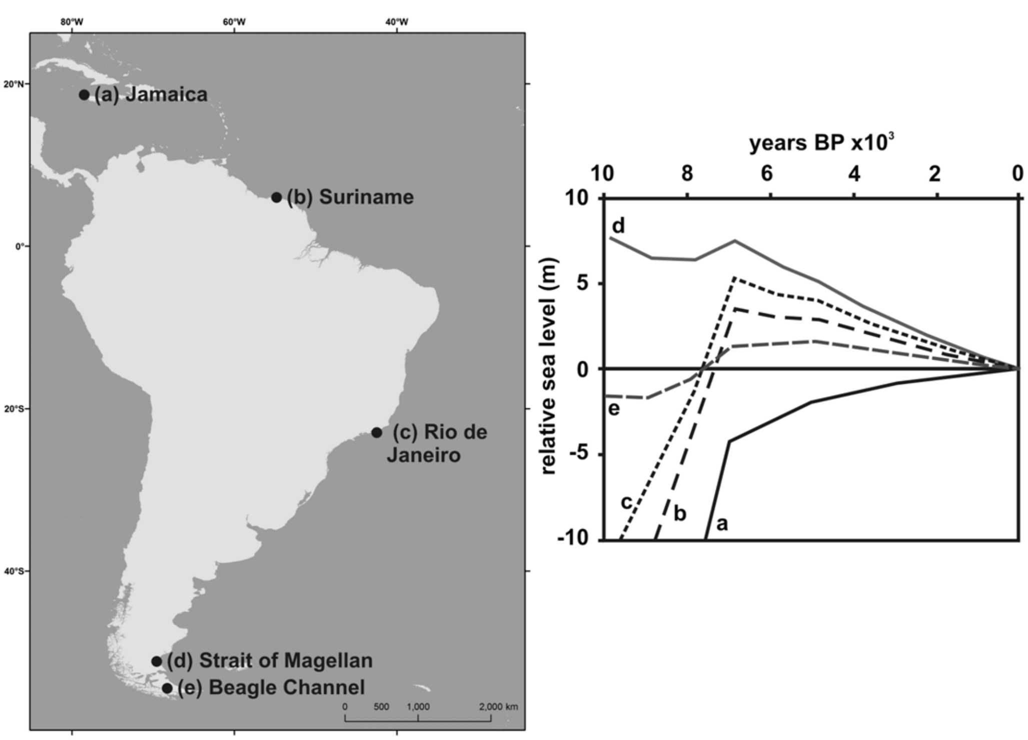

Fig. 10.4. Sea-level curves of the Atlantic coast of South America predicted by Global Isostatic Adjustment models (from Milne *et al* 2005).

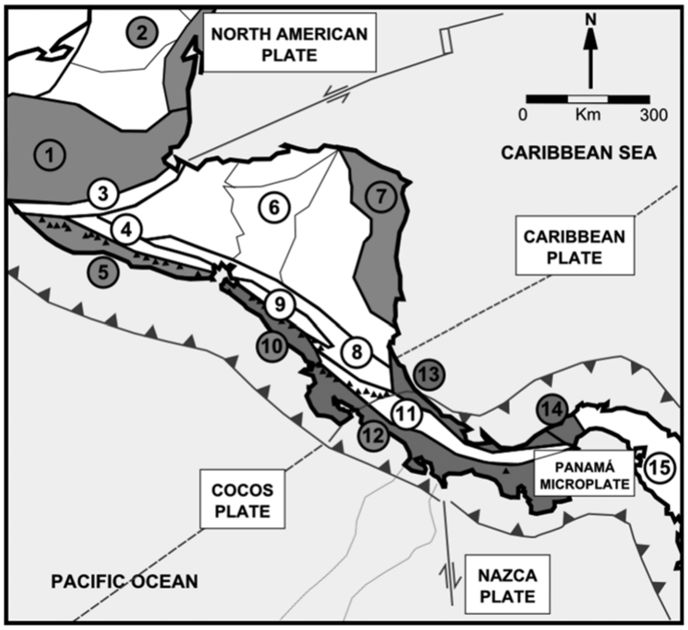

Fig. 10.5. Map of the physiographic provinces of Central America: 1, Maya Highlands; 2, Yucatán Platform (divided into four subzones); 3, Motagua Fault Zone; 4, Chortis Volcanic Front; 5, Chortis Fore arc; 6, Chortis Highlands (divided into four subzones); 7, Mosquito Coast Lowlands; 8, Nicaraguan Depression; 9, Nicaraguan Volcanic Front; 10, Sandino Fore Arc; 11, Chorotega Volcanic Front; 12, Chorotega Fore Arc; 13, Chorotega Back Arc; 14, Canal Zone Lowlands; 15, Darien Isthmus (numbers have their correspondent name in the text). Thin lines indicate subregions in Yucatán platform and Chortis highlands. The subregions into which Yucatán Platform (b) is divided are, from the shadowed coastal one: eastern block-faulted coastal plain; Peten karst Plateau and lowlands; Southern hilly karst plateau; and northern pitted karst plain. In the Chortis Highlands starting counter-clockwise from the coastal central one: Honduras borderlands; eastern dissected plateau; central Chortis Plateau; western rifted highland (modified from Marshall 2007).

Northern Central America includes the Maya and Chortis blocks (Dengo 1969; Dengo & Bohnenberger 1969; Donnelly *et al.* 1990; Burkart 1994), separated by the Motagua–Polochic fault zone in Guatemala (Fig. 10.6), which marks the Caribbean plate northern boundary (Marshall 2007). Differential lithology and structure between blocks, and Cenozoic subduction and volcanism exert control on geomorphology (Marshall 2007). Southern Central America is referred to as the Chorotega block and is a volcanic chain superimposed on oceanic rocks of Mesozoic age of the Caribbean plate (Dengo 1968, 1985; Dengo *et al.* 1970; Weyl 1980; Gardner *et al.* 1987; Escalante 1990; Mann & Corrigan 1990; Mann *et al.* 1990; Coates *et al.* 1992; Coates 1997; Wallace 1997). The boundary with the Chortis block is marked by a fault area from Costa Rica's Santa Elena peninsula eastward to the Caribbean Sea (Fig. 10.6).

The Chorotega block displays complex tectonics between four major converging and colliding plates: Caribbean, South America, Coco and Nazca (Dengo 1985; Mann *et al.* 1990) that have fragmented and created a system of fault-bounded microplates that absorb regional deformation (Adamek *et al.* 1988; Vergara-Muñoz 1988; Wadge & Burke 1983; Escalante 1990). Given this complex tectonic setting, with a subducting plate of irregular thickness just a few tens of kilometres far from the coast, earthquakes are very common and uplifted beaches and terraces are widespread.

Guatemala, El Salvador and Honduras. The lengths of the Pacific coasts of Guatemala, El Salvador and Honduras are, 250, 270 and 70 km, respectively. The first two are mainly formed by Quaternary coalescing alluvial fans forming coastal plains, being far narrower at El Salvador (Marshall 2007). The coast of Honduras is entirely inside the Gulf of Fonseca and is characterized by mangroves fringing a deltaic coastline (Scheffers & Browne 2010). Southeast from the Acajutla Peninsula (El Salvador), the coastline exhibits headlands and cliffs cut into resistant Pliocene volcanic rocks (Fig. 10.7; Marshall 2007).

Nicaragua. The Nicaraguan coast extends more than 300 km and represents the Sandino fore arc region (Fig. 10.5; Marshall 2007). It includes the rocky and steep volcanic Cosiguina Peninsula (Scheffers & Browne 2010) in the north (Fig. 10.6). There is also a basaltic dyke running parallel to the coastline near El Tránsito. It is sometimes separated a few metres from the beach, sometimes adjacent to it. At El Tránsito, it encloses partially the bay and it contributed to higher wave run-up causing many deaths during the 1992 Nicaraguan tsunami (Marshall 2007). The southern coast is characterized by rocky cliffs cut in the Cretaceous–Neogene marine folded sedimentary rocks of the Sandino fore-arc (Fig. 10.7; Marshall 2007), and exhibits pocket beaches, cliffy headlands and shore platforms controlled by structure (Fig. 10.7; Zoppis-Bracci & Del Giudice 1958; Rivera 1962; Weinberg 1992; INE 1995; Ranero & von Huene 2000). A late Pleistocene marine terrace dated at 135 ka (Walker *et al.* 1993) is cut in ash tuffs and Cretaceous–Neogene marine sediments are found at 17–22 m a.s.l. suggesting 0.1 m ka^{-1} of active uplift (Gerth *et al.* 1999). The terrace is adjacent to the Las Sierras volcanic massif, indicating that uplift could be due to thermal expansion or isostatic rebound after erosion of the shield (Marshall 2007).

Costa Rica. The Pacific coast of Coasta Rica is characterized by much more steep and rocky coasts than the countries described above, although extensive beaches, barrier islands, mangroves and coastal plains are also common. Active and intense tectonics in the Chorotega forearc and the presence of differential thickness and dip in the subducting Coco Ridge favour the formation of differential structural patterns and sharp morphologies, especially on the faulted blocks at the coast (Corrigan *et al.* 1990; Gardner *et al.* 1992; Fisher *et al.* 1994, 1998; Montero 1994; Kolarsky *et al*. 1995; Marshall *et al.* 2000, 2001, 2003*a*, 2004). Uplifted terraces are very common in the Costa Rican Pacific coast (Scheffers & Browne 2010), and show a northward decreasing rate of Quaternary uplift from 6–7 m ka^{-1} in the south to rates of less than 1 m ka^{-1} in the north (Marshall 2007).

Santa Elena Peninsula represents the northern margin of the Chorotega fore arc and is separated from the southern Sandino fore arc of the Chortis block, by the abrupt Murcielago fault zone (Madrigal 1982; Marshall & Vannuchi 2003). An indented and abrupt coastline south of Santa Elena Peninsula and on northern Nicoya Peninsula displays a pattern of pocket sandy beaches alternated with rocky headlands. Uplifted shallow marine and alluvial deposits of Holocene age in bays achieve 15–20 m elevation over some tens of kilometres inland, yielding uplift rates of 2.0–3.5 m ka^{-1} (Marshall & Vannuchi 2003). Shallow marine sediment wedges that crop out in the bays in this area attest to the continued and active uplift (Marshall & Vannuchi 2003).

Nicoya Peninsula is an emergent segment of the outer Chorotega fore arc (Fig. 10.7; Marshall 2007). To the west of Nicoya Peninsula lies the Gulf of Nicoya and Tempisque river alluvial plain (Madrigal & Rojas 1980; Bergoeing 1998). The peninsula is placed exactly above the seismogenic zone (Marshall & Anderson 1995; Marshall *et al.* 2003*a*, 2005) where seismic cycle deformation produced coseismic uplift of more than 1 m of the Nicoya Peninsula coastline during the 1950 M 7.7 earthquake (Marshall & Anderson 1995). After that, interseismic strain produced subsidence at the coast, and data suggest that the area is still seismically active (Protti *et al.* 2001; Norabuena *et al.* 2004). In fact, an M 7.6 earthquake that occurred on 5 September 2012, 24 km off the Nicoya Peninsula coast, seems to have

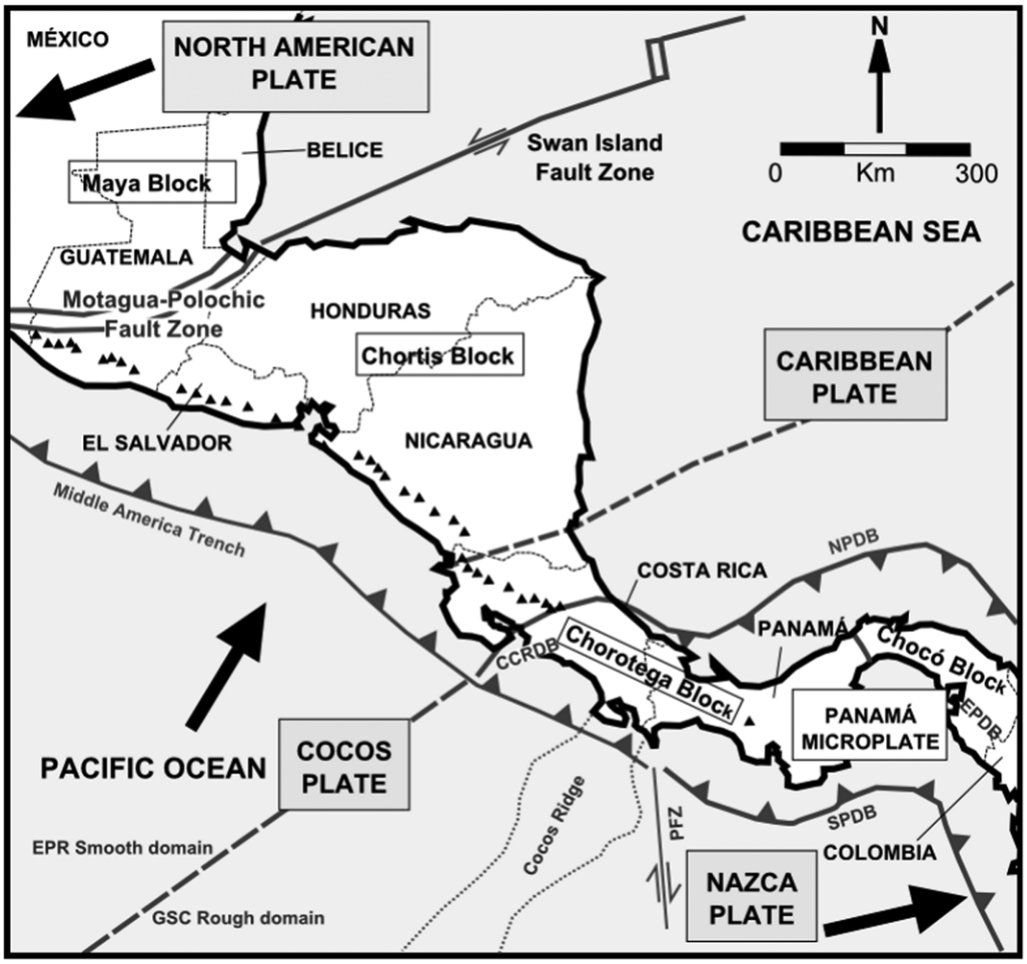

Fig. 10.6. Tectonic map of Central America, showing geometry of tectonic plates. Black arrows show plate motions relative to Caribbean plate. Active plate boundaries are shown with teeth on upper plate of convergent margins, and opposing arrows indicating transform motion). Dashed lines mark major bathymetric features. EPR, East Pacific Rise; GSC, Galapagos Spreading Center; PFZ, Panama Fracture Zone; CCRDB, Central Costa Rica deformed belt; NPDB, North Panama deformed belt; SPDB, South Panama deformed belt; EPDB, East Panama deformed belt (modified from Marshall 2007).

uplifted its western coast at least 1 m (there are no official data), suggesting that predictions made by Protti *et al.* (2001) were correct. There is a notable difference in uplift rates between the northern and southern coasts of Nicoya Peninsula; while northern Nicoya Peninsula lies onshore the 'smooth domain' of Coco's plate, the southern part lies inboard the subducting seamounts of the 'rough domain'. Therefore, these differential uplift rates are due to differences in thickness, roughness and dip of the subducting Coco Plate (Marshall 2007). Rocks coasts are formed by highly deformed mafic rocks and pelagic sediments dating to Cretaceous–early Cenozoic (Dengo 1962; de Boer 1979; Kuijpers 1980; Bourgois *et al.* 1984; Donnelly 1994). Four different coastal erosion surfaces have been recognized on the peninsula (Hare & Gardner 1985; Marshall & Anderson 1995; Marshall *et al.* 2001, 2003*a*, 2005; Gardner *et al.* 2001; Marshall 2007). In the north, the Iguanazul Surface is composed of a set of three marine late

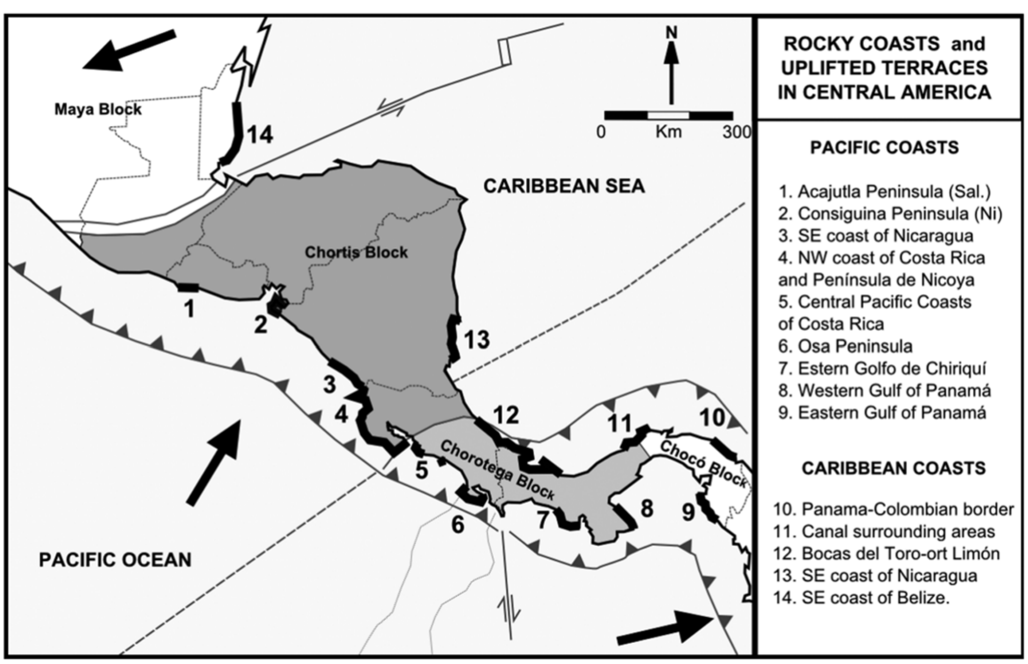

Fig. 10.7. Most important rocky coast segments in Central America are described in the text (modified from Marshall 2007).

Pleistocene palaeoshorelines at elevations between 10 and 32 m that yield uplift rates of 0.1–0.3 m ka^{-1} Radiocarbon dated beach deposits indicate Holocene ages consistent with recent uplift at less than 0.5 m ka^{-1} (Marshall *et al.* 2003*a*, 2005). The Cerro Azul Surface is a Plio-Pleistocene relict marine surface whose deformation suggests differential uplift across a series of faulted mountain blocks (Hare & Gardner 1985; Marshall 2007). The Cóbano Surface, on the southern Nicoya Peninsula, has at least four different uplifted late Pleistocene marine terraces, featuring an extensive incised mesa between the mountains and the uplifted sea cliffs near the coast (Hare & Gardner 1985; Marshall & Anderson 1995; Gardner *et al.* 2001; Marshall *et al.* 2001, 2003*a*, 2005). The marine terraces have been correlated to Pleistocene sea-level high stands at 60–215 ka (MIS 3–7), yielding uplift rates of 1.0–2.0 m ka^{-1} (Marshall *et al.* 2003*a*, 2005). Terraces range in elevation from 15 to 220 m a.s.l., increasing in elevation southwestward, in the direction of the trench (Marshall 2007). The Cabuya Surface is located on the seaward margin of the Cóbano Surface and landward from the present shoreline. It is composed of a set of small emerged Holocene terraces (<1 km wide, <20 m elevation) where uplift rates between 1.0 and 6.0 m ka^{-1} exceed late Holocene sea-level rise (Marshall 2007).

Differential Quaternary uplift rates owing to faults normal to the margin dissect the coast into several blocks with fluvial and marine terraces (Fisher *et al.* 1994, 1998; Marshall *et al.* 2000, 2001, 2003*b*). On the Esparza and Orotina fault blocks more than five late Quaternary valley fill terraces (10–260 m a.s.l.) were formed during sea-level rise towards eustatic highstands in the late Quaternary (Marshall *et al.* 2001). Herradura Headland (Fig. 10.7) is the highest promontory in the Chorotega fore arc (more than 1700 m) and late Cretaceous oceanic basalts crop out on it, revealing rapid Quaternary uplift and erosion that removed overlying marine sediments (Marshall 2007). Marine and fluvial terraces account for fast uplift rates in the Holocene that could be related to seamount subduction (Von Huene *et al.* 1995, 2000). Osa Peninsula (Fig. 10.7) is another emerged part of the outer Chorotega fore arc and it is formed by rapid uplift and crustal shortening exactly over the central part of the Coco Ridge (Gardner *et al*. 1992). It is composed of intensely folded Cretaceous–Palaeogene oceanic basement rocks and accreted marine sediments (Bourgois *et al.* 1984; Donnelly 1994). This area is known as a seismogenic area associated with subduction of Coco Ridge (Adamek *et al.* 1987; Tajima & Kikuchi 1995). Rapid uplift rates (2.1–6.5 m ka^{-1}) determined from marine, beach and alluvial deposits show a decrease northwestward (Gardner *et al*. 1992; Bullard 2002; Sak *et al.* 2004). Coastal sand deposits dated at 27–50 ka are exposed at the steep seaward-facing coast at more than 75 m a.s.l. (Sak *et al.* 2004). A series of uplifted beaches with radiocarbon ages ranging from less than 1 ka near the present shore to more than 30 ka achieve 25 m a.s.l. (Gardner *et al*. 1992).

Panama. Panama has the longest Pacific coast (more than 900 km) of the Central American countries. Deformation owing to the subducting Coco's Ridge and passage of the Panama Triple Junction (Corrigan *et al.* 1990) is revealed by the presence of uplifted shore platforms on the Burica Peninsula coast (Marshall 2007). The Gulf of Chiriquí is characterized by highly indented rocky coasts with steep cliffs (Fig. 10.7), especially on the steeply sided eastern Azuero peninsula (Scheffers & Browne 2010). The western and eastern coasts of the Gulf of Panama are steep and rocky. The eastern indented coastline encompasses drowned fluvial valleys flanking mountain chains (Scheffers & Browne 2010).

Caribbean coasts

The Caribbean coasts of Central America extend for about 2200 km from the Colombia–Panama border, to the Belize–Mexico border on the Yucatán Peninsula. Wave energy is medium to high owing to frequent storms and occasional hurricanes in the Caribbean Sea, but also varies depending on continental shelf width. Tidal ranges are less than 0.5 m. Coasts of the Caribbean exhibit wider coastal plains than Pacific coasts and often a wider continental shelf. Longer rivers in Central America mostly drain to the Caribbean Sea because the divide is located closer to the Pacific Ocean in most cases. Intense rainfall (5–6 m a^{-1}), especially when hurricanes occur, transports huge amounts of sediment to the Caribbean Sea forming beach ridges (Scheffers & Browne 2010). Costa Rica and Panama Caribbean coasts are the exception as streams are shorter and more deeply incised, so narrow sandy beaches, barrier islands with associated lagoons and large mangroves covering inlets and estuaries shores characterize most parts of this coast (Scheffers & Browne 2010). Coral reefs are common where there is little river suspended sediment and around offshore islands, especially on the Belize coast (Scheffers & Browne 2010).

Guatemala and Honduras. Amatique Bay in Guatemala is located on a graben stretching almost perpendicular to the coast, and it is enclosed at its eastern seaward part by a large sandy spit, Manabique Point. Small and dispersed beaches are present in this area associated with narrow lowlands and mangroves (Scheffers & Browne 2010). Honduras Coast extends for up to 600 km, excluding islands. The Bay Islands represent the continuation of the mountain system of Nuclear Central America (Scheffers & Browne 2010). Large rivers have provided a considerable amount of sediment, and westward longshore drift has created sand spits and long beaches, associated with mangrove- or marsh-covered estuaries and deltas (Scheffers & Browne 2010). The hinterland of the Catarasca Lagoon has many wide, low Plio-Pleistocene terraces (Scheffers & Browne 2010). Mountain ranges locally reach the coast west from the Patuca River delta.

Belize. Long and parallel to the coast, lagoons and barrier islands characterize the area north of Stann Creek, where mangrove shores are bordered inland by Plio-Pleistocene terraces formed predominantly of limestone fragments derived from the older carbonate rocks (Wright *et al.* 1959). Sharp cliffs carved in Cretaceous limestones crop out near Punta Gorda in southern Belize (Fig. 10.7). The second largest reef barrier in the world (more than 200 km long, with many islands and atolls), after Australia's Great Barrier Reef, is the most remarkable feature in this area. Coral reef distribution and morphology are controlled by a series of subparallel normal faults trending NNE in a horst-graben structure (Weidie 1985) owing to trans-tensional stress along the North American–Caribbean transform boundary (Marshall 2007). Geophysical research has shown that major reefs were built in the Pliocene (Scheffers & Browne 2010).

Nicaragua. The Caribbean coastline of Nicaragua runs north for more than 450 km. Sand and pebble deposits form wide Plio-Pleistocene low terraces in the northern part of the coast, near Puerto Cabezas (Scheffers & Browne 2010). Along the coast around Monkey Point in the south (Fig. 10.7), a series of prominent cliffs expose resistant basalt flows interbedded with Cenozoic volcaniclastic sediments. Cenozoic lavas also form the basement of the offshore Corn Islands, where coastal cliffs up to 100 m high expose massive basalt flows (Marshall 2007).

Costa Rica. Costa Rican Caribbean coasts are only 200 km in length. The rugged geomorphology of the Limón and Bocas Del Toro region (Fig. 10.7) is controlled by active crustal shortening within the north Panama deformation belt along the Caribbean margin of the Panama block (Escalante & Astorga 1994). During the 1991 M7.6 Valle de la Estrella earthquake, coseismic uplift of 0.5–1.5 m affected the southern Limón coast (Plafker & Ward 1992), while subsidence of 0.5–0.7 m resulted in drowning of swamps along the Bocas del Toro embayment (Phillips *et al.* 1994). From Puerto Limón, to South of Manzanillo in Costa Rica, Holocene relict coral and fringing reefs crop out as a consequence of 1991 earthquake rapid uplift around NE-verging thrust faults (Denyer *et al.* 1994).

This zone of active coastal deformation ends abruptly at the Limón headland, where thrust faulting gives way to the north to oblique slip along steeply dipping faults of the Central Costa Rica deformed belt (Tortuguero area; Denyer *et al.* 1994; Marshall *et al.* 2000). Tortuguero lowlands are composed of a sequence of huge alluvial fans incised by modern rivers, covered by deep-red, clay-rich soils (Wielemaker & Vogel 1993).

Panama. The state of Panama, with more than 600 km, has the longest Caribbean coastline of Central America. The coast is bordered by numerous small islands (Bocas del Toro and San Blas Archipelagos), made up of a drowned part of the basic basement of south-Central America. The 1991 M7.6 earthquake led to coseismic subsidence of about 0.5–0.7 m, resulting in flooding of peat swamps along the Bocas del Toro embayment (Phillips *et al.* 1994). Uplift around the Bocas del Toro coast has exposed a Neogene sequence of marine to terrestrial sediments and volcanic rocks along coastal cliffs and islands (Coates *et al.* 1992, 2003). As a whole, this rock sequence provides a detailed record of Neogene emergence along the Panama isthmus, resulting in closure of the oceanic strait between the Atlantic and Pacific Ocean basins (Coates & Obando 1996; Coates 1997). Uplifted shore platforms can be found close to the entrance of the Canal. Long areas of rocky cliffs owing to the proximity of mountain ridges alternate with small to medium beaches west from Cape Tiburón on the Colombian border (Scheffers & Browne 2010).

Colombia

Colombia is located on the northwestern corner of South America, a region with a complex geological history owing to the interactions among the Nazca, Caribbean and South American tectonic plates since Cretaceous times (Duque-Caro 1990; París *et al.* 2002; Cediel *et al.* 2003). Active tectonics, semidesert to humid tropical climatic conditions and a history of human interventions all play a fundamental role in the present geomorphology and plan-view configuration of Colombian Pacific and Caribbean continental coastlines (Correa & Morton 2010; Cantera & Restrepo 2011).

Cliffs of the Colombian Pacific coast

The Pacific coast of Colombia extends for about 1300 km from Punta Ardita (Panamá border) to Cabo Manglares (Ecuadorian border; Fig. 10.8). Cliffed coastlines along this high-seismic-risk, meso-macro tidal range, SW trade winds coast (West 1957; Correa 1996; Jaramillo & Bayona 2000; Correa & Morton 2010, 2011*a*) are found continuously between Punta Ardita (Panama border) and Cabo Corrientes cut mainly on basaltic rocks of the Serrania del Baudó coastal range (Fig. 10.9a). Cliffs are also found in the borderland of Málaga Bay and along the northern coastlines of the Buenaventura and Tumaco Bays. Between Cabo Corrientes and the San Juan River Delta, a continuous line of palaeo-cliffs marks the landward limit of a fringe of late Holocene mangrove swamps, lagoons and beach-barriers deposits up to 6 km wide from the present coastline (Fig. 10.8). Between Buenaventura and Tumaco bays (Fig. 10.9b) there is only one small patch of active cliffed coastline (Tortugas), and the present barrier islands–lagoon–mangrove swamp depositional systems are landward bordered by low-angle scarps marking the maximum advance of Holocene transgression in the area (Vélez *et al.* 2001; Correa & Morton 2010). The approximate total length of active cliffed coastlines along the Pacific coast of Colombia is of 350 km.

No detailed morphological studies have been made to date on any of the Pacific cliffs, but available information indicates that erosion rates are very low or negligible along most of the basaltic cliffs of the northern Pacific (Serranía del Baudò) and also along the cliffed areas to the south of Cabo Corrientes which are cut on stratified sequences of Cenozoic to Pleistocene mudstones and claystones. Episodic cliff retreat – rock falls, rotational slumps – along the active cliffs of the Colombian Pacific coast occurs in localized sectors and is triggered by high-magnitude seismic events common on this coast. The most famous of these are the 1906 and 1979 earthquakes that generated tsunami 2.5 m high that devastated the coast south of Buenaventura Bay (Herd *et al.* 1981; White *et al.* 2003). Episodic erosion of cliffs has also been reported during El Niño sea level positive anomalies (Morton *et al.* 2000). Preliminary comparisons of coastline positions on 1838 English Admiralty Charts for the Pacific coast of Colombia with Intera Canada Technologies radar images taken in 1992 suggest significant changes for some cliffed sectors of the northern Pacific coast. Soil mass movements along the steep slopes of the pacific cliffs are associated with the occurrence of earthquakes and with periods of high precipitation and high winds that cause soil saturation, tree falls and soil structure destruction.

Common erosional features along the cliffed coastlines of the Pacific coast of Colombia are mainly notches (found in all lithologies) and small islands, stacks and gentle steep-intertidal rock platforms found mainly in the bays and pocket beaches of the Serrania de Baudó. Flat surfaces that suggest emerged shore platforms or marine terraces have been reported in the Buenaventura area (10 m above present sea-level) and between Cabo Corrientes and the San Juan River Delta (40–80 m above present sea-level). Cantera *et al.* (1998) reported the importance of bioerosion as a first-order morphological process along the cliffed sectors between the bays of Málaga and Buenaventura.

Cliffs of the Caribbean coast

The Caribbean coast of Colombia has an approximate length of 1600 km and extends from Castilletes (Venezuelan border) to Cabo Tiburón (Panamá border; Fig. 10.10). Cliffed coastlines are exposed to a medium- to low-seismic risk, microtidal range and NE trade winds. These cliffs are found along the northern Guajira Penìnsula, the Sierra Nevada de Santa Marta massive, the Barranquilla–Cartagena shores and along the southern Caribbean, from the southern tip of Morrosquillo Gulf to the city of Turbo at the eastern borderland of the Urabá Gulf (Correa & Morton 2010, 2011*b*). The total length of active cliffs along the Colombian Caribbean coastlines is about 500 km.

Cliffs between the Santa Marta area and the Guajira Peninsula (Fig. 10.11) are mostly steep-sloping scarps up to 50 m high cut in Cenozoic sequences and also on igneous and metamorphic rocks such as serpentinite, granites and gneisses. South of Barranquilla, cliffs alternate with low sandy depositional shores and deltaic areas. Cliff types along the central and southern Caribbean are extremely variable with vertical scarps 30 m high cut on deformed Cenozoic rocks to 2–15 m-high scarps cut in mudstones and sandstones and also in semiconsolidated deposits resulting from the erosion of Quaternary and Holocene calcareous reefs most common along the Cartagena area (Vernette 1989; Martínez *et al.* 2010).

Evidence of recent tectonic deformation can be found all along the entire Caribbean coast of Colombia, but this is more noticeable along the southern Caribbean coast, between Galerazamba and the Urabá Gulf. The geological and geomorphological evolution of this coast has been controlled by compressional stresses and mud diapiric activity with numerous modern examples, including

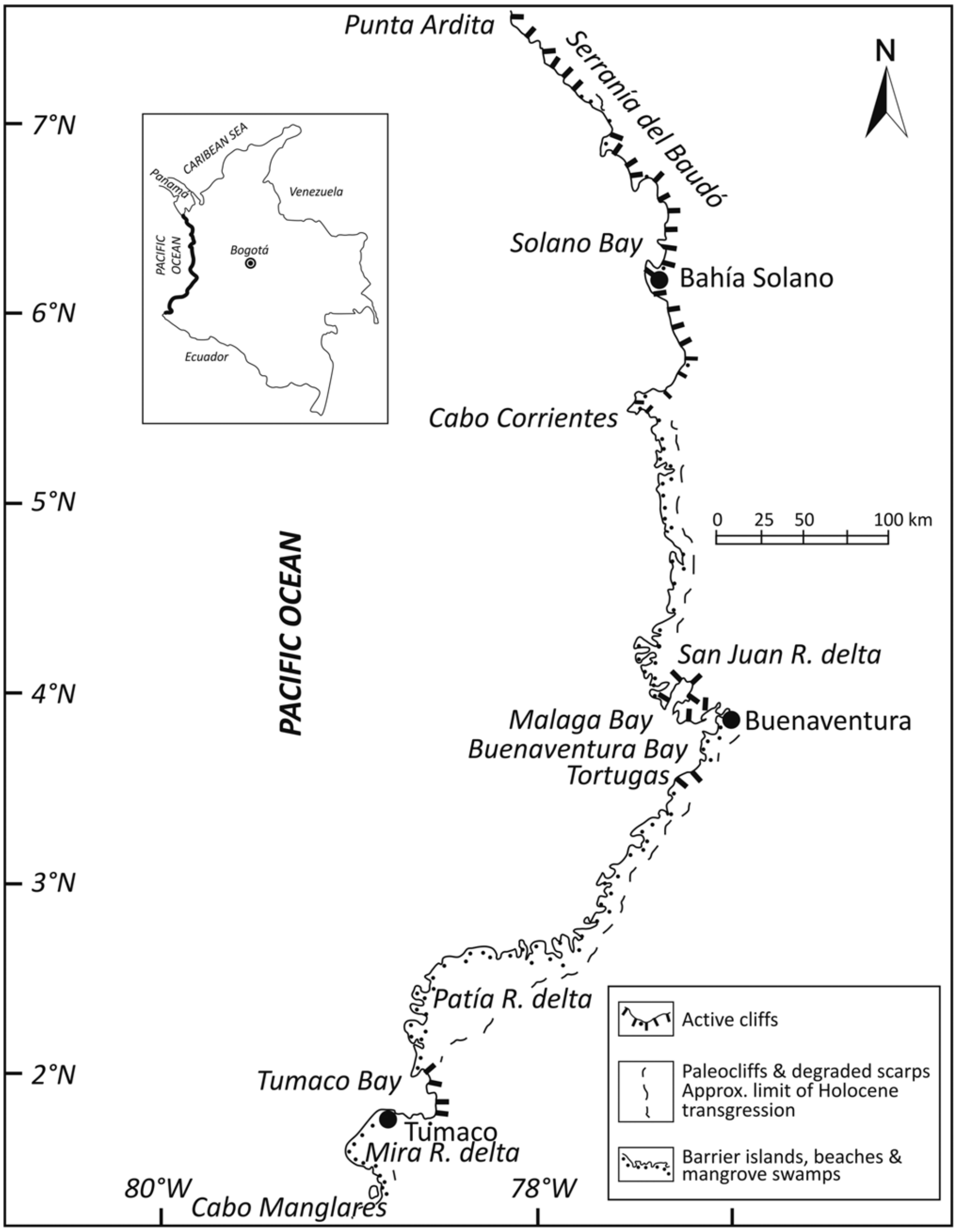

Fig. 10.8. Main coastline types of the Colombian Pacific Coast.

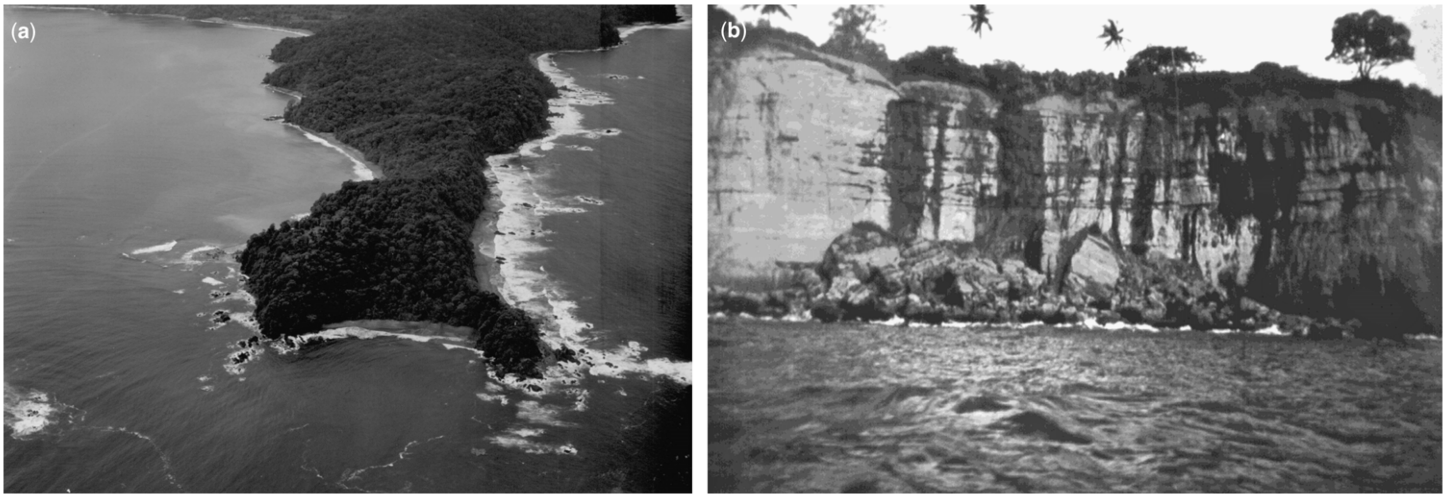

Fig. 10.9. Cliffed coastline at Solano bay cut on basaltic rocks ot the Serrania del Baudó coastal range (**a**). Active cliffs cut on Cenozoic rocks, eastern border of Tumaco bay (**b**).

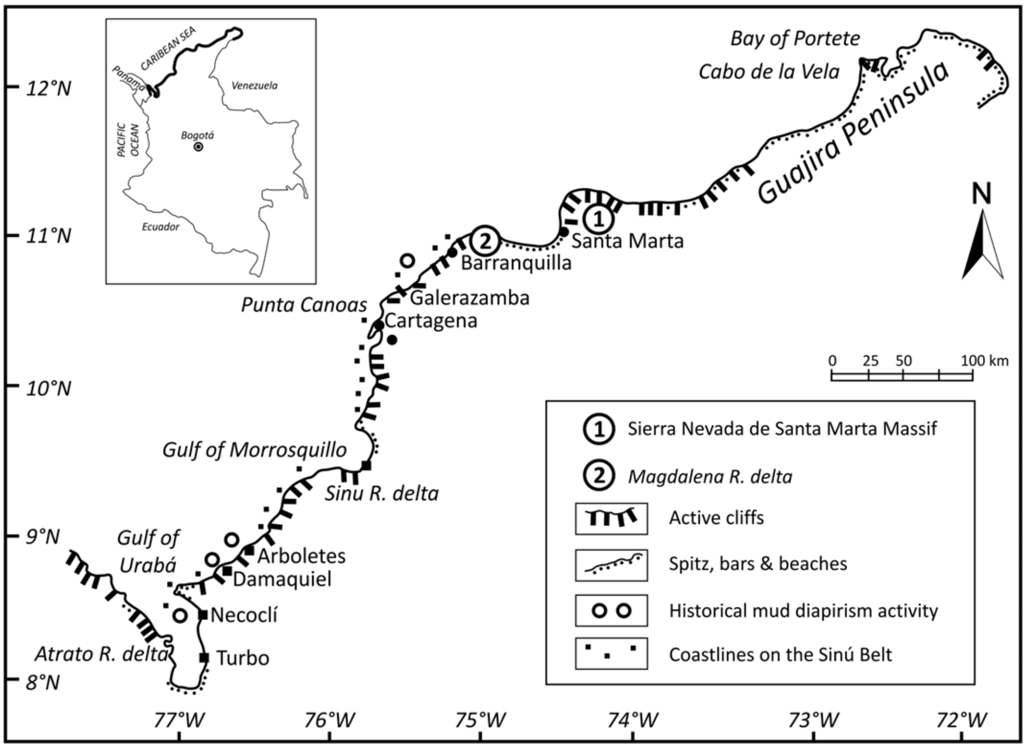

Fig. 10.10. Main coastline types of the Colombian Caribbean coast.

offshore and onshore domes, mud fluxes and mud volcanos, some of them with historical explosive events and nine human victims to date (Vernette 1989; Duque-Caro 1990; Correa *et al.* 2007). Using radiocarbon dates and the amount of uplift, Page (1983) estimated the rate of late Holocene deformation to be between 2 and 15 mm a^{-1} for the coastal fringe between the Morrosquillo and Urabá gulfs. This serrated (plain view) littoral shows strong historical erosional trends – up to 40 m a^{-1} at the Arboletes sector – and is dominated by emerged marine terraces 2–36 m high limited seaward by vertical to 30° scarps cut on sandstones (hard rocky points) and highly weathered mudstones receding at erosion rates up to 1–2 m a^{-1}, with higher values found along the zones affected by diapiric intrusions and/or human occupation – Galerazamba, Arboletes and Puerto Escondido. Cliff erosion along this coast proceeds in most sectors by natural and man-induced mass movements – rock falls, mud flows, debris flows – that occur mainly in the transition between the dry and wet periods, normally in April (Correa & Vernette 2004; Correa *et al.* 2007). Cliff profiles in this area continue offshore by some isolated small stacks and by a conspicuous rocky gentle sloping surface extending hundreds of metres and covered by thin deposits of muds. The southernmost cliffs of the Colombian Caribbean coastline are found on the NW area of the Urabá Gulf (Fig. 10.11) where coastal configuration is dominated by steep rocky slopes, stacks and small islands cut on *sheared* basalts and sandstones. Diaz *et al.* (2000) also report for this area the occurrence of shallow calcareous submarine terraces extending offshore to maximum depths of 10 m.

Fig. 10.11. Cliffs cut on serpentinite rocks. Cabo de la Vela, Guajira península. Courtesy of Mr Diego Zapata.

Brazil, Venezuela and Uruguay

Brazil

Brazil has the longest coastline on all the South American countires at more than 9200 km. The coast extends in latitude from 4°N to 3°S, with a predominant sedimentary shoreline with long beaches, deltaic plains and estuaries. Tidal amplitude progressively increases from less than 1 m in the south to 5 m in the north, although further north in the Amazon estuary the tide range can be up to 12 m. The north coast facing to the NE is exposed to low-energy waves generated by east and SE trade winds, whereas to the south wave energy increases southward, as this coast is increasingly exposed to swell waves from the South Atlantic (Dominguez 2006; Mueher 2010).

Coastal sectors of hard rocks appears when Precambrian igneous and metamorphic complexes reach the coastline and are exposed to open sea conditions, as happens in the SE, at the foot of the coastal mountains of Serra do Mar and Serra da Mantiqueira. Such areas, as with many other sectors of the Brazilian coasts, have a complex tectonic history that resulted in a horst and graben structure that configures the indented planform, with numerous islands and bays (Dominguez 2006). On Papagaio Island, in the area of Cabo Frio, Skrepnek *et al.* (2009) found typical morphological features of hard rock coasts such as sea caves, blowholes and boulder beaches derived from mass movements. These can be related to wave exposure and the different types of rock of the basement of the island. Most of these features develop on paragneisses and in other areas of weakness as lithological contacts and dykes.

Whereas the rock and cliffed coasts on the crystalline basements are crenulated and located in headlands, the longest extension of cliffed coastal is in the plains composed of Pliocene to Pleistocene deposits of the NE coast (Sugio *et al.* 2011). One of the most important features in the rock and cliffed coasts of Brazil is the Barreiras Formation, that crops out along more than 4000 km of the Brazilian coast from the Amazon to the Rio de Janeiro coast (Fig. 10.12). The formation covers the Precambrian basement and the overlying Cretaceous sandstones and carbonate rocks. The main facies of the formation are alluvial, marine and aeolian sediments that range from the Pleistocene to the Holocene (Bezerra *et al.* 2001). The sediments consist of intercalated layers of sandstone and claystone with conglomerates, and ferruginous cemented layers are common. The Barreiras Formation has been affected by faulting events since the Pliocene that are responsible for the present coastal configuration of the coast.

The strongly dissected uplifted blocks correspond to higher cliffs at the coast, whereas the downfaulted blocks are capped by alluvial and aeolian sediments (Bezerra *et al.* 2001; Furrier *et al.* 2006), and in some places by raised marine terraces formed during late Pleistocene transgressions with ages from 220 ± 2 to 110 ± 10 ka BP (Barreto *et al.* 2002). The elevation of the Pleistocene marine terraces suggests that northeastern Brazil has been subjected to differential subsidence and uplift in the late Quaternary.

The existence of a sea level between 2.5 and 4 m higher than today around 5000 cal. years BP (Bezerra *et al.* 2003; Angulo *et al.* 2006) eroded the Pliocene–Pleistocene sediments, forming cliffs that in many places remained abandoned with the late Holocene regression and the formation of modern sedimentary systems. Another highstand occurred around 2100 yr BP, causing a new episode of coastal erosion.

The cliffs in the Barreiras Formation alternate between areas where they are stable and areas of active retreat, with different modes of failure being evident. Santos *et al.* (2006, 2011) investigated the mechanisms of cliff retreat in the Barreiras Formation in the State of Rio Grande do Norte. They found that the different geotechnical properties of the sediment layers, the occurrence of protective features such as the width of the fronting beach and

Fig. 10.12. Coastal sectors where the Formation Barreiras crop out.

episodes of heavy rainfall are the main factors that control the retreat. The height of the cliff ranges between 10 and 40 m, with mean slopes between 20 and 60°, and cliffs are being eroded by falls of blocks, toppling and sliding that form debris talus at the base of the cliff. The most common mechanism is rock fall from the mid and upper parts of the cliff, because of the pressure exerted by the penetration of water into vertical tensional cracks at the top. The beaches fronting the cliffs range in width from 5 to 15 m, and the boulder accumulations at the cliff foot act as protective features; when this feature is absent, basal undercutting of the cliffs can be observed. Episodes of instability in these cliffs are mainly associated with heavy rainfall events, therefore affecting both active cliffs under wave attack and inactive cliffs not reached by waves (Furrier *et al.* 2006; Santos *et al.* 2006, 2011).

Another important feature along many stretches of the northeastern coast of Brazil is extensive beachrock ledges, located at the present intertidal zone that protects the coastline against the wave action. Beachrock ledges are commonly gently seaward-dipping, although when they are eroded the seaward edge is more abrupt, ranging in thickness from a few centimetres to 3 m, and in width from 2 to 50 m (Arai 2006; Vieira & Ros 2006; Irion *et al*. 2012). The age of the beachrock ranges from 7460 to 110 cal. years BP (Bezerra *et al.* 2003), although these ages can only be regarded as the maximum age for cementation, given that the time lapse between the deposition of a beach sediment and its subsequent cementation is still controversial (Vieira & Ros 2006). The beachrocks are conglomerates cemented by calcium carbonate and by limonite, the latter from the ferruginous sediments of the Barreira Formation (Irion *et al.* 2012). Several sedimentary facies are massive conglomerates; low-angle stratified conglomerate and sandstone, bioturbated conglomeratic sandstone and massive sandstone suggest that they were deposited

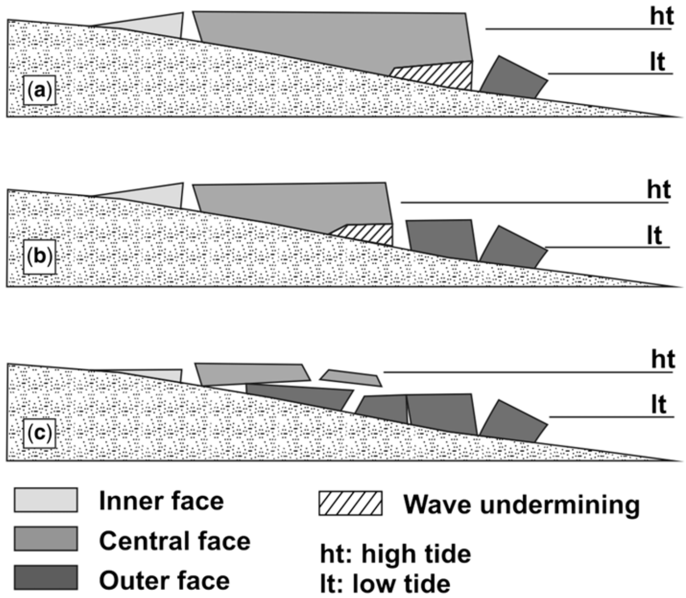

Fig. 10.13. Evolution model for the beachrocks. Undermining by waves (**a**), block detachment in the outer face (**b**) and breaking of the main body (**c**) (from Amaral & Bezerra 2006).

mainly in the upper shoreface zone (Vieira & Ros 2006). Although the occurrence of solution features in the upper face of the beachrock ais common (Vieira & Ros 2006), the most severe erosional processes occur at the high tide level.

Amaral & Bezerra (2006) used aerial photography and field mapping to study the mechanism of fracturing and erosion in beachrock, dated at 5310–4380 cal. years BP in the state of Rio Grande do Norte, 40 km to the south of Natal city. The beachrock is fractured by longitudinal joints parallel to the sedimentary bedding and trending north–south, and by an orthogonal joint set running east–west. Beachrock fracturing starts when waves erode the sandy basement of the beachrock, and the development of joints by the accommodation of the unconsolidated basement. The seaward part of the beachrock collapses and three areas can be identified (Fig. 10.13): a central face apparently unmoved, an inner face at the landward side, and an outer face at the seaside, where the undermining is more intense and most fracturing and erosion occur. The outer face acts as a protective feature for the beach, but when the central face also breaks, the beachrock is segmented, allowing waves to access the sandy beach.

Irion *et al.* (2012) present a model of beachrock construction in the coast of the state of Ceará, in which the spring tidal range of about 3.7 m is considered a main factor. During neap tide freshwater from the slopes of the Precambrian cliffs at the back is supplied, giving the conditions for carbonate cementation and the formation of a beachrock in the beach surface. When sea level rises, the beachrock is eroded because the underlying sands are washed, dislocating the cemented sediments, and new beachrock forms in the upper tidal zone.

Venezuela

The geology and topography of the coast of Venezuela are closely related to the contact of the Nazca, Caribe and South American tectonic plates. The north of Venezuela lies between the South American and Caribbean plates, whereas the western part of Venezuela has a more complex setting. The wave regime is moderate, with waves dominantly from the east and NE. Tide range is small, only exceeding 0.5 m in spring tides (Ellenberg 2010). The east coast of Venezuela corresponds to the western section of the sediments of the Orinoco delta. The swampy fluvial sediments change at the peninsulas of Parias and Araya, where the east end of the Cordillera de la Costa falls to the shoreline in steep and densely vegetated cliffs developed in strongly folded metamorphic rocks; these cliffs are interrupted by sandy beaches. The Gulf of Cariaco is closed in the north by the Peninsula of Araya, which is composed of Mesozoic schists, and by the deformed Cretaceous limestones of the Eastern Interior Range in the south. The geology and the topography of both the exposed north coasts of both Peninsulas and the more protected coastline of the Gulf of Cariaco are strongly controlled by the active system of the Cariaco and Pilar faults. The area is seismically active and has been affected by earthquakes generated by the El Pilar Fault, the last in 1997 with a magnitude of 6.9 (Van Daele *et al.* 2011).

The coast between Cariaco Gulf and Cordera Cape becomes low and with active sedimentation, with barriers, lagoons and mangroves. In Codera Cape the Cordillera de la Costa runs close to the sea, developing a steep cliffed coast, with several narrow plains at the foot. The cliffs are modelled on deformed and faulted metamorphic and intrusive rocks, and along the coast there is a discontinuous strip of Quaternary sandstones and conglomerates. To the west the coast alternates between cliffed headlands and small bays with beaches and mangroves. In Puerto Cabello the coast changes its orientation and runs northward and NW. The rock coast alternates between gentle and steep cliffs eroded in Cenozoic formations, with more frequent and effective erosive processes at the foot.

The Peninsula of Paraguaná (Fig. 10.14) is the last significat rock coast before the wide sedimentary coast of the Gulf of Venezuela. The peninsula was linked to the mainland by the Itsmo de Médanos during the Holocene. The east side of the isthmus is fringed by a long beach and protected by a beach rock. The peninsula is composed of Cenozoic limestone, with an exposed east coast with low cliffs and beaches.

On the more protected western coast, in the southern section between Punta Cardón and Punta Salinas are cliffs up to 20 m high cut in the Pliocene Paraguaná Formation, and there are lower cliffs eroded in fossil coral reefs. The cliffs are active and are being eroded between Punta Cardón and Astinave, whereas the cliffs between Astinave and Punta Salinas extended for 6 km and are abandoned and protected by a subhorizontal marine terrace. The terrace and the inactive cliffs are contemporary and are separated from wave action by a mud flat and the present sand barrier (Audemard 1996, 2001). In Punta Chaure, in the NW of the Peninsula of Paraguaná there is an area of 0.5 km with receding cliffs 3 m high cut in the Paraguaná Formation. The receding cliffs near the NE point are eroded in calcareous sandstones with a thickness between 0.23 and 1.5 m, identified as aeolianites, probably of Pleistocene age, although they have not been dated (Lara & González 2006). The aeolianites are affected by faults supposed to be of Quaternary age. Today the aeolianite cliffs are being undercut by waves, causing collapse, and they are also being eroded by dissolution processes developing a karst morphology with holes of up 1.5 m depth (Lara & González 2006). The coastal morphology of the Paraguaná Peninsula has been controlled in part by a slow tectonic uplift that was active until the middle Pleistocene with tectonic activity during the late Pleistocene and Holocene (Audemard 1996). Evidence of the slow uplifting has been also found in the islands of Aruba, Bonaire and Curaçao, where five groups of coral reef terraces range in elevation from 10 to 150 m (Hippolyte & Mann 2011).

Uruguay

The coast of Uruguay can be divided in two sectors: the first corresponds to the inner and outer estuary of the Rio de la Plata with 478 km of shoreline, and the second to the open ocean Atlantic coast with 236 km of coast (Goso *et al.* 2009). The Atlantic

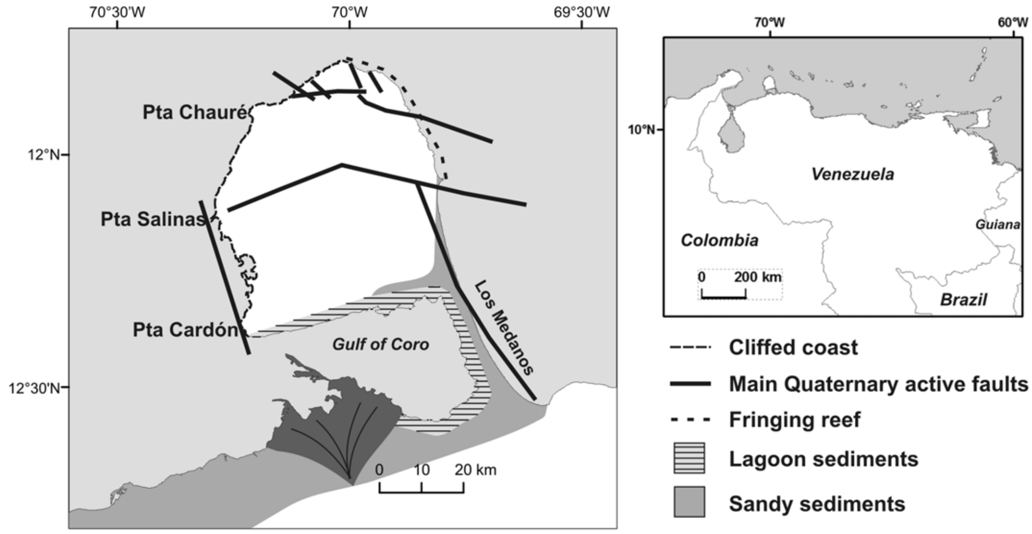

Fig. 10.14. Main faults and environments of the Peninsula of Paraguaná (from Audemard 2001 and Ellenberg 2010).

coast is exposed to swell waves from the SE and only the mouth of the Rio de la Plata receives waves from the SW. Wave energy increase to the north in part because of the shallow depths of the mouth river and the epicontinental sea (López-Laborde 2003; Bird 2010). It is a microtidal coast with a spring tidal range less than 0.5 m, although it increases inside the estuary up to 3.7 m in the compartment of Colonia.

The crystalline basement rock is composed of metamorphic and igneous rocks, and it mainly crops out on the coast of Montevideo and Canelones, whereas the most of the geology of the coast is composed of sedimentary formations deposited from the Miocene to the Holocene. The sediments have been eroded, forming cliffs, sometimes abandoned and not affected by waves, but in many places cliffs show active retreat. This type of cliffed coast has been named *Barrancas*, in the geomorphological literature, a local name that defines steep cliffs with incised gullies. The Cenozoic sediments comprise several continental and marine formations deposited from the Oligocene to the Holocene with varying facies from dominantly clay and sands to conglomerates, with different degrees of cementation and consolidation. This ares is the most affected by erosive processes, namely in the compartments of Colonia, San Jose and Canelones (Defeo *et al.* 2008). The sedimentary cliffs are eroded by mass movements and toppling caused directly by wave action but also by continental runoff forming deep gullies, or possibly by oscillations of the freatic layer. The more cohesive layers are more resistant to erosion and can develop subhorizontal platforms at the base of the cliffs, whereas the less consolidated sediments of the late Pleistocene and Holocene sediments collapse. The rate of cliff retreat has been estimated between 50 and 100 cm a^{-1}, although in the compartment of Canelones a maximum retreat of 2 m a^{-1} has been reported (Goso 2009; Goso *et al.* 2009).

In the compartments of Montevideo and Canelones the planform of the coast is controlled by the metamorphic (gneisses, schists, quartzites and conglomerates) and igneous rocks, forming embayments with sand beaches and dune complex separated by rock points with low cliffs and shore platforms with an irregular topography. In Canelones the coast shows an indented configuration resulting from the trend of the faulting of the basement, again with hard rock headlands and islands with low cliffs and shore platforms, where mechanical erosion is less effective and the dominant process is weathering.

Argentina

The coast of Argentina extends for 5700 km, covering a large difference in latitude. Waves arrive from the south, SE and SE, the north coast being mainly affected by swell waves and the south Patagonian and Tierra de Fuego by storm waves. Tide range decrease from a macro-tidal range of up to 10 m on the Patagonian coast to a micro-tidal range of 1 m in the area of Buenos Aires. The north coast of Argentina between the Rio de la Plata estuary and the Rio Colorado is in general low-lying, with sandy and gravel beaches and tidal flats alternating with cliffs cut in Pliocene and Pleistocene sediments but also in hard Palaeozoic rocks. To the south, on the Patagonian coast, rock and cliffed sectors are more frequent.

Patagonian coast

Many coastal areas of Argentinean Patagonia are characterized by rock shores that emerge as a relevant morphological feature of this area, bracketing long tracts of littoral plains built by sets of beach ridges separated by coastal lagoons (*salitrales*). High cliffs, sometimes more than 80 m high, are fronted by intertidal shore platforms; the platforms are frequently wider than a few tens of metres. Mixed gravel beaches are sometimes developed on top of the platforms. In some cases notches are carved at the base of cliffs. Ramps, marine caves, stacks and arches are quite rare features along the coastline of Argentinean Patagonia (Isla & Bujaleski 2008), owing to the massive character of the bedrock.

The morphological setting of his area is determined by its geological conditions, its climate and the particular meteorology and marine environment that characterizes it. The coastline is developed along the edge of the ancient basement of the south American craton, shaped in the form of tablelands locally called '*mesetas*', gently degrading from the Andes foothills through steps, coinciding with structural scarps, towards the sea. It is thus a typical passive margin, moderately but constantly uplifting throughout the Cenozoic. Uplift rates have been estimated for the Pleistocene in the order of 0.1 m ka^{-1} (Schellmann 1998).

For this reason the coastline has kept a similar position to the present at least during the Pleistocene, so that cliffs and platforms that developed are now raised and arranged in a staircase. Sediment-filled bays and drowned fluvial valleys occur in the lowlands.

From a geological point of view the coastal belt of Argentinean Patagonia belongs, from north to south, to: (a) the Northern Patagonian Tablelands, formed by Paleocene marine and continental sedimentary rocks, covered by Eocene–Oligocene pyroclastic rocks and Eocene to Miocene basaltic flows and necks (Ramos 1999); these rock types are exposed along the San Jorge Gulf; (b) the Deseado Massif (Leanza 1958), cropping out between the Deseado and Chico rivers, in Santa Cruz Province, formed by

Palaeozoic phyllites and schists intruded by granitoids and overlapped by continental and marine sedimentary rocks interbedded with volcanic sequences developed during the Mesozoic and the Cenozoic; and (c) the Southern Patagonian Tablelands (Ramos 1999) corresponding to Mesozoic and Cenozoic marine and continental sedimentary rocks.

Since the pioneering works of d'Orbigny (1834–1847), Darwin (1846) and Feruglio (1950), Pleistocene shorelines have been recognized in the form of at least five different levels of raised marine terraces between 6 and 185 m above present sea-level. For this reason the study of Patagonian coastal features has meant basically the study of the littoral deposits. These deposits are generally represented by series of storm beach-ridges and provide highly fossiliferous marine strata, with abundant shell concentrations that are useful as palaeoenvironmental tools (Aguirre 2003; Aguirre *et al.* 2005, 2011). Several studies have exploited the shell layers to date the littoral deposits and to try to reconstruct sea-level changes of the Atlantic coast of Patagonia (Rutter *et al.* 1989; Codignotto *et al.* 1992; Rostami *et al.* 2000; Schellman & Radtke 2003; Ribolini *et al.* 2011; Pedoja *et al.* 2011*b*; Isola *et al.* 2012; Zanchetta *et al.* 2012).

The most recent of these works (Pedoja *et al.* 2011*b*; Ribolini *et al.* 2011) have approached the study of erosional sea-level markers in the rocky tracts of the littoral, focusing therefore on their modern counterparts to state their relationship with sea level. In this framework the very first quantitative observations on Patagonia's rock coasts have started.

Apart from geological contingency the other two very important factors controlling the features of landforms forming along rock shores of Patagonian Argentina are climate and marine conditions. Climatic conditions (Coronato *et al.* 2008) are typical of mid-latitude cold semi-arid regions (BSk climate, according to Köppen climate classification), with an annual average temperature of around 13 °C (temperature range between extreme seasons of *c.* 10 °C) and rainfall not exceeding 300 mm, clustered during the summer (http://www.smn.gov.ar). Westerly air flows are dominant and strong gusts are frequent. Concerning the present modelling agents, thus, wind is dominant in most of the region, creating a peculiar landscape with abundant deflation features. Water runoff is constrained to winter and sediment discharge by rivers is poor.

The Atlantic coast of Patagonia is characterized by a semidiurnal macro-tidal cycle with a tidal range of 5–6 m. Tide effects increase inside gulfs and embayments. In addition, this tract of South American coast is an energetic environment characterized by oceanic waves, so that marine erosion is dominant along the coast. These environmental factors strongly affect the processes responsible for shaping the coastline. Rocky morphologies are thus concentrated on wave-exposed headlands, but are not exclusive to them.

Rocky shores are densely populated by many types of marine biota, the bioerosive/bioprotective role of which deserves to be investigated. Extensive beds of the mussel *Perumytilus purpuratus* are widespread, and cover 95% of the rock from the low to the extreme high intertidal (Bertness *et al.* 2006). Bare space is rare in spite of the strong wave forces in these habitats and the potential for wave-induced disturbance. *Perumytilus* mussel beds serve as critical foundation species or ecosystem engineers by providing protection from desiccation and wave-stress dislodgement to the wide variety of mobile (e.g. limpets, starfish, chitons and crabs) and sessile (e.g. barnacles) organisms that live within the mussel bed matrix.

Those tracts of Chubut and Santa Cruz provinces where rocky shores are currently under investigation (Pappalardo *et al.* 2012) are shown in Figure 10.15.

Active and raised abrasive notches have been found in different parts of the San Jorge Gulf (44–47°S), in particular in the Bahía Bustamante and Deseado areas. The efficiency of abrasion as a genetic process (Pirazzoli 1986; Trenhaile *et al.* 1998) is suggested

Fig. 10.15. General view of the Chubut and Santa Cruz provinces coastline. The rocky tracts are highlighted.

by the polished surface of the rock at the retreat point (Fig. 10.16) and the presence of a shore platform seaward of the notch covered by a thin veneer of sand and gravel transported by the littoral drift. A test was carried out in the Deseado area to assess relationship between sea level and morphometric parameters using a sample of 11 notches. A digital 3D method of surveying and analysis of notch features supported the traditional field methods (Favalli *et al.* 2012). This test showed a strong link between the elevation of retreat point of those notches that are currently being shaped by abrasion processes relative to medium high tide level. In fact, among the notches sampled, two clusters were identified, characterized by different elevations. The lower one approximates the medium level of high tide with a variability of elevation values within a range of ± 0.3 m. The higher exceeds the lower one by about 1.5 m in elevation and displays a variability of elevation values within the range of ± 0.2 m. The lower notches were interpreted as active owing to direct observation of water level reaching the retreat point during high tide but also evidence of biological zonation and coherence with morphological markers of high tide (Dickinson 2001; Kelletat 2005). The higher notches, instead, were interpreted as markers of raised Holocene shorelines.

Much less evidence has been collected so far for shore platforms at this site, although they are widespread in the area. Intertidal platforms can be observed especially along rocky headlands at Punta Tombo in northern Chubut, and at Cabo Dos Bahias between the well-known localities of Camarones and Bustamante, on the two peninsulas of Gravina and Aristizabal south of the Bustamante Village, at Punta Marques and Punta Delgada in the central part of San Jorge Gulf and Cabo Blanco at its southernmost edge. No specific study is available on the processes operating on these shore platforms. Abrasion is apparently the most effective shaping agent, as suggested by the presence of rockpools that can be observed at low tide. In Figure 10.17 the same holes

Fig. 10.16. Active abrasive notch in the Puerto Deseado area.

carved currently in the intertidal platform can be observed in a raised step backing the platform and provide evidence of the persistence of processes responsible for shore platforms development throughout at least the Upper Holocene.

Bioerosion and/or bioprotection should also be considered as possible effective processes in the current development of these shore platforms. Different categories of rocky shore organisms populate the study area such as algae, mussels, barnacles, limpets and chitons. Previous studies (Bertness *et al.* 2006; Silliman *et al.* 2011) showed that Patagonian rocky shore communities are exposed to unusually harsh physical conditions and consequently are more strongly organized by physical stress than rocky intertidal communities studied elsewhere.

A peculiar morphology characterizes coastline in the Puerto Deseado area. The harder rocks of the Deseado Massif form an irregular coast of capes, with cliffs and shore platforms. Northeast of Puerto Deseado village is characterized by two small promontories (Punta Cavedish and Punta Foca), embracing a pocket gravel beach. The most evident feature of this area is the presence of three well-defined steps of coastal aggradation. A small cave carved by marine action in the volcanic rocks (named Cueva del Indio) is characterized by the presence of a wonderfully preserved erosional notch located at an altitude of *c.* 6 m above high tide. A further spectacular cave with an erosional notch (named Cueva del Leon) is preserved close to the Punta Foca (Fig. 10.18). The elevation of the notch at Cueva del Leon allows for a confident correlation with the notch at the nearby Cueva del Indio cave.

South of the village of Puerto Deseado the coastline indentation forms a wide *ria*, corresponding to the mouth of the Deseado River. Invaded by the sea during high tides, the ria is bordered by cliffs, frequently mantled by Cormorant guano, that

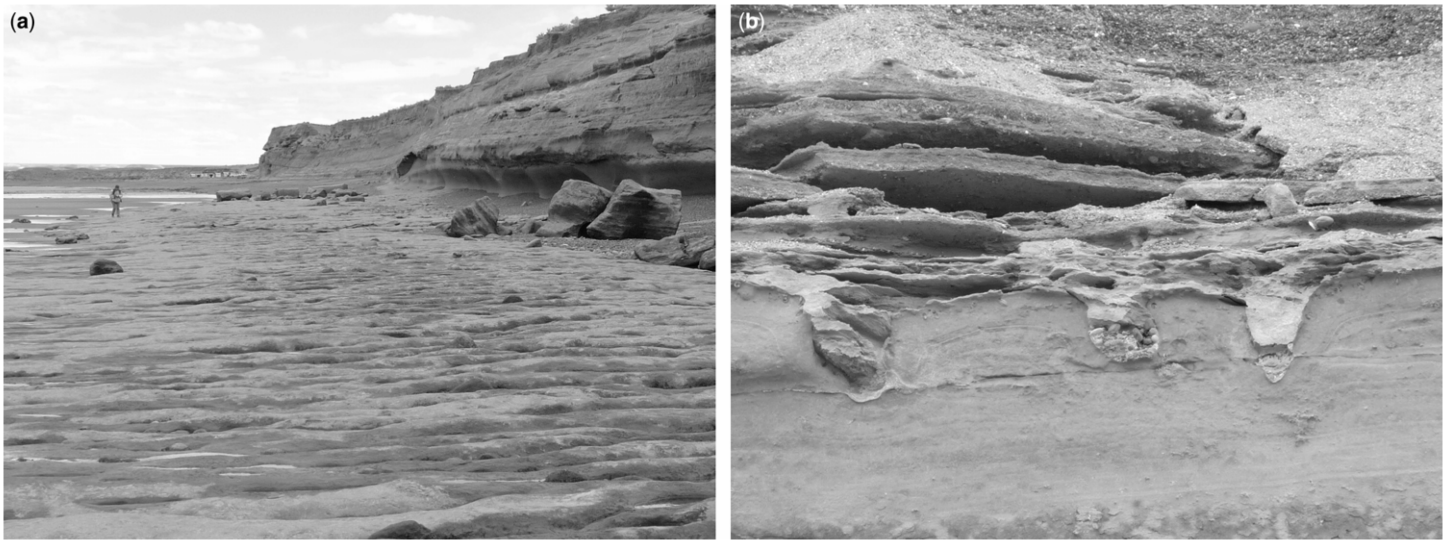

Fig. 10.17. Active (**a**) and raised (**b**) shore platforms in the Caleta Olivia area.

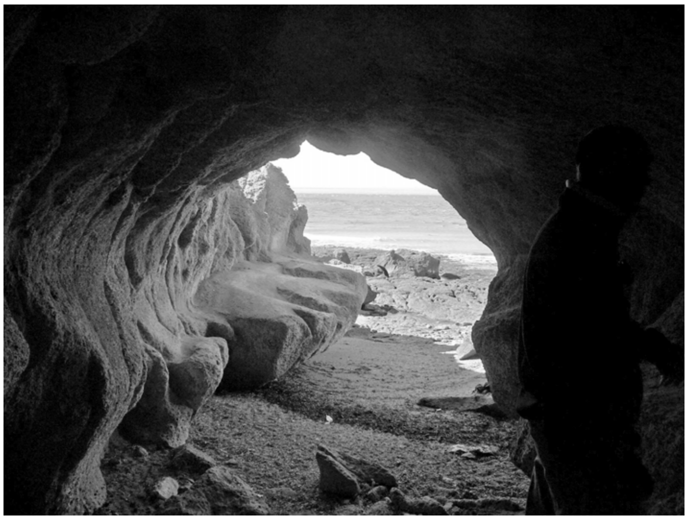

Fig. 10.18. Raised abrasive notch in a marine cave (Cueva del Leon, Puerto Deseado area).

forms stalactites (Fig. 10.19). At low tide conditions muddy tidal flats border the cliff foot.

Chile

The long coast of Chile extends about 6400 km. The tidal range increases southward from 1.5 m at Arica to 2 m near the southern end close to Cape Horn, although it reaches 5.8 m in the Gulf of Corcovado (Fig. 10.1). It is exposed to swell waves from the SW and to westerly storms waves at the south end. The desertic northern coast of Chile, between the border with Peru and the Peninsula Mejillones is characterized by the proximity of the mountain reliefs of the Great Coastal Cliff, alternating areas with cliffs cutted in the Palaeozoic rocks and areas where cliffs are eroded in Cenozoic sandstones (Quezada *et al.* 2010). The cliffs are usually fronted by transgressive dunes and with protruding headlands of hard rocks (Araya-Vergara 2010). Complex formations of marine sandstones and mudstones crop out forming bluffs near Hornitos (Hartley *et al.* 2001). On some prominent coastal features such as the Peninsula Mejillones there are high cliffs sculpted in hard Palaeozoic rocks but also in Miocene to Pleistocene thick regressive sedimentary formations of sandstones, mudstones and conglomerates severely affected by tectonic uplift (Di Celma & Cantalamessa 2007). Southward of the mouth of Copiapo river the coast is dominated by sand beaches and dunes with rock outcrops forming cliffs and shore platforms, but the Miocene sediments still crops out forming bluffs to the south of Valparaíso (Fig. 10.1). The coast passes to a more indented planform with rias formed by the submergence of river valleys incised into the schists rocks of the coastal mountains (Araya-Vergara 2010). In the south of Chile the coasts of Magellan Strait and Patagonia consist of fiords where the imprint of the last glaciation influences the coastal landforms, and where the rock coasts are modelled mainly in Palaeozoic and Jurassic and Cretaceous plutonic and metamorphic hard rocks.

Shore platforms and significance of sea arches in northern and central regions of Chile

Evolution of shore platforms

Figure 10.20 A shows the key features of high-tide platforms, which remain as subaerial landforms during high tide. As key elements, these platforms are interrupted by swash corridors associated with linear joint systems and enlarged circular potholes (Fig. 10.20b), which follow the joint direction and the points of joint crossing. If the corridors are very wide, only remnants of the high platform can be observed. Moreover, these corridors are frequently dissected and in their wide bottom appear lower platforms, which become a seaward-sloping (intertidal) or a low-tide platform. The seaward-sloping (intertidal) system operates between the high tide level and below low spring tide level.

Fig. 10.19. The Deseado *ria* at high tide. Cormorant colonies build their nests on the cliff face, mantling the rock surface with their guano.

Fig. 10.20. Left: Pichidangui (32°10′S): high-tide platform and swash corridors induced by joints in crystalline rocks. Right: Figure 10.2. Iquique (20°15′S): high-tide platform; swash corridor induced by joints and potholes following their direction in volcanic rocks.

In exchange, the low-tide platform is the step that remains subaerial during low tide. These levels can be interrupted by new swash corridors (Fig. 10.23, evolutionary stages 3 and 4, complementary profiles). These sets of features have been observed in volcanic rocks in northern regions, in crystalline rocks in the central part and in schists in the south-central region of Chile. The best examples appear in volcanic and crystalline rocks. The transformation of the progressively widened swash corridors into well-developed platforms is deduced in Arica, northern extreme of Chile (Fig. 10.21). Here, two high-tide platforms are observed. The higher one is expressed as lapies in hard rocks (type fairly common in many coasts) and is interrupted by old swash corridors. The lower one is very wide and flat and its height is correlative with that of the old swash corridors. This fact suggests that the low high-tide platform is an uplifted low-tide or intertidal swash-generated platform. In exchange, the lapies in the higher platform seems older than this lapse of uplift.

Figure 10.22 shows the key features of the low-tide platform, observed where the high-tide platform is absent. As key elements, these steps – which remain sub aerial during low tide – are very flat and commonly humid. A set of crossed joints is visible in the smooth surface. Embryonic, mini and widened potholes are observed in the points of joint crossing. The widened potholes are principally circular and contain gravels and sand in their bottom, which suggests that these features are produced by eddies of swash set up and set down, armed with trapped gravels and sand. Towards the edge of the platform appear embryonic swash corridors induced by the direction of principal joints. These sets of features are observed in sandstones and meta-sandstones in central Chile.

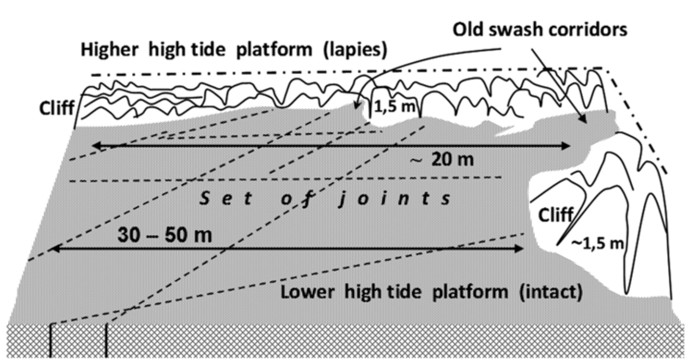

Fig. 10.21. Arica (18°30′ S). Block diagram showing two levels of high-tide platform. The correlative altitude between the old swash corridors and the intact lower high-tide platform suggests that this has been produced by widening of corridors and subsequently uplifted. See model in Figure 10.22, stage 4.

Detailed observations of platforms allow an evolutionary model to be proposed (Fig. 10.23). It is based on the increasing dissection at the same time as appear the stages of a high-tide platform, the processes of dissection with generation of new platforms, the lack of direct wave activity in the elevated high-tide platform and the previous observations of regional coastal uplift in the Chilean shoreline. In addition to observations in Chile, other workers identified factors that support the proposed model. They include the influence of deeply weathered igneous and metamorphic rocks (Blanco Chao *et al.* 2003), differences in joint spacing and persistence of discontinuities related to rock resistance (Kennedy 2010; Naylor & Stephenson 2010), interaction between waves and morphology (Marshall & Stephenson 2011) and evolution in rapidly uplifting coasts (Kennedy & Beban 2005).

Significance of natural arches

Until now, there has been a lack of specific descriptive terminology for the different elements of natural coastal arches. In order to establish types, according to their relative placing with respect to tide states, the following terms are proposed, keeping in mind the accepted names of arch elements used in architecture. Therefore, *intrados* is the inside curve or wall of the arch which defines the form of the tunnel (Fig. 10.24), *impost* is the rocky surface supporting the arch, which defines the tunnel bottom; *rise* is the height of the tunnel, and *span*, the width of the tunnel bottom at the impost level (Fig. 10.24). Different levels of impost show a sequence of continually active imposts and tunnels up to intermittent, episodic dormant or inactive imposts and tunnels. The example of plunging impost and span (Fig. 10.24) indicates a tunnel whose impost is permanently submerged and the rise is conjectural. In spite of the permanent work of the waves, the hardness of the granitic rock makes difficult a rapid enlargement of the span. In the case of intertidal impost and span, the arch has been elaborated in soft sandstones (Fig. 10.24); the subaerial exposition of the elements is rhythmically submitted to the tide states. During the high tide, the work of the waves is important because of the low rock strength, expressed both by the wider span and the high separation of the intrados walls in the upper part of the tunnel, which also suggest a present growth of the rise. In the example of low-tide impost and span (Fig. 10.24), the waves work these elements only during the high tide, but the hardness of the granitic rock makes difficult a rapid change of the impost, the span, the rise and the form of the intrados. Finally, in the case of high-tide impost and span (Fig. 10.24), the tunnel has been stabilized with regard to the marine activity. Therefore, it is observed that the degree of

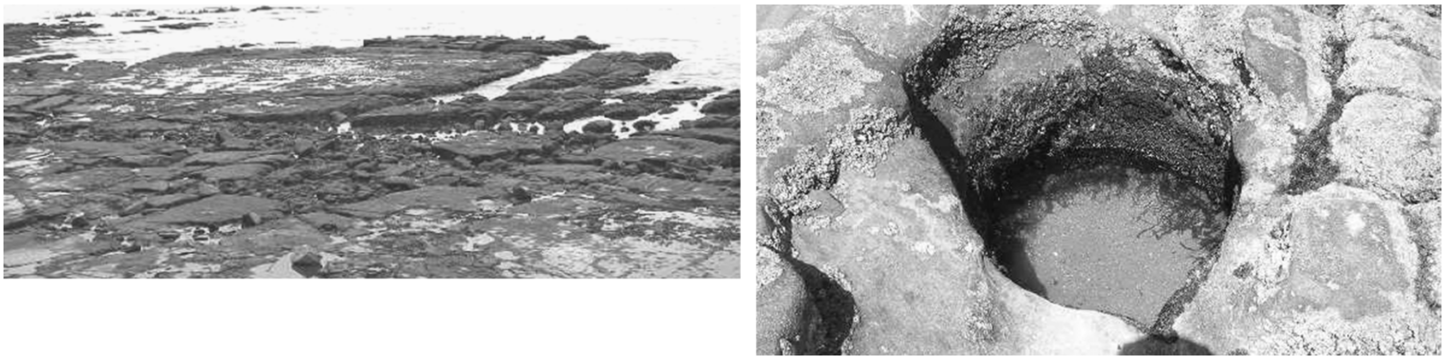

Fig. 10.22. Dichato (36°30′S): left, low-tide platform, joints and incipient corridors; right, pothole and joint crossing.

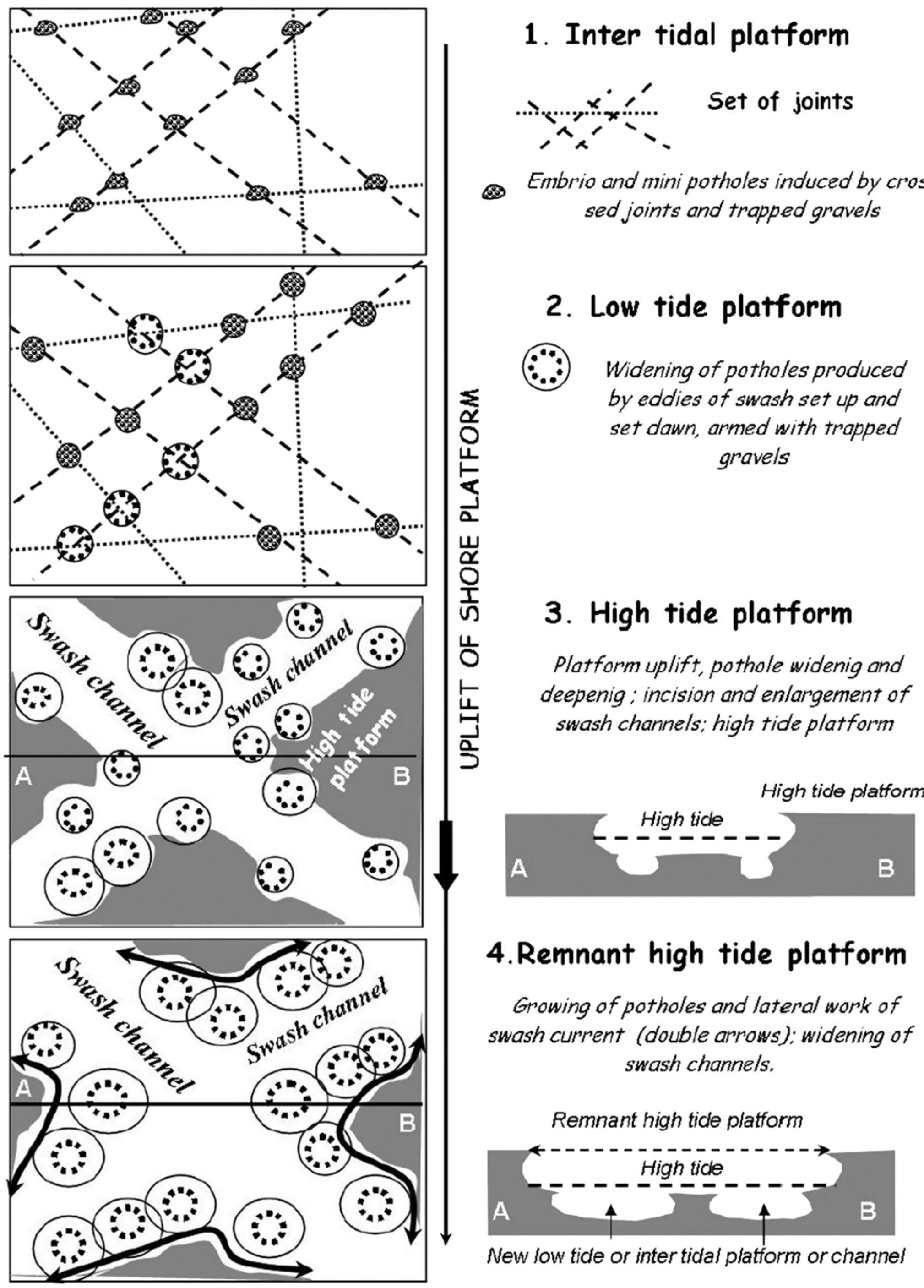

Fig. 10.23. Evolutive model of shore platform in northern and central Chile. The states in the moments 1–4 are thought to have been reached if a condition of platform uplift is accomplished.

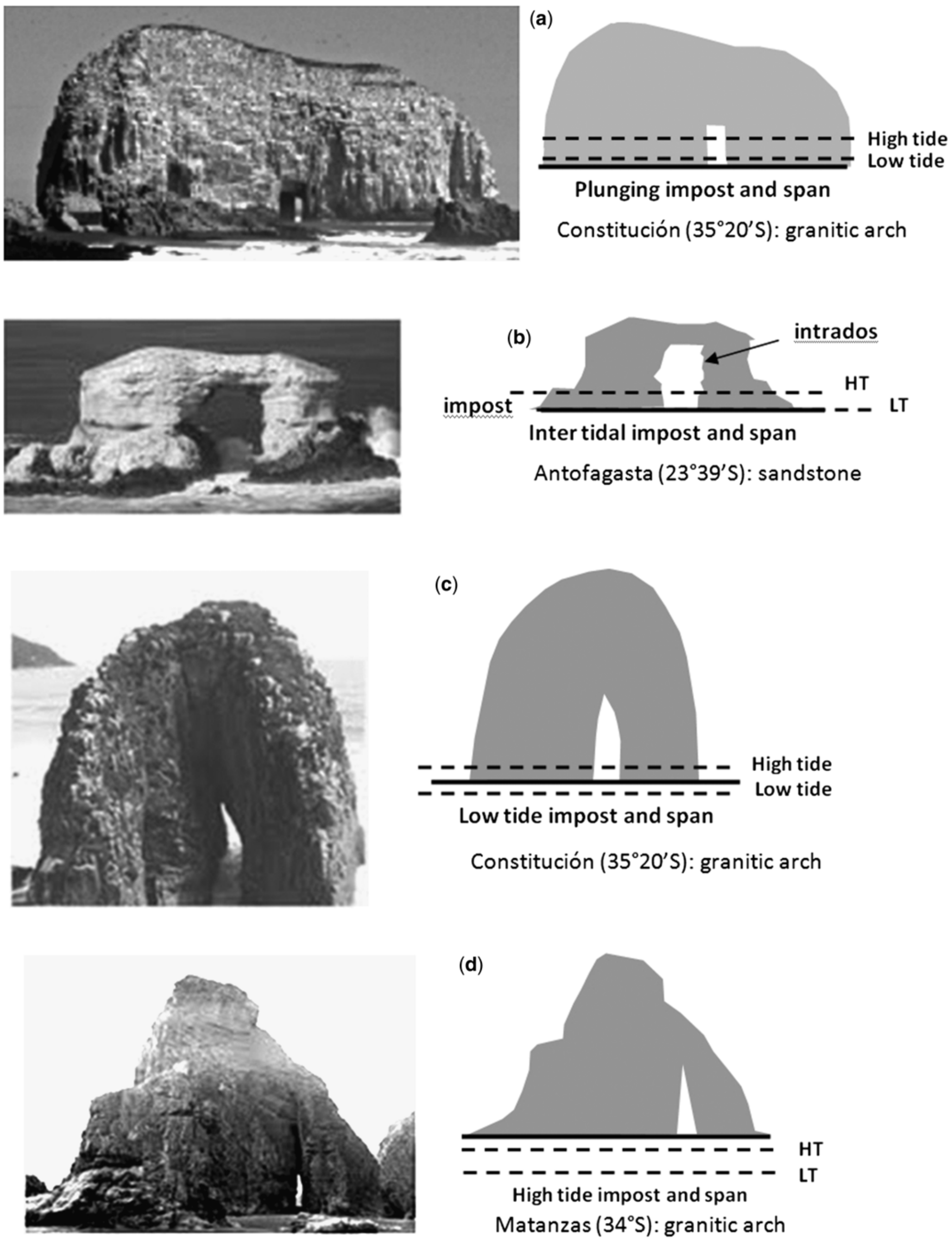

Fig. 10.24. Types of arch, according to the placement of their impost and span with respect to the tidal states.

transformation in the evolution of the active tunnels is related to the rock hardness. In sandstones the changes are relatively rapid. In hard rocks, the transformations in the tunnel elements are not perceptible for different levels of impost. The lack of rapid change can be related to the interference of tectonically controlled uplifts. For instance, Figure 10.25 indicates the tectonic control in the individualization of granitic arches and stacks, as evidenced by the lineament of two arches and one stack. A fault separates the seaward arch of plunging impost with respect to the stack and the landward arch of the high-tide impost.

These results can be compared with previous works carried out on recent uplifted coastlines, where the elements of arches show that they were formed partly as a result of exposure of an irregular coastline owing to recent block fault uplift (Shepard & Kuhn 1983). Overall attention has been directed to the dissection along prominent joint planes, parallel joint sets and the association between arches and stacks (Trenhaile *et al.* 1998).

As a general deduction, the compared observation of types of platform and arch impost placing in the Chilean coast indicates a possible synchronous operation in the morphogenesis of platforms and arches in an uplifted coastline.

Peru

The arid coast of Peru extends over 2300 km. Along the northern coast the main cliffed sections are cut into uplifted Plioceno and Pleistocene marine terraces capped by Quaternary sediments, locally named *tablazos*, which are incised by traverse valleys (Taype-Ramos & Bird 2010). Rock cliffs appear on the peninsulas of Paita and Illescas and in Punta Agula (Fig. 10.1). Further south between Chiclayo and Trujillo (Fig. 10.1), the Andean foothills approach and intersect the coastline, with cliffs cut in mesozoic rocks and granites. South of Chimbote the coast is more indented and hilly, with cliffs and shore platforms developed in volcanic rocks. The cliffed coast continues along the Peninsula of Ferrol, and near Huamey. The coast is exposed to swell from the SW, and the tide range is microtidal, with less than 1 m, increasing

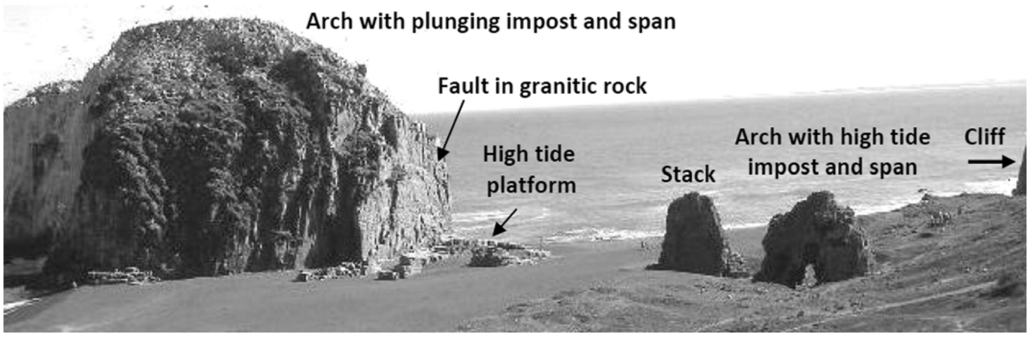

Fig. 10.25. Constitución (35°20′S): linear placing of granitic arches, stack and platform, indicating their tectonic relation and faulting operation in their disgregation.

northwards to the Gulf of Guayaquil. The cliffs of the Peruvian coast have been developed on sedimentary formations of Miocene and Quaternary age. These sediments, composed of marine, fluvial and alluvial sediments, were commonly affected by tectonic uplift.

Overall view of the sedimentology and geomorphology in the coastal area of Lima

Along Lima province on the central coast of Peru can be found many different landforms related to aeolian, marine, estuarine, fluvial and alluvial fan environments that are well seen through several sedimentary deposits that crop out along the Pacific Ocean and the western area of the Peruvian Andes representing the actual topographic surface that covers the lower areas from west to east, the coastal line and the coastal plain. This segment and sediment into it are attributed to the Quaternary (Macharé 1981; Palacios *et al.* 1992; Aleman *et al.* 2006) and Miocene (Noble *et al.* 2009). Those elements show stratigraphic features in field as a result of sedimentary and tectonic processes that affected the regional stratigraphy of Lima that ranges between Upper Jurasic and Upper Cretaceous (Palacios *et al.* 1992). To reconstruct the stratigraphy and genesis of these landforms, sedimentary data were sampled along the coast line of the province of Lima (Fig. 10.26).

The main sedimentary facies correspond to a large alluvial fan related to fluvial activity on Lima uptown and surroundings made by Rimac River, whose type of sediment is clearly defined by the NW–SE Costa Verde Cliffs. Stratigraphic and sedimentological surveys have been carried out by Le Roux *et al.* (2000), Guzmán *et al.* (1997) and Ayala & Macharé (2011), who identified bars of gravel and sand which are facing a small beach line as well as the Pacific Ocean with heights up to 50 m. Northwards, The Pativilca River forms large terraces at its mouth, composed of estuarine and fluvial facies. Here, at least three main levels of terraces can be observed from digital elevation models, showing slight

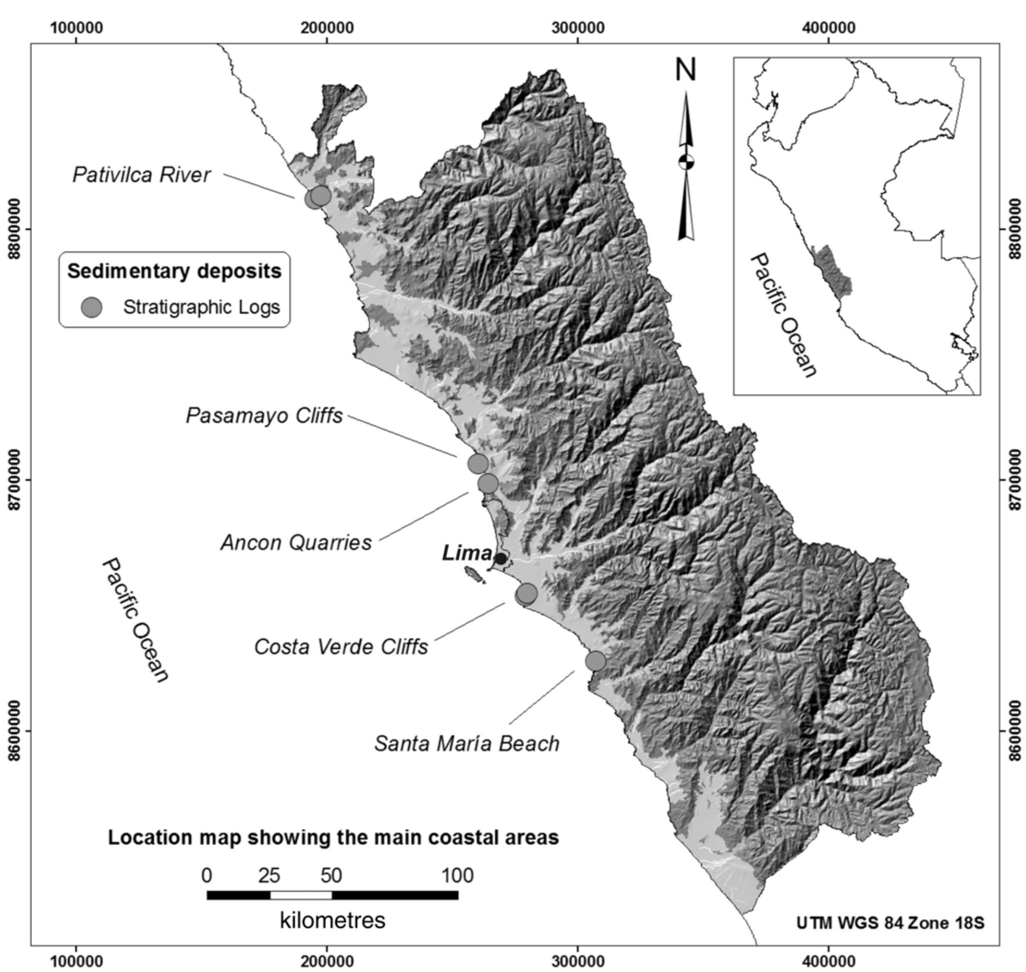

Fig. 10.26. Digital elevation model of the province of Lima. The five major areas of interest are indicated with arrows to the left; they are located along the Lima coastal line and coastal area (grey hatched).

Fig. 10.27. View of the cliffs located in Pasamayo towards to NW from the Lima capital. (**a**) The eolian deposits which covers the consolidated basement below. (**b**) Consolidated basement composed of the rocks from Morro Solar Group (sandstones); see the respective stratigraphy to the right.

differences in topography. These terraces are also facing the Pacific Ocean, restricted to Costa Verde Cliffs. The Pasamayo and Santa Maria cliffs (Fig. 10.27) are composed mainly of the sedimentary rocks of the Morro Solar Group and Pamplona Formation, respectively. Both of them are being eroded by the actual marine erosion. Behind those cliffs there is a coastal plain represented by the alluvial plain of Lima with a distinct topography of undulated hills and flat surfaces. One of the outcrops that define its present surface, that is, Ancon quarries, is mainly composed of deposits whose heights are roughly 10 m of well-stratified gravel and sand channels.

Ecuador

This section is a synthesis of several studies of the coast of Ecuador focused on the effect of active margin tectonics on coastal morphology. Three segments of coast are defined relative to their trend and structural setting: (a) the northern segment (Colombian border to the Galera point) which presents a transition from a subsiding sandy coast to a rising rocky coast; (b) the central segment running all along central Ecuador and showing about continuously a cliff bordering a shore platform; and (c) the southern segment, including all the coast of the Gulf of Guayaquil, characterized by structural coasts, either straight rocky coast along uplifted shoulders or mangrove along drowned segments. The discussion emphasizes the coherent long-term geological aspect of the coast of Ecuador, but also the complex short-term response to regional tectonics that makes difficult the evaluation of coastal evolution without careful studies.

The early synthesis of Daly (1989) pointing out a relationship between the vertical motion of the coastal margin of Ecuador and the rate of plate convergence led him to ask how the coastal morphology, and in particular the rocky coasts, can reflect plate motion conditions, in a more precise way than the historical observation of Suess (1888) on Pacific and Atlantic styles of coasts. Our studies of the coast of Ecuador began in 1995 as part of a broader project examining the subduction zone, developed by the Institut de Recherche pour le Développement, Villefranche sur mer, France, in cooperation with the Escuela Politécnica Nacional, Quito, Ecuador. The main purpose was the study of the Plio-Quaternary to present tectonics of the coastal margin, using principally structural methods such as the analysis of fault planes and slickensides (Carey & Mercier 1987), the analysis and dating of uplifted marine terraces, and later, with the participation of the Instituto Oceanográfico de la Armada, Guayaquil, Ecuador, the analysis and measurement of coastal erosion. A preliminary synthesis of ecuadorian coastal morphology was made as part of the Observatorio de la Línea de costa del Ecuador project of Escuela Politécnica del Litoral, Guayaquil. Microfauna dating and chemical analysis of the geological formations have been investigated with the cooperation of the Centro de Investigación Geológica de Guayaquil, Ecuador. The main results of these studies are summarized below.

Geological setting

The border of the South American plate in Ecuador is characterized by an up to 200 km-wide coastal margin made from an accreted oceanic basement covered by Cenozoic formations. The oceanic basement includes lower Cretaceous basalt (Piñon Formation) covered by upper Cretaceous and Paleocene volcanic sediments and cherts (Cayo Formation), both accreted to the Andean margin during the Eocene (Jaillard *et al.* 1995, 1990). This oceanic basement constitutes the backbone of the Coastal Cordillera, and is observed in the headlands, peninsulas and islands along the coast of central and south Ecuador.

According to Daly (1989), the Palaeogene and Neogene history of the coastal margin is represented by fore-arc basins filled with marine sediments during the periods of fast convergence (about 200 mm a^{-1} between 48 and 37 Ma), and erosion or continental deposition during periods of slow convergence (about 44 mm a^{-1} between 37 and 20 Ma). The present plate convergence is about east–west with a mean rate of 70–80 mm a^{-1} estimated from structural plate positioning by the NUVEL 1A model of relative plate motion (De Mets *et al.* 1989) and 50–70 mm a^{-1} from GPS measurements between the Nazca and South American plates (Kellogg & Vega 1995; Trenkamp *et al.* 2002). Kendrick *et al.* (2003) interpret the difference between the two methods in relation to a decrease in plate convergence during recent time, which is consistent with the uplift tendency of the coast.

Along the subduction zone of Ecuador, from the Gulf of Guayaquil to the Colombian border, the angle between the plate convergence and the trend of the subduction zone decreases from orthogonal to about 40°, providing evidence of an oblique subduction. This oblique subduction mechanism accounts for the northward motion of the North Andean Block (Ego *et al.* 1996) along the Dolores–Guayaquil Megashear (Baldock 1982), and the opening of the Gulf of Guayaquil (Deniaud *et al.* 1999).

Uplifted marine terraces are reported more or less continuously from 1°N (north Ecuador) to 6.5°S (north Peru), along the Talara Arc (CERESIS 1985; Pedoja 2003; Pedoja *et al.* 2006*a*). This arc is split into two parts by the Gulf of Guayaquil, a pull-apart structure including a central subsiding block (Deniaud *et al.* 1999). Along the coast of Ecuador three marine terraces are present at elevations of about 20–40, 60–80 and 100 m (Pedoja 2003; Pedoja *et al.* 2006*a*). These terraces are respectively correlated to the three last interglacial stages maxima (MIS 5e, 7 and 9) on the basis of infrared stimulated luminescence dating, giving uplift rates ranging from 0.15 to 0.3 mm a^{-1} (Pedoja *et al.* 2006*a*). The fastest uplift is observed in the Manta Peninsula (Central Ecuador) and is correlated to the subduction of the Carnegie Ridge (Gutscher *et al.* 1999; Pedoja *et al.* 2001).

Description of the Ecuadorian coast

The coast of Ecuador has a length of about 950 km (De Miro *et al.* 1976) from the estuary of the Mataje River to the north at the border with Colombia, to the Boca de Capones to the south at the border with Peru. Much of the coasts of Ecuador can be classified as rocky, even when a thin strip of sand along the foot of the sea cliff gives the appearance of sandy beaches. The Andean Cordillera is slightly oblique to the coast: the coastal margin is 60 km wide in northern Ecuador, but widens up to 180 km between the Santa Elena Peninsula and the Andean piedmont, just north of the Gulf of Guayaquil. According to the main trends of the coast of Ecuador the following description is divided into three parts, from north to south (Fig. 10.28): (a) Mataje River estuary to Galera Point; (b) Galera Point to Santa Elena Point (Puntilla); and (c) the Gulf of Guayaquil. The two northern parts are located respectively to the north and in front of the subduction of the Carnegie Ridge, and the southern one includes all the opening structure of the Gulf of Guayaquil.

Coast of northern Ecuador: from Mataje River to Galera Point

The north coast of Ecuador trends roughly NE–SW, and includes the Bay of Ancón de Sardinas and the southwestern continuation of the coast. Two different types of coast are observed: from the estuary of the Mataje River to Las Peñas, this is a low coast of sandy beach ridges and mangroves, and from Las Peñas to Galera Point a rocky coast with sea cliffs.

The hinterland of the Bay of Ancón de Sardinas is an area of dense drainage network identified as the El Placer alluvial fan (Winckell & Zebrowski 1997). The Cayapas, Santiago and Mataje rivers supply this fan with water. However the El Placer fan was principally constructed by the Mira River before this river was deviated to the north towards the area of Tumaco (Colombia), owing to the effect of the Canandé Fault (Dumont *et al.* 2006), identified as an active fault (Eguez *et al.* 2003). This change occurred during the Pleistocene. More recently during the Holocene the remaining drainage from the central part of the fan was diverted to the SW (Dumont *et al.* 2006). The drastic loss of water supply of the El Placer fan during the Quaternary explains the oversized tidal channels present in the estuary area, with capacity to receive sea vessels at any time in the San Lorenzo harbour despite the lack of drainage from the land. A cliff created by the Holocene fault tectonics limits now the upland of the old El Placer fan from the estuary formed since the last postglacial transgression. The estuary area is a 15 km-wide belt of mangrove, more or less drowned beach ridges and tidal channels. C14 dating of the oldest drowned beach ridges allows the calculation of a mean subsidence rate of 0.5 cm a^{-1} and a seaward sedimentary accretion of up to 2 m a^{-1} since the mid Holocene transgression (Dumont *et al.* 2006). However subsidence and sedimentary accretion reduce progressively southwards, as the beach ridges pattern becomes clearer, and the margin affected by tides is narrow. Northwards the subsidence stops at the fault that fixes the lower course of the Mataje River. This fault (Fig. 10.28, MAF) results in a high cliffed coast that extends from the border of the Mataje River estuary northwards to the Manglar Cap (Fig. 10.28, MC). West from Las Peñas begins a rocky coast, that continues in a similar style all along central Ecuador: a more or less continue sea cliff overlooking a shore platform. The change of coastal morphology is abrupt, and fits with the NW–SE trending Las Peñas Fault (Fig. 10.28). However the observation of a progressive decrease in the subsidence southwestward towards the fault, and an increase of the uplift rate from the fault to the west towards the Galera Point (Pedoja *et al.* 2006*a*) suggests a not so striking change, but a tilted coastal block with a hinge located near Las Peñas.

In order to understand the evolution of the coast between Las Peñas and Galera Point we must summarize now the late Cenozoic geological history of the Esmeraldas region. During the late Miocene up to the middle Pliocene the area was subsiding, registering the deposition of the Onzole Formation (late Miocene to middle Pliocene; Ordóñez *et al.* 2006) on the middle to upper continental shelf (Fig. 10.29). The fault deformations registered in the lower Onzole Formation (late Miocene to early Pliocene) show a west–east shortening, coherent with the plate convergence (Santana *et al.* 2001). During the middle Pliocene the deposition of the Upper Onzole Formation corresponds to sediments of continental origin (Aalto & Miller 1999) coming probably from the former estuary of the Esmeraldas River. After the late Pliocene and probably during the early to middle Pleistocene, the area emerged in response to the subduction of the Carnegie Ridge (Pedoja *et al.* 2006*a*). The erosion formed the Tonsupa Platform, that extends seaward down to a depth of 10 m (measured from the mean low-tide level) and 30 km off the coast (De Miro *et al.* 1977). However the coastal bathymetry shows a dual distribution of the Tonsupa Platform being distinct from the present shore platform, suggesting that a discontinuity between the two

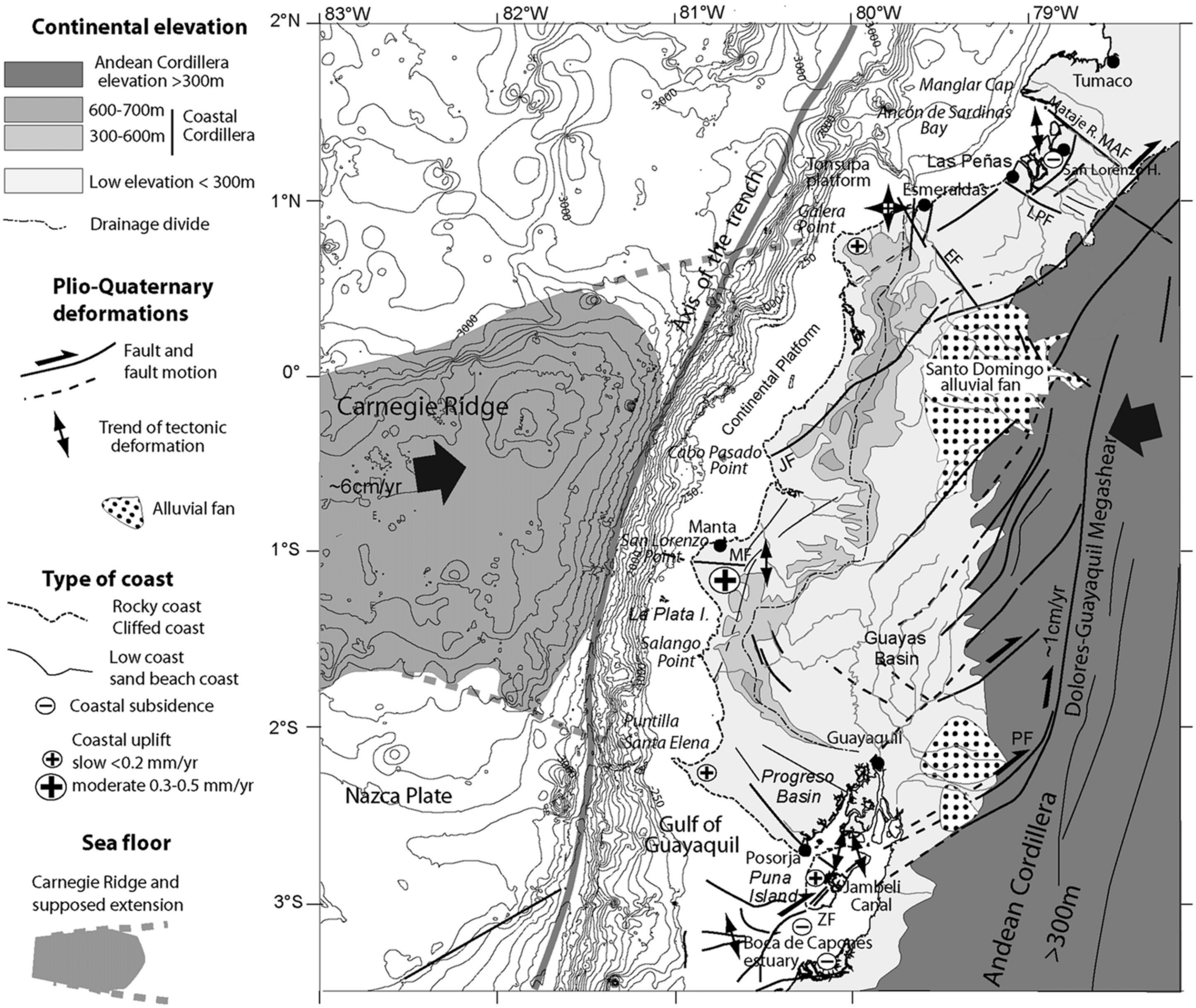

Fig. 10.28. Structural scheme of coastal Ecuador and eastern Nazca Plate. Main faults: MAF, Manglar fault; LPF, Las Peñas fault; EF, Esmeraldas Fault; JF, Jama Fault; MF, Manta Fault; PF, Pallatanga Fault; ZF, Zambapala Fault. Bathymetric chart from Michaud *et al.* (2006), simplified.

platforms and the Tonsupa Platform represents a continental shelf. The Tonsupa Platform belongs possibly to an early stage of the postglacial sea rising. Note that the Tonsupa Platform is the only wide shallow platform along the coast of Ecuador.

The Esmeraldas River enters the sea on the eastern border of the Tonsupa Platform, with a 20 km eastward shift of the estuary of the river from the axis of the old Pliocene sea fan to the present estuary (Figs 10.28 & 10.29). At present the Esmeraldas River does not form any fan at this estuary; a canyon begins at the coastline, extending the river channel seaward and driving the sediments transported directly to the oceanic trench through the canyon. A deep sea fan is now formed at the end of the canyon, at a depth of 3000 m (Collot *et al.* 2004).

Sedimentary dykes trending principally north–south, and a few west–east, are observed on the shore platform and in the cliff, 3 km west of the head of the canyon (Fig. 10.29). They are parallel to the upper part of the canyon, which present a main north–south trend with west–east deviations. The dykes are filled with thin clean sand that lacks marine fragments, and are probably of a fluvial origin. The dykes are clearly related to the Quaternary extension deformation observed in the Esmeraldas area (Santana *et al.* 2001; Dumont *et al.* 2006), and related here to the presence of the Esmeraldas Fault, a major structure in the region (Baldock 1982) that controls the position of the Esmeraldas River in the coastal margin. The interpretation is that sedimentary dykes channelized the river in the coastal area, helping in the formation of the canyon following downward erosion off the coast.

The analysis of sea cliff degradation between Punta Gorda and Puerto Balao shows that the normal faults and lithological characteristics (swelling clays) enhance erosion (Perrin *et al.* 1998). Mechanically the major effect of small faults is to slice the face off the cliff. Dense fracturing combines with thin stratification layers to produce small fragments sensitive to physical weathering by successive wetting and drying. Another affect is the presence of cross-cut faults in the cliff face, because cave development is much more likely at the fault intersections. Between Atacames and Punta Galera some stacks are abandoned on the shore platform and delimited by intersecting faults that are respectively more or less parallel and orthogonal to the cliff. They are all included in the shore platform of the last postglacial sea rise,

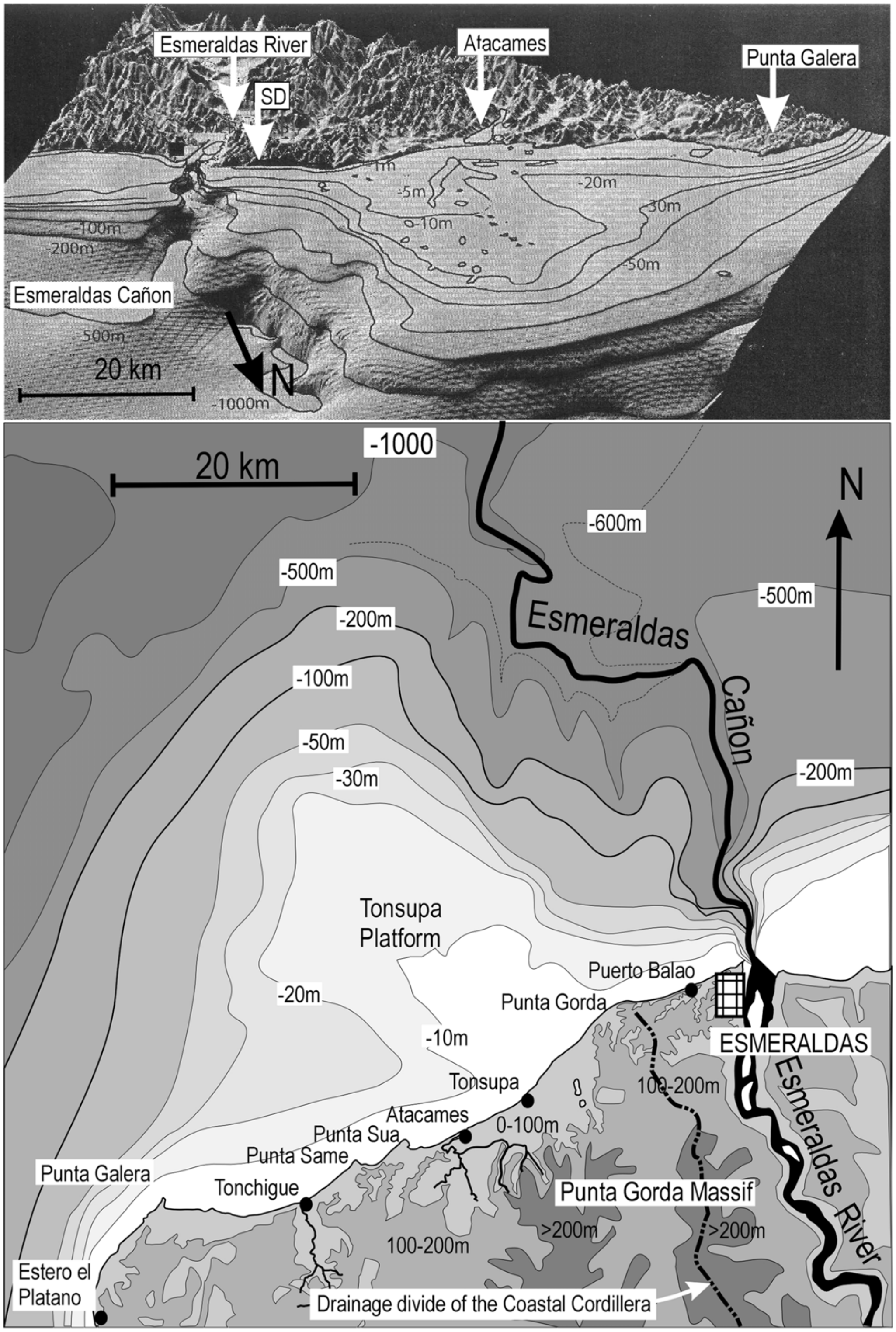

Fig. 10.29. Lower figure: topographic and batymetric map of the coastal area between Esmeraldas and Galera Point. The Esmeradas River marks presently a deviation to the east in the coastal region. The position of the Tonsupa platform (Upper Onzole Formation, Middle Pliocene) suggests that the river flowed previously straight, crossing the coastline between Gorda Point and Tonsupa, and feeding the Tonsupa platform with sediments. Upper figure: 3D model of the same area, looking from the north. SD arrow shows the place where north–south-trending sedimentary dykes cut the shore platform and the sea cliff.

and correspond to parts of the cliff that are more resistant, probably owing to better carbonate calcium cementation. In the Onzole Formation the foot of the cliff is frequently resistant to erosion when it is cut by a suspended valley way. This is due to carbonate deposition that strengthens the rock. Some extreme cases are observed in the Tonchigue area, west of Esmeraldas, showing the channel of the talweg protruding on the shore platform (Fig. 10.30). The calcium carbonate cementation of the cliff observed in some places from Tonchigue to Punta Galera is interpreted as the result of dissolution of calcium carbonate from the shell content of marine terraces located above in the topography, and transported by water drainage. The highest sea cliffs of the Esmeraldas region (Fig. 10.28) are observed in the area of Gorda Point, 8 km west of Esmeraldas and inland of the Tonsupa Platform. The free face of the sea cliffs reaches 100 m, and the elevation of coastal hills over 200 m. Cut in the Upper Onzole Formation, these high sea cliffs are very susceptible to erosion, especially during the El Niño events. The mean sea cliff retreat in the Gorda Point area range between 1 and 2 m a^{-1} for a 30 year period, which includes two major El Niño events, reaching locally up to 2.7 m a^{-1} (Santana *et al.* 2001). El Niño periods generate high precipitation that triggers landslides along the high cliffs of the coast. The front of the landslide is spread on the shore platform, giving locally the impression of a forward motion of the

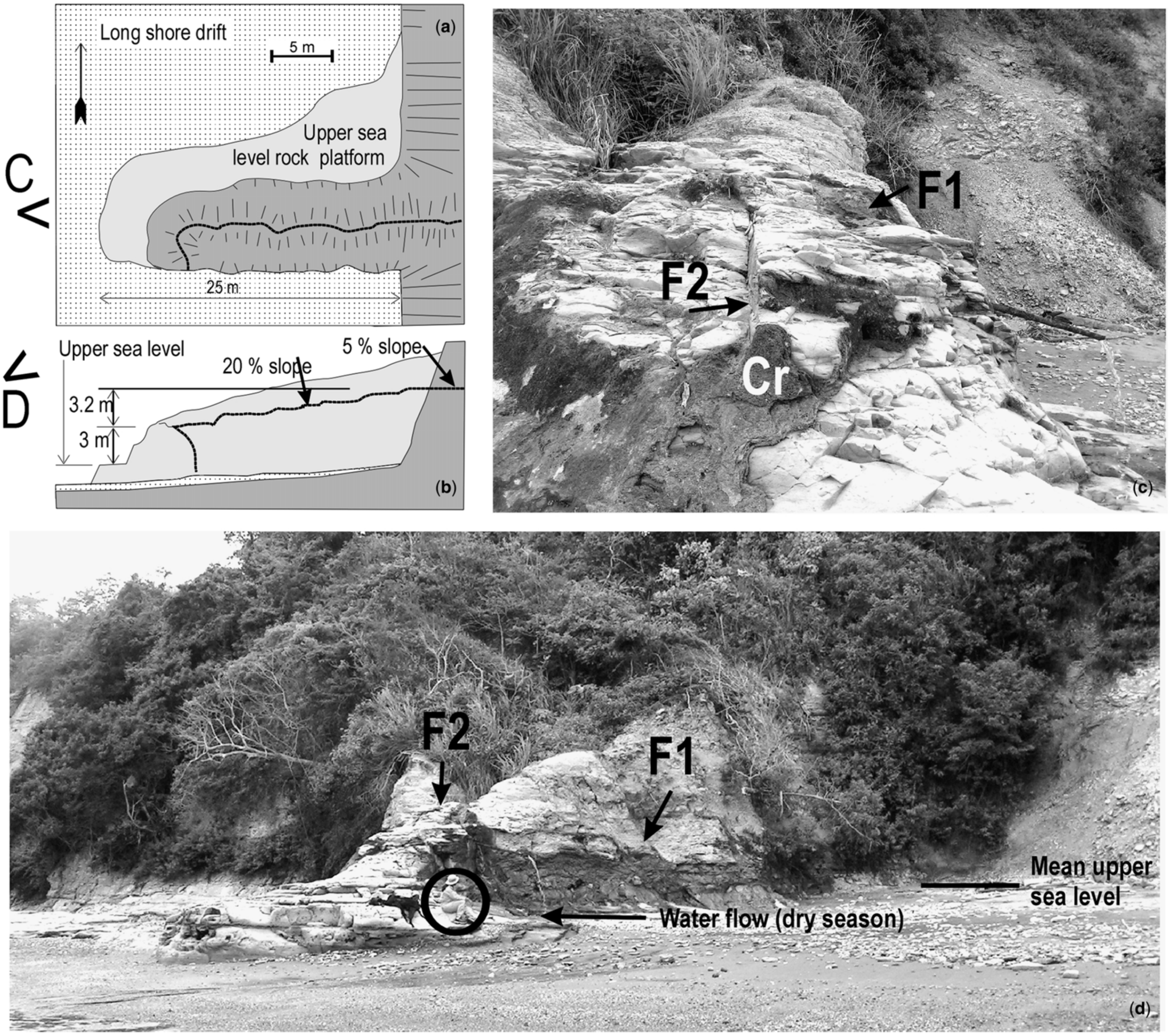

Fig. 10.30. Talweg protruding on the shore platform, west of the village of Tonchigue, 36 km west of the city of Esmeraldas. The person in the circle gives the scale. (**a** and **b**) Graphic sketch as a map (upper), and a lateral view (below). (**c** and **d**) Respectively front and lateral photos, the direction of view is indicated with a '<' in (a). F1 and F2 are faults respectively parallel and orthogonal to the coast. Cr is a crystal carbonate coating of the surface of the rock, up to 5 cm thick.

coastline (Fig. 10.31). However the slide material is quickly removed, so the higher sea cliff retreat is registered during the 2–4 years following the El Niño events. Along coast segments of relatively low cliff (10–40 m), such as the Tonchigue area, the mean sea cliff retreat since the Holocene transgression is about 4–7 cm a^{-1}.

Coast of central Ecuador: from Galera Point to Santa Elena Puntilla

The coast of Central Ecuador can be described as a wide curve punctuated by distinct headlands (from north to south: Galera, Pasado, San Lorenzo, Salango and Santa Elena; Fig. 10.28) and wide bays (Cojimes, Caraquez, Canoa, Santa Elena). The headlands are very close to the outer edge of the continental platform, about 10 km off the Manta Peninsula and the Santa Elena Puntilla. The three southern headlands (San Lorenzo, Salango and Santa Elena) expose the hard rock of the volcanic and clastic volcanic basement (Baldock 1982). North of the Manta Peninsula the coast is eroded in the Mio-Pliocene covering the Onzole and Borbon formations. The position of the points and peninsulas is determined by the main faults of the basement, such as the Jama and the Manta faults (Fig. 10.28, JM and MF).

An important characteristic of the coast of Central Ecuador is the presence of marine terraces (Pedoja *et al.* 2006*a*). They are well preserved on the sides of headlands and peninsulas, in particular on the Santa Elena and Manta peninsulas and Galera Point. The highest mean rate of coastal uplift calculated for the last interglacial period is observed in the Manta Peninsula, in front of the Carnegie Ridge (0.4 ± 0.05 mm a^{-1}). Lower uplift rates are calculated from the Galera Point to the north (0.3 ± 0.04 mm a^{-1}) and the Santa Elena Peninsula to the south (0.2 ± 0.03 mm a^{-1}; Pedoja *et al.* 2006*a*, *b*). The high

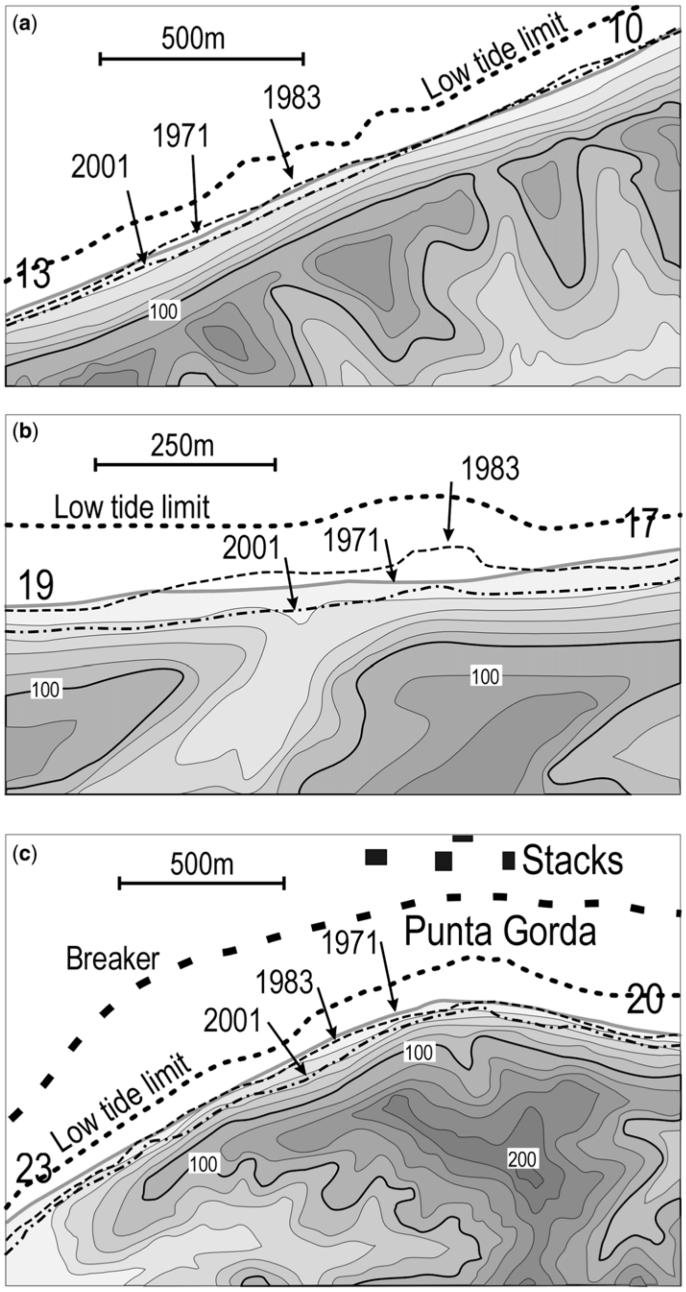

Fig. 10.31. Coastal retreats over a 30 year period, with coastline identified for 1971 and 1983 on aerial photos, and 2001 using GPS. (**a–c**) Successive coastal segments between Puerto Balao (3 km west of Esmeralda) and Gorda Point (10 km west of Esmeraldas). See on central sketch (b) that the landslides of the 1982–1983 El Niño event generated an irregular pattern of coastal erosion.

uplift observed in the Manta Peninsula is interpreted as the effect of the introduction of the Carnegie Ridge into the subduction trench.

The typical pattern of the rocky coast of Ecuador is a more or less clear and steep sea cliff overlooking a shore platform. The slope of the shore platform is generally 2–3° seaward. In some places a short ramp links the shore platform to the foot of the cliff. Comparisons between different places suggest that the presence of the ramp may be related to the lithology and the resulting rates of downwearing of the platform. A ramp is observed on the coast of Esmeraldas where the shore platform is cut in the poorly cemented Upper Onzole Formation, but absent on the platform around the Santa Elena Peninsula, which is cut in the harder chert of the Mesozoic basement (Santana *et al.* 2004). Notches carved at the foot of the cliff are infrequent on the rocky coast of Ecuador, with two possible explanations: most of the rocks are too quickly eroded to allow the formation and preservation of old notches, or the uplift is progressive. The only place where clear and continuous notches have been observed is the coast of the Santa Elena Peninsula: two superimposed notches about 1 m distant are cut in chert, giving evidence of jumps in the uplift of the coastal margin (Santana *et al.* 2004). In most places a thin layer of beach sand, issued from local rivers or the cliff, covers the upper part of the shore platform. However the Costal Cordillera prevents any significant river from reaching the coast, and the supply to the coast of sediment from the continent is poor or limited to specific places where local drainage reaches the coastline.

Coast of the Gulf of Guayaquil

The Gulf of Guayaquil represents the most important estuary system on the Pacific coast of South America (Cucalon 1983), and the Guayas River, with a mean annual discharge of 634 to 1160 $m^3 s^{-1}$ (Stevenson 1981; Gómez 1996), is the most important river on the Pacific coast of the Americas, surpassing the Colorado River. The mouth of the gulf is more than 200 km wide (north–south) and the marine entry extends 130 km inland (Fig. 10.28). The inner coast of the gulf is less than 10 km from the Andean piedmont. Stevenson (1981) defined an outer estuary that is basically the marine gulf bordered by rocky coasts (the southern coast of the Santa Elena Peninsula and the coast of northern Peru between Talara and Tumbez), and an inner estuary which is the estuary of the Guayas River, characterized by mangroves and sandy beach ridges. Stevenson (1981) classified the Guayas River estuary as a tectonic estuary, and this classification can be applied to the entire gulf. The Gulf of Guayaquil is schematically a pull-apart structure opened at the southern end of the Dolores–Guayaquil Megashear, between the piedmont of the Western Andean Cordillera and the subduction system (Deniaud *et al.* 1999). The coasts along the Gulf of Guayaquil are highly dependent upon the opening tectonic of the gulf, with rocky coast along the outer shelves, and low sandy or mangrove coasts in the inner drowned part. The system includes mainly longitudinal strike-slip faults (mainly NE–SW) and normal transverse faults (roughly NW–SE; Dumont *et al.* 2005*a*; Fig. 10.28). The Zambapala Fault in Puna (Fig. 10.28, IP and ZF) sets the limit between the rocky coast from the uplifted margin of the gulf that extends to the west and the drowned block of the pull-apart to the east, where low coasts bordering the alluvial estuary are observed (Dumont *et al.* 2005*b*). The rocky coasts observed along the north and south margins of the Gulf of Guayaquil are associated with uplifted marine terraces.

The distribution of rocky and sandy coasts in the inner part of the gulf is more complex. In the inner estuary of the Guayas River the important supply of alluvial sediments combines with the postglacial sea-level rise to fill the wide coastal plain that constitutes the present Guayas Basin (Baldock 1982; Dumont *et al.* 2007). The coast does not fit always with the structural limits, and some relief, such as the Santa Ana district of Guayaquil or the hills of Duran, can give local rocky coast alternating with alluvial fill.

Conclusion of the Ecuadorian coast section

The general characteristics of the Ecuadorian coast are: (a) parallelism with the orogenic belt; (b) large sections of uplifting coast; and (c) smaller but well delimited segments of subsiding coasts. Considering the detail of short-term coastal evolution, a pertinent question is how and why uplifting rocky coasts are eroding and regressive. Let us consider briefly these different points.

The parallelism of the coast with the orogenic belt that characterizes ‘Pacific type’ results because the coast occupies almost all the narrow width between the continental margin and the foot of the Andes on one side and the outer border of the shelf on the other side, although the coast can obviously zigzag along this relatively narrow belt as shown by the Ecuadorian coast.

Large sections of uplifted coast results in elevated marine terraces marking successive interglacial periods is another important characteristic of Pacific type coasts. These sequences have been widely analysed through models (Trenhaile 2001, 2002) and field work in Ecuador (Pedoja *et al.* 2006*a*, *b*): each interglacial transgression is marked by a different coastline, which is not going to be re-used, except in particular cases where former glacial terraces are uplifted to coincide with sea level. The first situation, which in Ecuador seems the most common (Pedoja 2003), allows consideration of the pre-transgression morphology with more confidence than in the case of coasts of passive margins, where complex inheritances must be considered.

The presence of limited sections of subsiding coast underlies the limit of the apparent continuous structural behaviour of this active margin coast. A particular tectonic situation (i.e. the Gulf of Guayaquil) or a change in the subduction zone (i.e. the subduction of the Carnegie Ridge) can drastically change the situation at the coast, introducing faster uplift and the change from a marine delta at the outlet of the Esmeraldas River to a canyon. Larger-scale elements such as the shape of the subduction zone are probably important; for example, the Arc of Talara probably determines the particular structure of the Gulf of Guayaquil opened at the apex of the arc (Bonnardot *et al.* 2008), or the change from uplifting to subsiding or stable coasts at the end of the arc segments (Pedoja 2003).

The erosion of rocky coasts along uplifting coastal margins shows that the vertical erosion of the shore platform is higher than the tectonic uplift. Kanyaya & Trenhaile (2005) showed from experiments that the downwearing owing to physical conditions, like successive wetting and drying, can vary from 0 to 4 mm a^{-1} according to tide range and lithology, and Stephenson & Finlayson (2009) measured a mean erosion of shore platforms from around the world of 1.486 mm a^{-1}. For coasts in siltstone from Australia Gill & Lang (1983) determined a 0.5–1 mm a^{-1} downwearing. Most of the coasts of central and northern Ecuador are cut in more or less indurate siltstone. The shore platform in silt-clay rocks of the coast of Esmeraldas shows evidences of repetitive fracturing related to plio-quaternary faulting, which allows the parting of the upper surface of the shore platform in small parallelepiped fragments easily removed by waves. However biological erosion of the shore platform by molluscs should also be considered here, although we do not have any measurements of respective physical and biological erosion. The most common burrowing bivalve in Ecuador is *Pholadidea esmeraldensis*, and burrowing activity is even more effective in the lower part of the shore platform (Cruz 1982). Both physical and biological downwearing are probably more than enough to compensate for the tectonic uplift of the coast of Ecuador, the mean rate of which is no higher than 0.4 mm a^{-1} (Pedoja 2003; Pedoja *et al.* 2006*a*). A comparison between shore platforms from different rock types observed in Ecuador suggests that the presence of a short ramp at the platform cliff junction may indicate more rapid downwearing of the platform. The shore platforms cut in the hard volcanic rock and chert of the Cretaceous–Eocene basement are much less susceptible to both physical and biological downwearing, thus giving a narrow but well-defined shore platform joining the base of the cliff without ramp.

As far as the coast of Ecuador is associated with an active margin showing large segments of uplifting coasts, how may the short-term tectonic activity, in particular tectonic jump v. progressive uplift, be identified from the coastal morphology? A definitive argument for the identification of tectonic jump should be the observation of superposed notches and/or staircase morphology at the foot of the cliffs. We presently lack enough arguments to give a definitive answer; however, the following remarks can be made. We never observed superposed notches or staircase morphology along the coasts of central and northern Ecuador. Even if the relatively easy erosion of the cliff makes difficult the formation and preservation of notches, a jump of the shore platform should have risen, or at least some part of it, out of further physical and biological erosion related to successive tides. Such a situation is clearly observed on the north and south sides of the Santa Elena Point, with both superposed notches and a staircase shore platform. The Santa Elena Point is located in an area of relatively low mean uplift rate, but precisely on the border of the structural transition between uplifting (towards central Ecuador to the north) and subsiding (towards the Gulf of Guayaquil to the south) coasts. All that gives the impression of a slow, progressive and relatively fast uplift in most part of the coast of central Ecuador facing the subducting Carnegie Ridge, but vertical motion with jumps at the structural transition between uplifting and subsiding segments of the Talara Arc.

Final remarks

The combination of tectonic movements and Quaternary Pleistocene–Holocene sea-level changes can be considered as two of the major factors affecting rock and cliffed coasts of South and Central America. It is important to keep in mind the different meaning of cliffed coast and hard rock coasts. For example, the extensive Cenozoic sedimentary formations that cover a long section of the Atlantic coasts in Brazil and Uruguay define the typology and present processes in the cliffs eroded in the sediments. Climate is also an important factor, and Holocene and Present climatic conditions exert a great influence on the mechanisms of cliff stability, rock weathering and the development of some features such as beachrock. As with the rest of the world, research in South and Central America has focused on sedimentary coastal systems such as beaches, lagoons or fluvio-marine systems rather than rock coasts. Today, research into rock coast in South America is still very scarce and much work is required to catalogue landforms and to describe the range of operating processes and evolutionary histories. Although coastal research in South and Central America is today at a high scientific and technical level, interest in rock coasts is still low. Attention has been give to the sedimentology and tectonic evolution of sedimentary formations that crop out in the coast forming cliffs, which is the basis of progress in the study of rock coasts. Much less attention has been given to the geomorphology and processes of cliffs and rock coasts. The complex tectonic scenario and the occurrence of extensive Pliocene and early to mid Pleistocene sedimentary formations can be highlighted as a very important factor in the morphodynamics and evolution of cliffs and rock coast. These facts make the coasts of South and Central America of special interest, and hold future insights into rock coast geomorphology.

References

Aalto, K. R. & Miller, W. 1999. Sedimentology of the Pliocene Upper Onzole Formation, an inner-trench slope succession in northwestern Ecuador. *Journal of South American Earth Sciences*, **12**, 69–85.

Adamek, S., Tajima, F. & Wiens, D. A. 1987. Seismic rupture associated with subduction of the Cocos Ridge. *Tectonics*, **6**, 757–774.

Adamek, S. H., Frolich, S. & Pennington, W. 1988. Seismicity of the Caribbean–Nazca boundary: Constrains on microplate tectonics of the Panama region. *Journal of Geophysical Research*, **93**, 2053–2075.

Aguirre, M. L. 2003. Late Pleistocene and Holocene palaeoenvironments in Golfo San Jorge, Patagonia: molluscan evidence. *Marine Geology*, **194**, 3–30.

Aguirre, M. L., Sirch, Y. N. & Richiano, S. 2005. Late Quaternary molluscan assemblages from the coastal area of Bahía Bustamante

(Patagonia, Argentina): paleoecology and paleoenvironments. *Journal of South American Earth*, **20**, 13–32.

Aguirre, M. L., Donato, M., Richiano, S. & Farinati, E. A. 2011. Pleistocene and Holocene interglacial molluscan assemblages from Patagonian and Bonaerensian littoral (Argentina, SW Atlantic): palaeobiodiversity and palaeobiogeography. *Palaeogeography, Palaeoclimatology, Palaeoecology*, **308**, 277–292.

Aleman, A., Benavides, V. & León, W. 2006. *Estratigrafía, Sedimentología y evolución tectónica del área de Lima*. Guía de campo N°11 (Segunda Edición).

Amaral, R. F. & Bezerra, F. H. R. 2006. Mapping beachrock fracturing and erosion using small format aerial photography in northeastern Brazil. *Journal of Coastal Research*, SI**39**, 270–274.

Angulo, R., Lessa, G. C. & de Souza, M. C. 2006. A critical review of mid- to late-Holocene sea-level fluctuations on the eastern Brazilian coastline. *Quaternary Science Reviews*, **25**, 486–506.

Arai, M. 2006. A Grande Elevação Eustática do Mioceno e Sua Influência na Origem do Grupo Barreiras. *Geologia Série Científica*, **6**, 1–6.

Araya-Vergara, J. 2010. Chile. *In*: Bird, E. C. F. (ed.) *Encyclopedia of the World's Coastal Landforms*. Springer, Dordrecht, 213–218.

Argus, D. F., Gordon, R. G. *et al.* 2010. The angular velocities of the plates and the velocity of Earth's centre from space geodesy. *Geophysical Journal International*, **180**, 913–960.

Armijo, R. & Thiele, R. 1990. Active faulting in northern Chile: ramp stacking and lateral decoupling along a subduction plate boundary? *Earth and Planetary Science Letters*, **98**, 40–61.

Audemard, F. M. 1996. Late Quaternary marine deposits of the Paraguaná Peninsula, State of Falcon, Northwestern Venezuela: preliminary geological observations and neotectonic implications. *Quaternary International*, **31**, 5–11.

Audemard, F. M. 2001. Quaternary tectonics and present stress tensor of the inverted northern Falcón Basin, northwestern Venezuela. *Journal of Structural Geology*, **23**, 431–453.

Audin, L., Lacan, P., Tavera, H. & Bondoux, F. 2008. Upper plate deformation and seismic barrier in front of Nazca subduction zone: the Chololo Fault System and active tectonics along the Coastal Cordillera, southern Peru. *Tectonophysics*, **459**, 174–185.

Ayala, L. & Macharé, J. 2011. Geología y conservación de los acantilados de la Costa Verde-Lima. *Guía de excursión Sociedad Geológica del Perú*, **36**, 1–24.

Baldock, J. W. 1982. *Geología del Ecuador: Boletín de la explicación del Mapa Geológico de la República del Ecuador, Esc. 1:1'000.000*. Ministerio de Recursos Naturales y Energía, Quito, **10**.

Barreto, A. M. F., Bezerra, F. H. R., Sugio, K., Tatumi, S. H., Yee, M., Paiva, R. P. & Munita, C. S. 2002. Late Pleistocene marine terrace deposits in northeastern Brazil: sea-level change and tectonic implications. *Palaeogeography, Palaeoclimatology, Palaeoecology*, **179**, 57–69.

Bergoeing, J. P. 1998. *Geomorphología de Costa Rica*. Instituto Geográfico Nacional, San José, CA.

Bertness, M. D., Crain, C. M., Silliman, B. R., Bazterrica, M. C., Reyna, M. V., Hildago, F. & Farina, J. K. 2006. The community structure of western atlantic patagonian rocky shores. *Ecological Monographs*, **76**, 439–460.

Bezerra, F. H. R., Amaro, V. E., Vita-Finzi, C. & Saadi, A. 2001. Pliocene–Quaternary fault control of sedimentation and coastal plain morphology in NE Brazil. *Journal of South American Earth Sciences*, **14**, 61–75.

Bezerra, F. H. R., Barreto, A. M. F. & Suguio, K. 2003. Holocene sea-level history on the Rio Grande do Norte State coast, Brazil. *Marine Geology*, **196**, 73–89.

Bird, E. C. F. 2010. Uruguay. *In*: Bird, E. C. F. (ed.) *Encyclopedia of the World's Coastal Landforms*. Springer, Dordrecht, 227–229.

Blanco Chao, R., Costa Casais, M., Martínez Cortizas, A., Pérez Alberti, A. & Trenhaile, A. S. 2003. Evolution and inheritance of a rock coast: Western Galicia, Northwestern Spain. *Earth Surface Processes and Landforms*, **28**, 757–775.

Blisniuk, P. M., Stern, L. A., Chamberlain, P., Idleman, B. & Zeitler, P. K. 2005. Climatic and ecologic changes during Miocene surface uplift in the southern Patagonian Andes. *Earth and Planetary Science Letters*, **230**, 125–142.

Bonnardot, M.-A., Hassani, R., Tric, E., Ruellan, E. & Régnier, M. 2008. 3-D mechanical modelling of subduction. *Geophysical Journal International*, **173**, 1084–1094.

Bourgois, J., Azema, J., Baumgartner, P. O., Tournon, J., Desmet, A. & Aubouin, J. 1984. The geologic history of the Caribbean–Cocos plate boundary with special reference to the Nicoya ophiolite complex (Costa Rica) and D.S.D.P. results (legs 67 and 84) off Gautemala: a synthesis. *Tectonophysics*, **108**, 1–32.

Bracco, R., del Puerto, L., Inda, H. & Castiñeira, C. 2005. Mid–late Holocene cultural and environmental dynamics in Eastern Uruguay. *Quaternary International*, **132**, 37–45.

Bullard, T. F. 2002. Geomorphic history and fluvial responses to active tectonics and climate change in an uplifted forearc region, Pacific coast of southern Costa Rica, Central America. *Z. Geomorphol*, **129**, 1–29.

Burkart, B. 1994. Northern Central America. *In*: Donovan, S. & Jackson, T. (eds) *Caribbean Geology: An Introduction*. University of the West Indies Publisher's Association, Kingston, 265–284.

Cande, S. C. & Leslie, R. B. 1986. Late Cenozoic tectonics of the southern Chile trench. *Journal of Geophysical Research – Solid Earth and Planets*, **91**, 471–496.

Cantalamessa, G. & Di Celma, C. 2004. Origin and chronology of Pleistocene marine terraces of Isla de la Plata and of flat, gently dipping surfaces of the southern coast of Cabo San Lorenzo (Manabì, Ecuador). *Journal of South American Earth Sciences*, **16**, 633–648.

Cantera, J. & Restrepo, J. D. 2011. Discharge diversion in the Patia River delta, the Colombian Pacific: geomorphic and ecological consequences for mangrove ecosystems. *Journal of South American Earth Sciences*, **33**, 1–16.

Cantera, J., Neira, R. & Ricaurte, C. 1998. *Bioerosión en la Costa Pacífica de Colombia*. Fondo FEN, Colombia.

Carey, E. & Mercier, J. L. 1987. A numerical model for determining the state of stress using focal mechanisms of earthquake population: application to Tibetan teleseims and microseismicity of Southern Peru. *Earth Planetary Science Letters*, **82**, 165–177.

Cavallotto, J. L., Violante, R. A. & Parker, G. 2004. Sea-level fluctuations during the last 8600 years in the de la Plata river (Argentina). *Quaternary International*, **114**, 155–165.

Cediel, F., Shaw, R. P. & Cáceres, C. 2003. Tectonic Assembly of the Northern Andean Block. *In*: Bertolini, C., Buffer, R. T. & Blickwede, J. (eds) *The Circum-Gulf of Mexico and the Caribbean: Hydrocarbon Hábitats, Basin fFrmation, and Plate Tectonics*. American Association of Petroleum Geologists, Tulsa, OK, Memoirs, **79**, 815–848.

CERESIS. 1985. *Mapa Neotectonico Preliminar de America del Sur*. Centro Regional de Sismología para América del Sur.

Clift, P. & Hartley, A. 2007. Slow rates of subduction erosion and coastal underplating along the Andean margin of Chile and Peru. *Geology*, **35**, 503–506.

Coates, A. G. 1997. The forging of Central America. *In*: Coates, A. G. (ed.) *Central America: A Natural and Cultural History*. Yale University Press, New Haven, CT, 1–37.

Coates, A. G. & Obando, J. A. 1996. Geological evolution of the Central American Isthmus. *In*: Jackson, J. B. C., Budd, A. F. & Coates, A. G. (eds) *Evolution and Environment in Tropical America*. University of Chicago Press, Chicago, IL, 21–56.

Coates, A. G., Jackson, J. B. C. *et al.* 1992. Closure of the Isthmus of Panama; the near-shore marine record of Costa Rica and western Panama. *Geological Society of America Bulletin*, **104**, 814–828.

Coates, A. G., Aubry, M. P., Berggren, W. A., Collins, L. S. & Kunk, M. 2003. Early Neogene history of the Central American arc from Bocas del Toro, western Panama. *Geological Society of America Bulletin*, **115**, 271–287.

Codignotto, J. O., Kokot, R. R. & Marcomini, S. C. 1992. Neotectonism and sea-level changes in the coastal zone of Argentina. *Journal of Coastal Research*, **8**, 125–133.

Cogné, N., Gallagher, K. & Cobbold, P. R. 2011. Post-rift reactivation of the onshore margin of southeast Brazil: evidence from apatite (U–Th)/He and fission-track data. *Earth and Planetary Science Letters*, **309**, 118–130.

Collot, J. Y., Marcaillou, B. *et al.* 2004. Are rupture zone limits of great subduction earthquakes controlled by upper plate structures? Evidence from multichannel seismic reflection data acquired across the Northern Ecuador – southwest Colombian margin. *Journal of Geophysical Research*, **109**, B11103.

Coronato, A. M. J., Mazzoni, E. & Vásquez, M. 2008. The physical geography of Patagonia and Tierra del Fuego. *In*: Rabassa, J. (ed.) *The late Cenozic of Patagonia and Tierra del Fuego. Developments in Quaternary Science*, **11**, 13–55.

Correa, I. D. 1996. *Le Littoral Pacifique Colombien: interdependance des Agents morphostructuraux et hydrodynamiques*. PhD thesis, Universite Bordeaux I, France.

Correa, I. & Morton, R. A. 2010. *Coasts of Colombia*. Coastal and Marine Geology Program, St. Petersburg Coastal and Marine Science Center, United States Geological Survey, http://coastal.er.usgs.gov/coasts-colombia/index.html (accessed 26 July 2012).

Correa, I. D. & Morton, R. A. 2011*a*. Pacific coast of Colombia. *In*: Bird, E. C. F. (ed.) *Encyclopedia of Worlds Coastal Landforms*. Springer, Dordrecht, 139–199.

Correa, I. D. & Morton, R. A. 2011*b*. Caribbean coast of Colombia. *In*: Bird, E. C. F. (ed.) *Encyclopedia of Worlds Coastal Landforms*. Springer, Dordrecht, 259–264.

Correa, I. D. & Vernette, G. 2004. Introducción al problema de la Erosión Litoral en Urabá (sector- Arboletes-Turbo) Costa caribe colombiana. *Boletín de investigaciones marinas y costeras*, **33**, 5–26.

Correa, I. D., Acosta, S. & Bedoya, G. 2007. *Análisis de las causas y monitoreo de la Erosión litoral en el departamento de Córdoba*. Convenio de transferencia horizontal de Ciencia y tecnología No. 30. Corporación Autónoma de los valles del Sinú y San Jorge – CVS – Universidad Eafit, Departamento de Geología/Area de Ciencias del Mar. Fondo Editorial Universidad Eafit.

Corrigan, J., Mann, P. & Ingle, J. C. 1990. Forearc response to subduction of the Cocos Ridge, Panama-Costa Rica. *Geological Society of America Bulletin*, **102**, 628–652.

Cruz, M. 1982. *Estudio sistemático de los bivalvos recientes de la plataforma superior interna de la Prov. de Manabí*. Previa a la obtención del título de Doctor en Biología thesis, Universidad de Guayaquil, Guayaquil.

Cucalon, E. 1983. Temperature, salinity and water mass distribution off Ecuador during an El Nino event in 1976. *Revista Ciencias del Mar y Limnología*, **2**, 1–25.

Daly, M. C. 1989. Correlations between Nazca/Farallon plate kinematics and forarc basin evolution in Ecuador. *Tectonics*, **8**, 769–790.

Darwin, C. R. 1846. *Geological Observations on South America. Being the Third Part of the Geology of the Voyage of the Beagle, Under the Command of Capt. Fitzroy, R.N. During the Years 1832 to 1836*. Smith Elder and Co., London.

Davila, F. M., Lithgow-Bertelloni, C. & Gimenez, M. 2010. Tectonic and dynamic controls on the topography and subsidence of the Argentine Pampas: the role of the flat slab. *Earth and Planetary Science Letters*, **295**, 187–194.

de Boer, J. 1979. The outer arc of the Costa Rica orogen (oceanic basement complexes of the Nicoya and Santa Elena peninsulas). *Tectonophysics*, **56**, 221–259.

Defeo, O., Vincent, P. & Acuña, A. 2008. *Geo-Uruguay 2008. Capitulo 3. Zona Costera*. PNUMA-DINAMA-CLAES, Montevideo. 118–176.

Delouis, B., Philip, H., Dorbath, L. & Cisternas, A. 1998. Recent crustal deformation in the Antofagasta region (northern Chile) and the subduction process. *Geophysical Journal International*, **132**, 302–338.

De Mets, C., Gordon, R. G., Argus, D. F. & Stein, S. 1989. Current plate motions. *Geophysical Journal*, **101**, 425–478.

De Mets, C., Gordon, R. G., Argus, D. F. & Stein, S. 1994. Effect of recent revisions to the geomagnetic reversal time-scale on estimates of current plate motions. *Geophysical Research Letters*, **21**, 2191–2194.

De Mets, C., Gordon, R. G. & Argus, D. F. 2010. Geologically current plate motions. *Geophysical Journal International*, **181**, 1–80.

De Miro, M., Ayon, H. & Benites, B. 1976. *Morfología y estructura del margen continental del Ecuador*, **1**. Instituto Oceanográfico de la Armada (INOCAR), Guayaquil.

De Miro, M., Coronel, V., Franco, I. & Cuenca, J. 1977. *Morfología y sedimentos de la plataforma continental de la provincia de Esmeraldas, Ecuador*, **1**. Instituto Oceanográfico de la Armada (INOCAR), Guayaquil.

Dengo, G. 1962. Tectonic-Igneous sequence in Costa Rica. *In*: Engel, A. E. J., James, H. L. & Leonard, B. F. (eds) *Petrologic Studies: A Volume to Honor A.F. Buddington* Geological Society of America, Boulder, CO, 133–161.

Dengo, G. 1968. *Estructura geológica, historia tectónica y morfología de América Central*. Instituto Centroamericano de Investigación y Tecnología Industrial, Guatemala City.

Dengo, G. 1969. Problems of tectonic relations between Central America and the Caribbean. *Transactions of the Gulf Coast Geological Society*, **19**, 311–320.

Dengo, G. 1985. Mid-America: Tectonic setting for the Pacific margin from southern Mexico to northwestern Colombia. *In*: Nairn, A. E. M. & Stehli, F. G. (eds) *The Ocean Basins and Margins*. Plenum Press, New York, **7**, 123–180.

Dengo, G. & Bohnenberger, O. 1969. Structural development of northern Central America. *In*: McBirney, A. R. (ed.) *Tectonic Relations of Northern Central America and the Western Caribbean: The Bonacca Expedition, Memoir 11*. American Association of Petroleum Geologists, Tulsa, OK, 203–220.

Dengo, G., Bohnenberger, O. H. & Bonis, S. 1970. Tectonics and volcanism along the Pacific marginal zone of Central America. *Geologische Rundschau*, **59**, 1215–1232.

Deniaud, Y., Baby, P., Basile, C., Ordoñez, M., Montenegro, G. & Mascle, G. 1999. Opening and tectonic and sedimentary evolution of the Gulf of Guayaquil: Neogene and Quaternary fore-arc basin of the south Ecuadorian Andes. *Comptes Rendus de l'Académie des Sciences – Séries II A – Earth and Planetary Science*, **328**, 181–187.

Denyer, P., Arias, O. & Personius, S. 1994. Efecto tectonico del terremoto de Limón. *Revista Geológica América Central*, Vol. Especial – Terremoto de Limón, 22 de Abril, **199**, 39–52.

DeVries, T. J. 1988. The geology of late Cenozoic marine terraces (tablazos) in northwestern Peru. *Journal of South American Earth Sciences*, **1**, 121–136.

Díaz, J. M., Díaz-Pulido, G. & Sanchez, J. A. 2000. Distribution and structure of the southernmost caribbean coral reefs: Golfo de Urabá, Colombia. *Scientia Marina*, **64**, 327–336.

Di Celma, C. & Cantalamessa, G. 2007. Sedimentology and high-frequency sequence stratigraphy of a forearc extensional basin: the Miocene Caleta Herradura Formation, Mejillones Peninsula, northern Chile. *Sedimentary Geology*, **198**, 29–52.

Dickinson, W. R. 2001. Hydro-isostatic and tectonic influences on emergent Holocene paleoshorelines in the Mariana Islands western Pacific Ocean. *Journal of Coastal Research*, **16**, 725–746.

Dominguez, J. M. L. 2006. The Coastal Zone of Brazil: an overview. *Journal of Coastal Research, SI*, **39**, 16–20.

Donnelly, T. W. 1994. The Caribbean Cretaceous basalt association: A vast igneous province that includes the Nicoya complex of Costa Rica. *In*: Seyfried, H. & Hellmann, W. (eds) *Geology of an Evolving Island Arc, Profil*. Universität Stuttgart, Stuttgart, **7**, 17–45.

Donnelly, T. W., Horne, G. S., Finch, R. C. & López-Ramos, E. 1990. Northern Central America: the Maya and Chortis blocks. *In*: Dengo, G. & Case, J. E. (eds) *The Caribbean Region: The Geology of North America*, **H**. Geological Society of America, Boulder, CO, 37–76.

D'Orbigny, A. 1834–1847. *Voyage dans l'Amérique Méridionale. Mollusques*. Bertrand, Paris and Levrault, Strasbourg, **V**(3).

Duerto, L., Escalona, A. & Mann, P. 2006. Deep structure of the Merida Andes and Sierra de Perija mountain fronts, Maracaibo Basin, Venezuela. *AAPG Bulletin*, **90**, 505–528.

Dumont, J. F., Santana, E. *et al.* 2005*a*. Morphological and microtectonic analysis of Quaternary deformation from Puná and Santa Clara Islands, Gulf of Guayaquil, Ecuador (South America). *Tectonophysics Andean Geodynamics*, **399**, 331–350.

Dumont, J. F., Santana, E. & Vilema, W. 2005*b*. Morphologic evidence of active motion of the Zambapala Fault, Gulf of Guayaquil (Ecuador). *Geomorphology*, **65**, 223–239.

Dumont, J. F., Santana, E., Valdez, F., Tihay, J. P., Usselmann, P., Iturralde, D. & Navarette, E. 2006. Fan beheading and drainage diversion as evidence of a 3200–2800 BP earthquake event in the

Esmeraldas-Tumaco seismic zone; a case study for the effects of great subduction earthquakes. *Geomorphology*, **74**, 100–123.

Dumont, J.-F., Santana, E., Soledispa, B. & King, A. 2007. El Islote El Palmar, resultado de una evolución a largo plazo de la distribución del drenaje entre los ríos Daule y Babahoyo en la cuenca del Guayas. *Acta Oceanográfica del Pacifico*, **14**, 169–180.

Duque-Caro, H. 1990. Neogene stratigraphy, paleoceanography and paleobiogeography in northwest South America and the evolution of the Panamá Seaway. *Paleogeography, Paleoclimatology, Paleoecology*, **77**, 203–214.

Ego, F., Sébrier, M., Lavenu, A., Yepes, H. & Eguez, A. 1996. Quaternary state of stress in the Northern Andes and the restraining bend model for the Ecuadorian Andes. *Tectonophysics*, **259**, 101–116.

Eguez, A., Alvarado, A., Yepez, H., Machette, M. N., Costa, C. & Dart, R. L. 2003. *Database and map Map of Quaternary Faults and Folds of the Ecuador and its Offshore Regions*. International Lithosphere Program Task Group II-2, Major Active Faults of the World. US Department of the Interior, US Geological Survey, Denver, CO.

Ellenberg, L. 2010. Venezuela. *In*: Bird, E. C. F. (ed.) *Encyclopedia of the World's Coastal Landforms*. Springer, Dordrecht, 282–290.

Escalante, G. 1990. The geology of southern Central America and western Colombia. *In*: Dengo, G. & Case, J. E. (eds) *The Caribbean region: The Geology of North America*, **H**. Geological Society of America, Boulder, CO, 201–230.

Escalante, G. & Astorga, A. 1994. Geología del este de Costa Rica y el norte de Panamá. *Revista Geológica América Central, Especial – Terremoto de Limón, 22 de Abril de 1991*, 1–14.

Espurt, N., Funiciello, F., Martinod, J., Guillaume, B., Regard, V., Faccenna, C. & Brusset, S. 2008. Flat subduction dynamics and deformation of the South American plate: Insights from analog modeling. *Tectonics*, **27**, TC3011, http://dx.doi.org/10.1029/2007TC002175

Favalli, M., Fornaciai, A., Isola, I., Tarquini, S. & Nannipieri, L. 2012. Multiview 3D reconstruction in geosciences. *Computer & Geosciences*, **44**, 168–176.

Feruglio, E. 1933. I terrazi marini della Patagonia. *Giornale di Geologia Annali Reale Museo geologico di Bologna*, **8**, 1–288.

Feruglio, E. 1950. *Descripcion geologica de la Patagonia, v. T3*. Direccion General de Y.P.F., Buenos Aires.

Fisher, D. M., Gardner, T. W., Marshall, J. S. & Montero, W. 1994. Kinematics associated with late Cenozoic deformation in central Costa Rica: western boundary of the Panama microplate. *Geology*, **22**, 263–266.

Fisher, D. M., Gardner, T. W., Marshall, J. S., Sak, P. B. & Protti, M. 1998. Effect of subducting sea-floor roughness on fore-arc kinematics, Pacific coast, Costa Rica. *Geology*, **26**, 467–470.

Furrier, M., Araújo, M. E. & Menesses, L. F. 2006. Geomorfologia e Tectônica da Formação Barreiras no Estado da Paraíba. *Geologia Série Científica*, **6**, 61–70.

Gardner, T. W., Back, W. *et al.* 1987. Central America and the Caribbean. *In*: Graf, W. L. (ed.) *Geomorphic Systems of North America: GSA Centennial Special Volume 2*. Geologic Society of America, Boulder, CO, 343–402.

Gardner, T. W., Verdonck, D., Pinter, N. M., Slingerland, R., Furlong, K. P., Bullard, T. F. & Wells, S. G. 1992. Quaternary uplift astride the aseismic Cocos Ridge, Pacific coast, Costa Rica. *Geologic Society of America Bulletin*, **104**, 219–232.

Gardner, T. W., Marshall, J. S. *et al.* 2001. Holocene fore arc block rotation in response to seamount subduction, southeastern Península de Nicoya, Costa Rica. *Geology*, **29**, 151–154.

Gerth, R., Silver, E. *et al.* 1999. La Boquita terrace, Nicaragua: evidence for uplift of the central Pacific coastal zone. *American Geophysical Union, Supplement Abstracts*, **80**, T42C-13.

Gierloff-Emden, H. G. 1982. Central America, coastal morphology. *In*: Schwartz, M. L. (ed.) *The Encyclopedia of Beaches and Coastal Environments*. Hutchinson and Ross, Stroudsburg, PA, 188–191.

Gill, E. D. & Lang, J. G. 1983. Microerosion meter measurement of rock wear onthe Otway Coast of southeast Australia. *Marine Geology*, **52**, 141–156.

Gómez, N. E. 1996. *Elementos de Geografía del Ecuador*. Instituto Geográfico Militar, Ministerio de Educación y Cultura.

Gorring, M. L., Kay, S. M., Zeitler, P. K., Ramos, V. A., Rubiolo, D., Fernandez, M. I. & Panza, J. L. 1997. Neogene Patagonian plateau lavas: continental magmas associated with ridge collision at the Chile Triple Junction. *Tectonics*, **16**, 1–17.

Goso, C. 2009. Geología y problemática costera del departamento de Canelones (Uruguay). *In*: Álvaro López, R. & Cristina Marcomini, S. (eds) *Problemática de los ambientes costeros*. Sur de Brasil, Uruguay y Argentina. Croquis, Buenos Aires, 77–105.

Goso, C., Mesa, V. & Alvez, M. C. 2009. Sinopsis geológico-ambiental de la costa Platense y Atlántica de Uruguay. *In*: Álvaro López, R. & Cristina Marcomini, S. (eds) *Problemática de los ambientes costeros*. Sur de Brasil, Uruguay y Argentina. Croquis, Buenos Aires, 59–76.

Guillaume, B., Martinod, J., Husson, L., Roddaz, M. & Riquelme, R. 2009. Neogene uplift of central eastern Patagonia: dynamic response to active spreading ridge subduction? *Tectonics*, **28**, TC2009, http://dx.doi.org/10.1029/2008TC002324

Guillaume, B., Moroni, M., Funiciello, F., Martinod, J. & Faccenna, C. 2010. Mantle flow and dynamic topography associated with slab window opening: Insights from laboratory models. *Tectonophysics*, **496**, 83–98.

Gutscher, M. A., Malavieille, J. S. L. & Collot, J.-Y. 1999. Tectonic segmentation of the North Andean margin: impact of the Carnegie Ridge collision. *Earth and Planetary Science Letters*, **168**, 255–270.

Guzmán, A., Zavala, B. & Valenzuela, G. 1997. *Proyecto: mapa de suelos de fundación de Lima-Callao, incluyendo los taludes de los acantilados del suroeste*. Estudio de la seguridad física de los acantilados de la Costa Verde, INGEMMET.

Hampel, A. 2002. The migration history of the Nazca Ridge along the Peruvian active margin: a re-evaluation. *Earth and Planetary Science Letters*, **203**, 665–679.

Hare, P. W. & Gardner, T. W. 1985. Geomorphic indicators of vertical neotectonism along converging plate margins, Nicoya Peninsula, Costa Rica. *In*: Morisawa, M. & Hack, J. T. (eds) *Tectonic Geomorphology: Proceedings of the 15th Geomorphology Symposia Series*. Allen and Unwin, Boston, MA, Binghamton, NY, 76–104.

Hartley, A. J., May, G., Chong, G., Turner, P., Kape, S. J. & Jolley, E. J. 2000. Development of a continental forearc: a Cenozoic example from the Central Andes, northern Chile. *Geology*, **28**, 331–334.

Hartley, A., May, G., Chong, G., Turner, P., Kape, S. & Jolley, E. 2001. Development of a continental forearc: a Cenozoic example from the Central Andes, northern Chile. *Geology*, **28**, 331–334.

Herd, D. G., Youd, T. L., Meyer, H., Arango, J. L., Person, W. J. & Mendoza, C. 1981. The great Tumaco, Colombia earthquake of 12 December 1979. *Science*, **211**, 441–445.

Hippolyte, J. C. & Mann, P. 2011. Neogene-Quaternary tectonic evolution of the Leeward Antilles islands (Aruba, Bonaire, Curacao) from fault kinematic analysis. *Marine and Petroleum Geology*, **28**, 259–277.

Hoffstetter, R. 1948. Notas sobre el Cuaternario de la Peninsula de Santa Elena (Ecuador). *Boletin de Informaciones Cientificas Nacionales*, **2**, 19–44.

Hsu, J. T. 1992. Quaternary uplift of the Peruvian coast related to the subduction of the Nazca Ridge: 13.5 to 15.6 degrees south latitude. *Quaternary International*, **15–16**, 87–97.

Hulton, N. R. J., Purves, R. S., McCulloch, R. D., Sugden, D. E. & Bentley, M. J. 2002. The Last Glacial Maximum and deglaciation in southern South America. *Quaternary Science Reviews*, **21**, 233–241.

Husson, L., Conrad, C. P. & Faccenna, C. 2008. Tethyan closure, Andean orogeny, and westward drift of the Pacific Basin. *Earth and Planetary Science Letters*, **271**, 303–310.

Iaffaldano, G., Bunge, H. P. & Dixon, T. H. 2006. Feedback between mountain belt growth and plate convergence. *Geology*, **34**, 893–896.

INE 1995. *Geological Field Guide of Sandino Basin.Onshore*. Instituto Nicaragüense de Energía, Managua.

Inman, D. L. & Nordstrom, C. E. 1971. On the tectonic and morphologic classification of coasts. *Journal of Geology*, **79**, 1–21.

Irion, G., Morais, J. O. & Bungenstock, F. 2012. Holocene and Pleistocene sea-level indicators at the coast of Jericoacoara, Ceará, NE Brazil. *Quaternary Research*, **77**, 251–257.

Isla, F. I. & Bujalesky, G. G. 2008. Coastal Geology and Geomorphology of Patagonia and the Fuegian Archipelago. *In*: Rabassa, J. (ed.) *The Late Cenozic of Patagonia and Tierra del Fuego. Developments in Quaternary Science*, **11**, 227–240.

Isola, I., Bini, M. *et al.* 2012. Geomorphologic map of the northeastern sector of San Jorge Gulf (Chubut, Argentina). *Journal of Maps*, **7**, 476–485.

Ivins, E. R. & James, T. S. 2004. Bedrock response to Llanquihue Holocene and present-day glaciation in southernmost South America. *Geophysical Research Letters*, **31**, L24613, http://dx.doi.org/10.1029/2004GL021500

Jaillard, E., Soler, P., Carlier, G. & Mourier, T. 1990. Geodynamic evolution of the northern and central Andes during Early to Middle Mesozoic times: a Tethyan model. *Geological Society of London*, **147**, 1009–1022.

Jaillard, E., Ordoñez, M., Benítez, S., Berrones, G., Jimenez, N., Montenegro, G. & Zambrano, I. 1995. Basin development in an accretionary, oceanic-floored fore-arc setting: southern coastal Ecuador during Late Cretaceous–Late Eocene times. *In*: Tankard, A. J., Suarez, S. R. & Welsink, H. J. (eds) *Petroleum Basins of South America*. American Association of Petroleum Geologists, Tulsa, OK, 615–631.

Jaillard, E., Lapierre, H., Ordonez, M., Alava, J. T., Amortegui, A. & Vanmelle, J. 2009. Accreted oceanic terranes in Ecuador: southern edge of the Caribbean Plate? *In*: James, K. H., Lorente, M. A. & Pindell, J. L. (eds) *The Origin and Evolution of the Caribbean Plate*. Geological Society, London, Special Publications, **328**, 469–485.

Jaramillo, C. & Bayona, G. 2000. Mangrove distribution during the Holocene in Tribugá Gulf, Colombia. *Biotrópica*, **1**, 14–22.

Kanyaya, J. I. & Trenhaile, A. S. 2005. Tidal wetting and drying on shore platforms: An experimental assessment. *Geomorphology*, **70**, 129–146.

Kelletat, D. H. 2005. Notches. *In*: Schwartz, M. L. (ed.) *Encyclopedia of Coastal Science*. Springer, 728–729.

Kellogg, J. N. & Vega, V. 1995. Tectonic development of Panama, Costa Rica, and the Colombian Andes: constraints from Global Positioning System geodetic studies and gravity. *In*: Mann, P. (ed.) *Geologic and Tectonic Development of the Caribbean Plate Boundary in Southern Central America*. Geological Society of America, Boulder, CO, Special Papers, 75–90.

Kendrick, E., Bevis, M., Smalley, R. J., Brooks, B., Barriga Vargas, R., Lauria, E. & Souto Fortes, L. P. 2003. The Nazca-South America Euler vector and its rate of change. *Journal of South American Earth Science*, **16**, 125–131.

Kennedy, D. M. 2010. Geological control on the morphology of estuarine shore platforms: Middle Harbour, Sydney, Australia. *Geomorphology*, **114**, 71–77.

Kennedy, D. M. & Beban, J. G. 2005. Shore platform morphology on a rapidly uplifting coast, Wellington, New Zealand. *Earth Surface Processes and Landforms*, **30**, 823–832.

Klemann, V., Ivins, E. R., Martinec, Z. K. & Wolf, D. 2007. Models of active glacial isostasy roofing warm subduction: case of the South Patagonian Ice Field. *Journal of Geophysical Research*, **112**, B09405, http://dx.doi.org/10.1029/2006JB004818

Kolarsky, R. A., Mann, P. & Montero, W. 1995. Island arc response to shallow subduction of the Cocos Ridge, Costa Rica. *In*: Mann, P. (ed.) *Geologic and Tectonic Development of the Caribbean Plate Boundary in Southern Central America, GSA Special Paper 295*. Geological Society of America, Boulder, CO, 235–262.

Kuijpers, E. P. 1980. The geologic history of the Nicoya ophiolite complex, Costa Rica and its geotectonic significance. *Tectonophysics*, **68**, 233–255.

Lagabrielle, Y., Suarez, M., Rossello, E., Hérail, G., Martinod, J., Régnier, M. & de La Cruz, R. 2004. Neogene to Quaternary tectonic evolution of the Patagonian Andes at the latitude of the Chile Triple Junction. *Tectonophysics*, **385**, 211–241.

Lamb, S. & Davis, P. 2003. Cenozoic climate change as a possible cause for the rise of the Andes. *Nature*, **425**, 792–797.

Lara, S. & González, L. F. 2006. Las eolianitas de Punta El Chaure en la costa noroccidental de la Península de Paraguaná, Edo. Falcón, Venezuela. *Acta Científica Venezolana*, **57**, 149–158.

Leanza, A. F. 1958. *Geología regional. La Argentina. Suma de Geograía*, **1**, 217–349.

Leonard, E. M. & Wehmiller, J. F. 1991. Geochronology of marine terraces at Caleta Michilla, northern Chile; implications for late Pleistocene and Holocene uplift. *Revista Geologica De Chile*, **18**, 81–86.

Leonard, E. M. & Wehmiller, J. F. 1992. Low uplift rates and terrace reoccupation inferred from mollusk aminostratigraphy, Coquimbo bay area, Chile. *Quaternary Research*, **38**, 246–259.

Le Roux, J. P., Correa, C. T. & Alayza, F. 2000. Sedimentology of the Rimac–Chillon alluvial fan at Lime, Peru, as related to Plio-Pleistocene sea-level changes, glacial cycles and tectonics. *Journal of South American Earth Sciences*, **13**, 499–510..

Leroy, M., Dauteuil, O. & Cobbold, P. R. 2004. Incipient shortening of a passive margin: the mechanical roles of continental and oceanic lithospheres. *Geophysical Journal International*, **159**, 400–411.

Lomnitz, C. 2004. Major earthquakes of Chile: a historical survey, 1535–1960. *Seismological Research Letters*, **75**, 368–378.

Lopez-Laborde, J. 2003. *República Oriental del Uruguay; Caracterización y diagnóstico del litoral costero sobre el Río de la Plata y el Océano Atlántico (Nueva Palmira a Chuy)*. FREPLATA Project Technical Report. CARP-CTMFM.

Macharé, J. 1981. *Geología del Cuaternario de la costa del Perú Central*. PhD thesis, Universidad Nacional de Ingeniería.

Macharé, J. & Ortlieb, L. 1992. Plio-Quaternary vertical motions and the subduction of the Nazca Ridge, central coast of Peru. *Tectonophysics Andean Geodynamics*, **205**, 97–108.

Madrigal, R. 1982. *Geología de Santa Rosa*. Universidad Estatal a Distancia, San José, CA.

Madrigal, R. & Rojas, E. 1980. *Manual Descriptivo del Mapa Geomorfológico de Costa Rica*. Secretaría Ejecutiva de Planificación Sectorial Agropecuaria (SEPSA), San José, CA.

Mann, P. & Corrigan, J. 1990. Model for late Neogene deformation of Panama. *Geology*, **18**, 558–562.

Mann, P., Schubert, C. & Burke, K. 1990. Review of Caribbean neotectonics. *In*: Dengo, G. & Case, J. E. (eds) *The Caribbean Region: The Geology of North America, **H***. Geological Society of America, Boulder, 307–338.

Marquardt, C., Lavenu, A., Ortlieb, L., Godoy, E. & Comte, D. 2004. Coastal neotectonics in Southern Central Andes: uplift and deformation of marine terraces in Northern Chile (27°S). *Tectonophysics*, **394**, 193–219.

Marshall, J. S. 2007. The Geomorphology and physiographic provinces of Central America. *In*: Bundschuh, J. & Alvarado, G. (eds) *Central America: Geology, Resources and Hazards, Overview of Plate Tectonic History and Its Unresolved Tectonic Problems*. Taylor & Francis, London, 201–237.

Marshall, J. S. & Anderson, R. S. 1995. Quaternary uplift and seismic cycle deformation, Península de Nicoya, Costa Rica. *Geologic Society of America Bulletin*, **107**, 463–473.

Marshall, J. S. & Vannuchi, P. 2003. Forearc deformation influenced by subducting plate morphology and upper plate discontinuity, Pacific Coast, Costa Rica. *Geological Society of America Abstracts with Programs*, **35**, 74.

Marshall, J. S., Fisher, D. M. & Gardner, T. W. 2000. Central Costa Rica deformed belt: Kinematics of diffuse faulting across the western Panama block. *Tectonics*, **19**, 468–492.

Marshall, J. S., Gardner, T. W., Fisher, D. M., Sak, P. B. & Protti, M. 2001. *Quaternary Neotectonics of the Costa Rican Coastal Fore Arc. Field Trip Guide*. National Science Foundation MARGINS Program: Central America Tectonics Workshop, Heredia, Costa Rica.

Marshall, J. S., Khaw, F., Parra, J. G., Annis, L. K. & Protti, M. 2003*a*. Marine terraces, subduction earthquakes and Quaternary uplift of the Nicoya Peninsula, Costa Rica, Central America. *Geological Society of America Abstracts with Programs*, **35**, 515.

Marshall, J. S., Idleman, B. D., Gardner, T. W. & Fisher, D. M. 2003*b*. Landscape evolution within a retreating volcanic arc, Costa Rica, Central America. *Geology*, **31**, 419–422.

Marshall, J. S., Annis, L. K., Khaw, F., Parra, J. G. & Protti, M. 2004. Coastal deformation patterns along the Nicoya seismic gap, Pacific coast, Costa Rica, Central America. *EOS, Transactions, American Geophysical Union, Supplement Abstracts*, **85**, T13C–1393.

Marshall, J. S., Lafromboise, E. J., Utick, J. D., Khaw, F., Annis, L. K., Parra, J. G. & Protti, M. 2005. Variations in Quaternary coastal emergence along the Nicoya Peninsula seismic gap, Costa Rica, Central America. *Geologic Society of America Bulletin Abstracts with Programs*, **37**, 560.

Marshall, R. J. E. & Stephenson, W. J. 2011. The morphodynamics of shore platforms in a micro-tidal setting: interaction between waves and morphology. *Marine Geology*, **288**, 18–31.

Martin, L., Suguio, K. & Flexor, J. M. 1988. Hauts niveaux marins Pleistocenes du littoral bresilien. *Palaeogeography, Palaeoclimatology, Palaeoecology Quaternary Coastal Changes*, **68**, 231–239.

Martin, L., Suguio, K., Flexor, J. M., Dominguez, J. M. L. & Bittencourt, A. C. S. P. 1996. Quaternary sea-level history along the central Part of the Brazilian Coast. Variations in coastal dynamics and their consequences on coastal plain construction. *Anais da Academia Brasileira de Ciencias*, **68**, 304–354.

Martínez, J. I., Yokoyama, Y., Gomez, A., Delgado, A., Matsuzaki, H. & Rendon, E. 2010. Late Holocene marine terraces of the Cartagena region, southern Caribbean: the product of neotectonism or a former high stand in sea-level? *Journal of South American Earth Sciences*, **29**, 214–224.

Martinod, J., Husson, L., Roperch, P., Guillaume, B. & Espurt, N. 2010. Horizontal subduction zones, convergence velocity and the building of the Andes. *Earth and Planetary Science Letters*, **299**, 299–309.

Melnick, D. & Echtler, H. P. 2006. Inversion of forearc basins in south-central Chile caused by rapid glacial age trench fill. *Geology*, **34**, 709–712.

Melnick, D., Bookhagen, B., Strecker, M. R. & Echtler, H. 2009. Segmentation of megathrust rupture zones from forearc deformation patterns over hundreds to millions of years, Arauco Peninsula, Chile. *Journal of Geophysical Research*, **114**, B01407, http://dx.doi.org/10.1029/2008JB005788

Mercer, J. H. 1983. Cenozoic glaciation in the southern hemisphere. *Annual Reviews of Earth and Planetary Science*, **11**, 99–132.

Michaud, F., Collot, J.-Y., De la Torre, G., Alvarado, A., Pazmino, N. & Lopez, E. 2006. *Batimetria y topografia del Ecuador, escala 1:1 000 000*. INOCAR, Quito.

Michaud, F., Witt, C. & Royer, J. Y. 2009. Influence of the Carnegie ridge subduction on Ecuadorian geology: reality and fiction. *In*: Kay, S., Ramos, V. & Dickinson, W. R. (eds) *Backbone of the Americas: Shallow Subduction, Plateau Uplift and Ridge and Terrane Collision*. Geological Society of America, Boulder, CO, Special Publications, **204**, http://dx.doi.org/10.1130/2009.1204.10

Milne, G. A. & Shennan, I. 2007. Isostasy. *In*: Elias, S. A. (ed.) *Encyclopedia of Quaternary Science*. Elsevier, Amsterdam, 3043–3051.

Milne, G. A., Long, A. & Bassett, S. E. 2005. Modelling Holocene relative sea-level observations from the Caribbean and South America. *Quaternary Science Reviews*, **24**, 1183–1202.

Mitrovica, J. X. & Milne, G. A. 2002. On the origin of late Holocene sea-level highstands within equatorial ocean basins. *Quaternary Science Reviews*, **21**, 2179–2190.

Montero, W. 1994. Neotectonics and related stress distribution in a subduction-collisional zone, Costa Rica. *In*: Seyfried, H. & Hellmann, W. (eds) *Geology of an Evolving Island Arc: The Isthmus of Southern Nicaragua, Costa Rica, and Western Panamá. Profil*. Universität Stuttgart, Stuttgart, **7**, 126–141.

Moreno, M., Melnick, D. *et al.* 2012. Toward understanding tectonic control on the Mw 8.8 2010 Maule Chile earthquake. *Earth and Planetary Science Letters*, **321–322**, 152–165.

Mörner, A. N. 2005. Changing sea-levels. *In*: Schwartz, M. L. (ed.) *Encyclopedia of Coastal Sciences*. Springer, Dordrecht, 229–233.

Morton, R. A., González, J. L., López, G. & Correa, I. D. 2000. Frequent non-storm washover of Barrier Islands, Pacific Coast of Colombia. *Journal of Coastal Research*, **16**, 82–87.

Mueher, D. 2010. Brazil. *In*: Bird, E. C. F. (ed.) *Encyclopedia of the World's Coastal Landforms*. Springer, Dordrecht, 231–238.

Naylor, L. A. & Stephenson, W. J. 2010. On the role of discontinuities in mediating shore platform erosion. *Geomorphology*, **114**, 89–100.

Noble, D., Wise, J., Zanetti, K., Vidal, C. & McKee, E. 2009. Edad Miocena Tardía para los conglomerados y gravas del 'cuaternario' en las planicies costaneras del Perú central y otras evidencias concernientes a la evolución Neógena en la vertiente occidental de los Andes Peruanos. *Sociedad Geológica del Perú SGP*, Volumen especial, **7**, 90.

Norabuena, E., Dixon, T. H. *et al.* 2004. Geodetic and seismic constraints on some seismogenic zone processes in Costa Rica. *Journal of Geophysical Research*, **109**, B11403, http://dx.doi.org/10.1029/2003JB002931

Okal, E. A. 2005. A re-evaluation of the great Aleutian and Chilean earthquakes of 1906 August 17. *Geophysical Journal International*, **161**, 268–282.

Ordóñez, M., Jimenez, N. & Suarez, M. 2006. *Micropaleontologia equatoriana*. Petroproduccion, CIGG, Guayaquil.

Ortlieb, L., Zazo, C., Goy, J., Hillaire-Marcel, C., Ghaleb, B. & Cournoyer, L. 1996. Coastal deformation and sea-level changes in the northern Chile subduction area (23°S) during the last 330 ky. *Quaternary Science Reviews: Records of Rapid Events in Late Quaternary Shorelines*, **15**, 819–831.

Ota, Y., Miyauchi, T., Paskoff, R. & Koba, M. 1995. Plio-Quaternary marine terraces and their deformation along the Altos de Talinay, north-central Chile. *Revista Geológica de Chile*, **22**, 89–102.

Page, W. 1983. Holocene deformation of the caribbean coast, northwestern Colombia. *In*: Duque-Caro, H. *et al.* (eds) *Field trip C: General Geology, Geomorphology and Neotectonics of Northwestern Colombia. 10th Caribbean Geol Conference*, Cartagena, Appendix, 1–20.

Palacios, O., Caldas, J. & Vela, C. H. 1992. *Geología de los cuadrángulos de Lima, Lurín, Chancay y Chosica*. Boletín No. 43, Serie A: Carta Geológica Nacional. INGEMMET, Lima.

Pappalardo, M., Aguirre, M. *et al.* 2012. *Morphological evidence interpreted in terms of sea level indicators along the coast of Patagonia*. SLALOM2012 Abstract volume, Athens.

Pardo-Casas, F. & Molnar, P. 1987. Relative Motion of the Nazca (Farallon) and South-American Plates since Late Cretaceous Time. *Tectonics*, **6**, 233–248.

Paris, G., Machette, M. N., Dart, R. I. & Haller, M. K. 2002. Map and Database of Quaternary Faults and Folds in Colombia and its Offshore Regions. U.S.G.S Open File Report **00-0284**, 1–64.

Paskoff, R. 1970. *Recherches géomorphologiques dans le Chili semi-aride*. Biscaye Freres, Bordeaux.

Paskoff, R. 1977. Quaternary of Chile: The State of research. *Quaternary Research*, **8**, 2–31.

Paskoff, R. 1980. Late Cenozoic crustal movements and sea level variations in the coastal area of Northern Chile. *In*: Morner, N. A. (ed.) *Earth Rheology, Isostasy, and Eustasy*. John Wiley, Chichester, 487–495.

Pedoja, K. 2003. *Les terrasses marines de la marge Nord Andine (Equateur et Nord Pérou): relations avec le contexte géodynamique*. PhD thesis, Paris VI, Villefranche sur Mer.

Pedoja, K., Dumont, J. F., Sorel, D. & Ortlieb, L. 2001. Marine terraces and subducting asperities: the Manta Case, Ecuador. *In*: *Fifth International Conference on Geomorphology. Transaction of the Japanese Geomorphological Union*, Tokyo.

Pedoja, K., Dumont, J. F. *et al.* 2006*a*. Plio-Quaternary uplift of the Manta Peninsula and La Plata Island and the subduction of the Carnegie Ridge, central coast of Ecuador. *Journal of South American Earth Sciences*, **22**, 1–21.

Pedoja, K., Ortlieb, L., Dumont, J. F., Lamothe, M., Ghaleb, B., Auclair, M. & Labrousse, B. 2006*b*. Quaternary coastal uplift along the Talara Arc (Ecuador, Northern Peru) from new marine terrace data. *Marine Geology*, **228**, 73–91.

Pedoja, K., Regard, V., Husson, L., Martinod, J. & Iglesias, M. 2008. Why is the passive margin of Argentinean Patagonia uplifting? An insight by marine terrace and tidal notches sequences. *7th International Symposium Andean Geodynamics (Nice)*, Ed. IRD, Paris, France, September 2008.

Pedoja, K., Dumont, J. F. & Ortlieb, L. 2009. Levantamiento Cuaternario costero del Arco de Talara (Ecuador y norte del Perú): cuantificaciones con las secuencias de terrazas marina. *In*: Collot, J.-Y., Sallares, V. & Pazmiño, N. (eds) *Geologia y Geofisica marina y terrestre del Ecuador desde la costa continental hasta las* *islas Galapagos*. Comisión Nacional del Derecho del Mar, Institut de Recherche pour le Développement and Instituto Oceanográfico de la Armada (INOCAR), Guayaquil, 107–129.

Pedoja, K., Ortlieb, L., Devries, T. J., Macharé, J., Audin, L. & Regard, V. 2011*a*. Comment on 'Tectonic record of strain buildup and abrupt coseismic stress release across the northwestern Peru coastal plain, shelf, and continental slope during the past 200 kyr' by Jacques Bourgois *et al. Journal of Geophysical Research*, **116**, B09401, http://dx.doi.org/10.1029/2011JB008321

Pedoja, K., Regard, V. *et al*. 2011*b*. Uplift of Quaternary shorelines in Eastern Patagonia: Darwin revisited. *Geomorphology*, **127**, 121–142.

Pedoja, K., Husson, L. *et al*. 2011*c*. Relative sea-level fall since the last interglacial stage: Are coasts uplifting worldwide? *Earth-Science Reviews*, **108**, 1–15.

Perrin, J. L., Jeanneau, J. L. & Podwojeski, P. 1998. *Deslizamientos de tierra, inundaciones y flujos de lodo en Esmeraldas; diagnostico general de la situacion actual en la ciudad, mision de expertos*, 020005212. Informe ORSTOM, Quito.

Phillips, S., Bustin, R. M. & Lowe, L. E. 1994. Earthquake-induced flooding of a tropical coastal peat swamp: A modern analogue for high-sulfur coals? *Geology*, **22**, 929–932.

Pino, M., Moreno, K. & Paz Riedemann, M. 2002. La terraza del ultimo interglacial en la costa de Valdivia: observaciones, interpretaciones y desafios. *Simposio Internacional de Geología Ambiental para Planificación del Uso del Territorio*, 165–169.

Pirazzoli, P. A. 1986. Marine notches. *In*: Van de Plassche, O. (ed.) *Sea Level Research: a Manual for the Collection and Evaluation of Data*. Geo Books, Norwich, 361–400.

Pirazzoli, P. A. 1991. *World Atlas of Holocene Sea-level Changes*. Elsevier, Oxford, Oceanographic Series, **58**.

Plafker, G. & Savage, J. C. 1970. Mechanism of the Chilean Earthquakes of May 21 and 22, 1960. *Geological Society of America Bulletin*, **81**, 1001–1030.

Plafker, G. & Ward, S. N. 1992. Backarc thrust faulting and tectonic uplift along the Caribbean Sea coast during the April 22, 1991, Costa Rica earthquake. *Tectonics*, **11**, 709–718.

Prawirodirdjo, L. & Bock, Y. 2004. Instantaneous global plate motion model from 12 years of continuous GPS observations. *Journal of Geophysical Research*, **109**, B08405, http://dx.doi.org/10.1029/2003JB002944

Protti, M., Güendel, F. & Malavassi, E. 2001. *Evaluación del potencial sísmico de la Península de Nicoya*. Editorial Fundación UNA, Heredia.

Quezada, J., Cerda, J. L. & Jensen, A. 2010. Efectos de la tectónica y el clima en la configuración morfológica del relieve costero del norte de Chile. *Andean Geology*, **37**, 78–109.

Quinteros, J. & Sobolev, S. V. 2013. Why has the Nazca plate slowed since the Neogene? *Geology*, **41**, 31–34.

Ramos, V. A. 1999. Plate tectonic setting of the Andean Cordillera. *Episodes*, **22**, 183–190.

Ranero, C. R. & von Huene, R. 2000. Subduction erosion along the Middle America convergent margin. *Nature*, **404**, 748–752.

Regard, V., Saillard, M. *et al*. 2010. Renewed uplift of the Central Andes Forearc revealed by coastal evolution during the Quaternary. *Earth and Planetary Science Letters*, **297**, 199–210.

Ribolini, A., Aguirre, M. L. *et al*. 2011. Holocene beach ridges and coastal evolution in the Cabo Raso bay (Atlantic Patagonian coast, Argentina). *Journal of Coastal Research*, **27**, 973–983.

Rivera, N. P. 1962. Reconocimiento geológico de la costa del Pacífico de Nicaragua. *Boletín del Servicio Geológico Nacional de Nicaragua*, **6**, 71–87.

Rostami, K., Peltier, W. R. & Mangini, A. 2000. Quaternary marine terraces, sea-level changes and uplift history of Patagonia, Argentina: comparisons with predictions of the ICE-4G (VM2) model of the global process of glacial isostatic adjustment. *Quaternary Science Reviews*, **19**, 1495–1525.

Russo, R. & Silver, P. G. 1996. Cordillera formation, mantle dynamics, and the Wilson cycle. *Geology*, **24**, 511–514.

Russo, R. M., Gallego, A., Comte, D., Mocanu, V. I., Murdie, R. E. & VanDecar, J. C. 2010. Source-side shear wave splitting and upper mantle flow in the Chile Ridge subduction region. *Geology*, **38**, 707–710.

Rutter, N., Schnack, E. J. d., Rio, J., Fasano, J. L., Isla, F. I. & Radtke, U. 1989. Correlation and dating of Quaternary littoral zones along the Patagonian coast, Argentina. *Quaternary Science Reviews*, **8**, 213–234.

Saillard, M., Hall, S. R. *et al*. 2009. Non-steady long-term uplift rates and Pleistocene marine terrace development along the Andean margin of Chile (31°S) inferred from 10Be dating. *Earth and Planetary Science Letters*, **277**, 50–63.

Saillard, M., Hall, S. R., Audin, L., Farber, D. L., Regard, V. & Hérail, G. 2011. Andean coastal uplift and active tectonics in southern Peru: 10Be surface exposure dating of differentially uplifted marine terrace sequences (San Juan de Marcona, ~15.4°S). *Geomorphology*, **128**, 178–190.

Saillard, M., Riotte, J., Regard, V., Violette, A., Hérail, G., Audin, L. & Riquelme, R. 2012. Beach ridges U–Th dating in Tongoy bay and tectonic implications for a peninsula-bay system, Chile. *Journal of South American Earth Sciences*, **40**, 77–84.

Sak, P. B., Fisher, D. M. & Gardner, T. W. 2004. Effects of subducting seafloor roughness on upper plate vertical tectonism: Osa Peninsula, Costa Rica. *Tectonics*, **23**, TC1017, http://dx.doi.org/10.1029/2002TC001474

Santana, E., Dumont, J. F. & King, A. 2001. Los efectos del fenomeno El Niño en la ocurencia de una alta tasa de erosion costera en el sector de Punta Gorda, Esmeraldas. *Acta Oceanografica del Pacifico*, **11**, 1–5.

Santana, E., Dumont, J. F., Armas, V., Burbano, L., Gutierrez, L. & Valdez, F. 2004. Evolución morfológica de la costa en la península de Santa Elena; Evidencias de plataformas marinas y socavones superpuestos. *Acta Oceanográfica del Pacifico*, **12**, 155–167.

Santos, J. O. F., Amaral, R. F. & Scudelari, A. C. 2006. Failure Mechanisms of a Coastal Cliff in Rio Grande do Norte State, NE Brazil. *Journal of Coastal Research*, SI**39**, 629–632.

Santos, J. O. F., Scudelari, A. C., Costa, Y. D. & Costa, C. M. 2011. Sea Cliff Retreat Mechanisms in Northeastern Brazil. *Journal of Coastal Research*, SI**64**, 820–824.

Scalabrino, B., Lagabrielle, Y. *et al*. 2010. A morphotectonic analysis of central Patagonian Cordillera: negative inversion of the Andean belt over a buried spreading center? *Tectonics*, **29**, TC2010, http://dx.doi.org/10.1029/2009TC002453

Scheffers, & Browne, 2010: *Pacific Coasts of Guatemala, El Salvador, Honduras, Nicaragua, Costa Rica and Panama*. *In*: Bird, E. C. F. (ed.) *Encyclopedia of the World's Coastal Landforms*. Springer, Dordrecht, 227–229.

Schellmann, G. 1998. Coastal development in Southern South America (Patagonia and Chile) since the Younger Middle Pleistocene — sea-level changes and neotectonics. *In*: Kelletat, D. (ed.) *German Geographical Coastal Research: The Last Decade*. Institute for Scientific Co-operation Tübingen, IGU Sonderband, Tübingen, 289–304.

Schellmann, G. & Radtke, U. 2003. Coastal Terraces and Holocene Sea-level changes along the Patagonian Atlantic Coast. *Journal of Coastal Research*, **19**, 983–996.

Schellmann, G. & Radtke, U. 2010. Timing and magnitude of Holocene sea-level changes along the middle and south Patagonian Atlantic coast derived from beach ridge systems, littoral terraces and valley-mouth terraces. *Earth Science Reviews*, **103**, 1–30.

Sdrolias, M. & Muller, R. D. 2006. Controls on back-arc basin formation. *Geochemistry Geophysics Geosystems*, **7**, Q04016, http://dx.doi.org/10.1029/2005GC001090

Sheppard, G. 1927. Geological observations on Isla de la Plata, Ecuador, South America. *American Journal of Science*, **13**, 480–486.

Shepard, F. P. & Kuhn, G. G. 1983. History of sea arches and remnant stacks of La Jolla, CValiofornia, and their bearing on similar features elsewhere. *Marine Geology*, **51**, 139–161.

Shephard, G. E., Müller, R. D., Liu, L. & Gurnis, M. 2010. Miocene drainage reversal of the Amazon River driven by plate–mantle interaction. *Nature Geosciences*, **3**, 870–875.

Silliman, B. R., Bertness, M. D. *et al*. 2011. Whole-community facilitation regulates biodiversity on patagonian rocky shores. *PLoS ONE*, **6**, 24502.

Silver, P. G., Russo, R. M. & Lithgow-Bertelloni, C. 1998. Coupling of South American and African Plate motion and Plate deformation. *Science*, **279**, 60–63.

Skrepnek, C. C., Schmitt, R. S. & Guerra, J. V. 2009. Geology and Geomorphology of Papagaios Island, Cabo Frio, SE Brazil. *Journal of Coastal Research*, SI**56**, 761–771.

Somoza, R. 1998. Updated Nazca (Farallon)–South America relative motions during the ñast 40 My: implications for mountain building in the Central Andean region. *Journal of South American Earth Sciences*, **11**, 211–215.

Somoza, R. & Ghidella, M. E. 2012. Late Cretaceous to recent plate motions in western South America revisited. *Earth and Planetary Science Letters*, **331–332**, 152–163.

Stephenson, W. J. & Finlayson, B. L. 2009. Measuring erosion with the micro-erosion meter. *Contributions to Understanding Landform Evolution. Earth-Sciences Reviews*, **95**, 53–62.

Stevenson, M. R. 1981. Seasonal variation in the Gulf of Guayaquil, a tropical estuary. *Boletin Cientifico y Téchnico INP*, **4**, 1–133.

Suess, E. 1888. *Das Antlitz der Erde*. F. Tempsky, Vienna.

Sugio, K., Bezerra, F. H. R. & Barreto, A. M. F. 2011. Luminescence dated Late Pleistocene wave-built terraces in northeastern Brazil. *Anais da Academia Brasileira de Ciências*, **83**, 907–920.

Taboada, A., Rivera, L. A. *et al.* 2000. Geodynamics of the northern Andes: Subductions and intracontinental deformation (Colombia). *Tectonics*, **19**, 787–813.

Tajima, F. & Kikuchi, M. 1995. Tectonic implications of the seismic ruptures associated with the 1983 and 1991 Costa Rica earthquakes. *In*: Mann, P. (ed.) *Geologic and Tectonic Development of the Caribbean Plate Boundary in Southern Central America, GSA Special Paper 295*. Geological Society of America, Boulder, CO, 327–340.

Taype-Ramos, V. & Bird, E. 2010. Peru. *In*: Bird, E. C. F. (ed.) *Encyclopedia of the World's Coastal Landforms*. Springer, Dordrecht, 208–211.

Thomas, C., Livermore, R. & Pollitz, F. 2003. Motion of the Scotia Sea plates. *Geophysical Journal International*, **155**, 789–804.

Trenhaile, A. S. 2001. Modeling the effect of Late Quaternary interglacial sea levels on wave-cut shore platforms. *Marine Geology*, **172**, 205–223.

Trenhaile, A. S. 2002. Modeling the development of marine terraces on tectonically mobile rock coasts. *Marine Geology*, **185**, 341–361.

Trenhaile, A. S., Pepper, D. A., Trenhaile, R. W. & Dalimonte, M. 1998. Stack and notch development, Hopewell Rocks, New Brunswick. *Canadian Geographic*, **42**, 94–99.

Trenkamp, R., Kellogg, J. N., Freymueller, J. T. & Mora, H. P. 2002. Wide plate margin deformation, southern Central America and northwestern South America, CASA GPS observations. *Journal of South American Earth Sciences*, **15**, 157–171.

Van Daele, M., van Welden, A. *et al.* 2011. Reconstruction of Late-Quaternary sea- and lake-level changes in a tectonically active marginal basin using seismic stratigraphy: the Gulf of Cariaco, NE Venezuela. *Marine Geology*, **279**, 37–51.

Vélez, M. I., Wille, M., Hooghiemstra, H., Metcalfe, S., Vanderberghe, J. & van der Borg, K. 2001. Late Holocene environmental history of Southern Chocó region, Pacific Colombia; sediment, diatom and pollen analysis of core El Caimito. *Paleogeography, Paleoclimatology, Paleoecology*, **173**, 177–214.

Vergara-Muñoz, A. 1988. Tectonic patterns of the Panama block deduced from seismicity, gravitational data and earthquake mechanisms: implications to the seismic hazard. *Tectonophysics*, **154**, 253–267.

Vernette, G. 1989. Impact du diapirisme argileus sur les recifs de la plate-forme colombienne des Caraibs. *Bulletin de l'Institut de Geologie du Bassin d'Aquitaine*, **45**, 97–106.

Victor, P., Sobiesiak, M., Glodny, J., Nielsen, S. N. & Oncken, O. 2011. Long-term persistence of subduction earthquake segment boundaries: evidence from Mejillones Peninsula, northern Chile. *Journal of Geophysical Research-Solid Earth*, **116**, B02402, http://dx.doi.org/10.1029/2010JB007771

Vieira, M. M. & Ros, L. F. 2006. Cementation patterns and genetic implications of Holocene beachrocks from northeastern Brazil. *Sedimentary Geology*, **192**, 207–230.

Von Huene, R. & Lallemand, S. 1990. Tectonic erosion along the Japan and Peru convergent margins. *Geological Society of America Bulletin*, **102**, 704–720.

Von Huene, R. & Ranero, C. R. 2003. Subduction erosion and basal friction along the sediment-starved convergent margin off Antofagasta, Chile. *Journal of Geophysical Research*, **108**, 2079.

Von Huene, R., Bialas, J. *et al.* 1995. Morphotectonics of the Pacific convergent margin of Costa Rica. *In*: Mann, P. (ed.) *Geologic and Tectonic Development of the Caribbean Plate Boundary in Southern Central America*. Geological Society of America, Boulder, CO, Special Papers, **295**, 291–307.

Von Huene, R., Ranero, C., Weinrebe, W. & Hinz, K. 2000. Quaternary convergent margin tectonics of Costa Rica: segmentation of the Cocos Plate and Central American volcanism. *Tectonics*, **19**, 314–334.

Wadge, G. & Burke, K. 1983. Neogene Caribbean plate rotation and associated tectonic evolution. *Tectonics*, **2**, 633–643.

Walker, J. A., Williams, S. N., Kalamarides, R. I. & Feigenson, M. D. 1993. Shallow open-system evolution of basaltic magma beneath a subduction zone volcano: the Masaya caldera complex, Nicaragua. *Journal of Volcanology and Geothermal Research*, **56**, 379–400.

Wallace, D. R. 1997. Central American landscapes. *In*: Coates, A. G. (ed.) *Central America: A Natural and Cultural History*. Yale University Press, New Haven, CT, 72–96.

Weidie, A. E. 1985. Geology of the Yucatan Platform, Part 1. *In*: Ward, W. C., Weidie, A. E. & Back, W. (eds) *Geology and Hydrogeology of the Yucatan and Quaternary Geology of Northeastern Yucatan Peninsula*. New Orleans Geological Society, New Orleans, LA, 1–19.

Weinberg, R. F. 1992. Neotectonic development of western Nicaragua. *Tectonics*, **11**, 1010–1017.

West, R. 1957. *The Pacific Lowlands of Colombia: a Negroid area of the American Tropics*. Louisiana State University Press, Baton Rouge, LA.

Weyl, R. 1980. *Geology of Central America*. Gebrüder Borntraeger, Berlin.

White, S. M., Trenkamp, R. & Kellog, J. N. 2003. Recent crustal deformation and the earthquake cycle along the Ecuador-Colombia subduction zone. *Earth and Planetary Science Letters*, **216**, 231–242.

Wielemaker, W. G. & Vogel, A. W. 1993. *Un Sistema de Información de Suelos y Tierras para la Zona Atlantica de Costa Rica*. Atlantic Zone Program Report 22, Wageningen Agricultural University, Wageningen.

Winckell, A. & Zebrowski, C. 1997. Los paisajes costeros. *In*: Winckel, A. (ed.) *Los paisajes naturales del Ecuador. Geografía básica del Ecuador*. CEDIG, Quito, 208–319.

Witt, C., Bourgois, J., Michaud, F., Ordoñez, M., Jimenez, N. & Sosson, M. 2006. Development of the Gulf of Guayaquil (Ecuador) during the Quaternary as an effect of the North Andean Block tectonic escape. *Tectonics*, **25**, TC3017, http://dx.doi.org/10.1029/2004TC001723

Wong, T. E. 1992. Quaternary stratigraphy of Suriname. *In*: Prost, M. T. & Charron, C. (eds) *Evolution des littoraux de Guyane et de la zone caraïbe méridionale pendant le Quaternaire, SymposiumPICG 274/Orstom, Cayenne (Guyane)*. Orstom, Paris, 559–578.

Wright, A. C. S., Romney, D. H., Arbuckle, R. H. & Vial, V. E. 1959. *Land in British Honduras*. Colonial Research Publications, London.

Yanez-Arancibia, A. 2005. Middle America, coastal ecology and geomorphology. *In*: Schwartz, M. (ed.) *Encyclopedia of Coastal Science*. Springer, Dordrecht, 639–645.

Zanchetta, G., Consoloni, I. *et al.* 2012. New insights on the Holocene marine transgression in the Bahía Camarones (Chubut, Argentina). *Italian Journal of Geosciences (Bollettino della Società Geologica Italiana e del Servizio Geologico d'Italia)*, **131**, 19–31. http://dx.doi.org/10.3301/IJG.2011.20

Zong, Y. 2007. Tropics. *In*: Elias, S. A. (ed.) *Encyclopedia of Quaternary Science*. Elsevier, Amsterdam, 3087–3094.

Zoppis-Bracci, L. Z. & Del Giudice, D. 1958. Geología de la costa del Pacífico de Nicaragua. *Boletín del Servicio Geológico Nacional de Nicaragua*, **2**, 21–65.